T-2238

An Investigation into the Influences of Alkali Additions to the Manganese Silicate Welding Flux System

by

Theodore L. Reinhart

A Thesis submitted to the Faculty and the Board of Trustees of the Colorado School of Mines in partial fulfillment of the requirements for the degree of Master of Science in Metallurgical Engineering.

Signed: Theodore L. Reinhart   Date: 6 June 1980
Theodore L. Reinhart
Student
Golden, Colorado

Approved: David LeRoy Olson   Date: 6 June 1980
Dr. David L. Olson
Thesis Advisor
Golden, Colorado

W D Copeland   Date: 10 June 1980
Dr. William D. Copeland
Head of Department
Golden, Colorado

Abstract

The effect of alkali additions to the $MnO-SiO_2$ welding flux system on flux properties was studied in this investigation. Fused $MnO-SiO_2$ fluxes containing varying amounts of sodium, lithium, and potassium were made and used to perform bead-on-plate submerged arc welds on 1020 and 4340 steels. The effect of alkalis on flux behavior--flux viscosity, arc stability, and flux-weld bead interfacial tensions--were observed. Changes in flux behavior were then related to changes in weld bead morphology. These three factors were successfully related to penetration in 1020 steel welds using the equation developed by Schwemmer, but the equation did not agree with data from 4340 steel welds. The effects of alkalis and/or alloying agents from the steel on flux-weld interfacial tensions is believed responsible for this disagreement.

Table of Contents

Table of Contensts (continued)

Table of Contents (concluded)

List of Tables

List of Tables (concluded)

List of Figures

List of Figures (continued)

List of Figures (continued)

List of Figures (continued)

List of Figures (continued)

List of Figures (concluded)

ACKNOWLEDGEMENTS

Without help from other people this thesis would not have been possible. The author would like to acknowledge the inspiration, patience, and guidance of Prof. D. L. Olson. Thanks also go to the other committee members, Prof. W. M. Mueller and Prof. D. K. Matlock. Also, thanks to Enrique Carmona and other graduate students in the Department of Metallurgical Engineering. A very special thanks also goes to Vicky Zuber for preparing this document.

I. INTRODUCTION

The welding industry has seen tremendous advances since its birth nearly a century ago. Filler materials have been developed which can be used to make welded joints with properties often as good as those of the parent metal. Advanced welding processes now exist which employ lasers, electron beams, and plasma torches. Even ultra-high frequency sonic waves are being used to join some materials.

Despite these amazing new concepts, the welding industry is constantly being pressed to develop new techniques and improve existing ones to meet the welding requirements of an increasing array of materials and quality specifications. In order to meet this challenge, much more knowledge of the mechanisms of welding processes is needed. One area where this need is apparent is the behavior of welding consumables, especially welding fluxes.

A. Commercial Fluxes

A Welding flux is a granular fusible material made up mostly of oxides, flourides, and in the case of covered electrode coatings, carbonates. The American Welding Society definition of a flux[1] is as follows: "... a material used to prevent, dissolve, or facilitate removal of oxides and other undesirable substances ..." Of course, a welding flux must perform other functions as well; these are discussed in a later section.

Commerical welding fluxes are made up of essentially unrefined minerals such as limestome, silicates, kaolin, etc. Because the compositions of such minerals vary widely with the location of their origin, typical fluxes contain a great variety of compounds. Some of these compounds can be detrimental to weld quality. For the same reason, one can find considerable compositional variations in different shipments of the same grade flux. These variations do indeed cause welding problems; more than one shipment of welding flux has been returned to the manufacturer because its composition made it unuseable.[2] Table 1 gives some typical compositional variations in raw materials used in flux manufacture. Since flux manufacturers have been known to buy raw materials from several suppliers, it is easy to see why flux compositions vary so much. Besides this reason, chemical refining of such minerals is often expensive and difficult, and to date, the marketplace has not demanded it. However, as the demand for better weld quality increases, it is quite possible that higher grade fluxes with more carefully controlled compositions will be developed.

Table 2 gives the compositions of some electrode coatings and submerged arc welding fluxes. The numbers reflect the raw materials compositions; a typical flux will often contain over a dozen different compounds. Covered electrode coatings contain not only impurities but also some intentionally added ingredients, e.g., "borcote" (gound coconut shells) and sodium silicate, to act as binders and strengthening agents.

B. Functions of a Weld Flux

A flux must serve many functions in order to produce acceptable welds. Most of all it must protect the weld puddle from atmospheric gases and stabilize the arc. Table 3 is a detailed list of the many possible functions of a welding flux. In order to function properly the flux must have certain properties. It must have a lower solidus point than the parent metal so that the metal solidifies before the flux. If the flux solidifies first, it

TABLE 1

TYPICAL ANALYSES OF SELECTED RAW MATERIALS[3]

Manganese Ore	Total Mn	MnO_2	SiO_2	Fe_2O_3	K_2O	Na_2O	Al_2O_3	CaO	MgO	BaO	P	S	C
Africa	54.84	81.64	5.20	1.76	0.36	0.13	1.95	0.06	0.14	0.21	0.110	0.008	0.04
Ghana	56.59	19.84	8.13	8.79	0.63	0.20	5.01	0.08	0.08	0.28	0.140	0.025	0.45
Angola	53.99	73.89	3.46	2.32	0.54	0.05	2.27	0.49	0.00	2.65	0.032	0.100	0.10
Chile	50.37	53.64	7.18	1.72	0.24	0.59	1.88	3.06	0.80	1.72	0.018	0.380	0.10
Mexico	40.82	53.11	23.18	3.22	0.43	0.16	1.33	1.96	0.48	1.29	0.100	0.100	0.38
Indonesia	48.15	74.32	10.12	3.95	0.30	0.08	2.35	0.96	0.54	1.53	0.100	0.027	0.16
African Mn	64.79	85.14	2.01	2.15	0.35	0.30	2.32	1.00	ND	ND	0.070	0.020	ND
Brown Mn oxide	64.84	68.56	3.28	1.60	ND	ND	2.50	ND	ND	ND	0.020	0.003	ND

	$CaCO_3$	$MgCO_3$	MgO	CaF_2	S	P	Fe_2O_3	Al_2O_3	TiO_2	SiO_2	Pb	CaO	FeO
Calcium carbonate	97.7		0.7		0.03	0.01	0.2	0.6					
Dolomite	54.1	43.9								1.8			
Fluorspar	1.10			97.6	0.06	Trace				1.2	0.07		
Silica			0.04				0.02	0.05		99.0		0.02	
Talc			30.9							56.7		4.8	
Rutile					0.02	0.01			93.0	0.50			6.0
Ilmenite					0.01	0.03	24.6	1.2	55.9				12.3
Wollastonite			1.0				0.30	0.45		49.8		46.5	

TABLE 2

TYPICAL COMPOSITION OF VARIOUS COATINGS AND FLUXES

COVERED ELECTRODES

E6010

Component	Wt. %
Borcote (ground coconut shells)	26.0
TiO_2	13.0
Ilmenite	10.0
Asbestos	10.0
Calcium carbonate	3.0
SiO_2	5.0
Talc	3.0
Bentonite	2.0
HC Fe-Mn	12.0
Fe-Si	3.0
Na_2SiO_3 (N Brand)	13.0
Moisture content	3 to 6
Amount of coating	10 to 14

E6024

Component	Wt. %
Rutile	22.0
Cellulose	1.0
Feldspar	8.2
Silica	2.7
Clay	3.3
Fe powder	39.0
Fe-Si	4.4
Fe-Mn	5.4
Sodium silicate	7.0
Potassium silicate	7.0
Moisture content	0.4 to 0.6
Amount of coating	45 to 55

SUBMERGED-ARC FLUXES

Component	Flux 1 Wt. %	Flux 2 Wt. %	Flux 3 Wt. %
CaF_1	2.6	15.0	6.9
CaO	2.5	7.2	1.2
MnO	43.9		42.0
MgO	1.2	2.4	0.3
FeO	3.4	27.7	1.5
Na_2O			0.4
Al_2O_3	5.4	23.0	2.0
TiO_2	17.7	4.6	0.1
SiO_2	22.7	3.1	45.0
Other	V_2O_5 0.6	Fe_2O_3 17.0	PbO 0.1 BaO 0.1

TABLE 3

FUNCTIONS OF A FLUX

1. Stabilize the arc (liberate electrons at relatively low temperature to ionize the arc gap before the metal melts).

2. Provide a slag of low melting point (sometimes nearly the same as base metal so that both melt at the same rate).

3. Provide a slag of low density.

4. Provide a slag of low viscosity (not too viscous, otherwise slag is trapped in weld metal).

5. Replenish the losses of metallic elements.

6. Add alloying elements to the weld metal (to raise the tensile strength, or to reduce aging, or to produce nuclei for grain size control).

7. Perform metallurgical refining operations, such as deoxidation.

8. Change the apparent resistance of the arc gap, in this way controlling deposit efficiency.

9. Retard the rate of cooling and solidification of weld metal. (The annealing effect of the slag, particularly if it protects the weld from oxidation is said to reduce shrinkage stresses.)

10. Facilitate specific welding operations, such as overhead welding and fillet welding.

11. Permit use of different types of current.

12. Reduce spatter or fume.

13. Produce a weld of desired smooth contour.

14. Provide slag that is easily separated from the deposit (low coefficient of expansion or transformations).

15. Provide a slag that is immiscible in weld metal.

16. Dissolve scale or rust on surfaces to be welded.

17. Provide a slag to cover the weld puddle completely.

may crack and expose molten weld metal to the atmosphere; this can also cause pock marks in the weld bead. The density of the molten flux must be considerably less than that of the weld metal to prevent entrapment of flux particles in the fusion zone. Flux viscosity is always an important consideration. The viscosity must be low enough to cover the entire weld puddle and allow gases to escape from the metal. However, if the flux is too fluid, inadequate weld penetration and/or atmospheric contamination may result. A relatively viscous flux is required for overhead and vertical welding to contain the weld puddle, but undercutting of the bead can occur if it is too viscous. Thus, the situation is complex.

Fluxes can also serve other purposes. Sometimes powdered aluminum is added to deoxidize the weld metal. Alloying can be accomplished by the addition of ferroalloys to the flux. Calcium fluoride is often added to fluxes to give a weld possessing greater toughness. The remaining functions in Table 3 are self-explanatory.

C. Flux Classification Systems

Although there are a limited number of commercial flux compositions, at present there are no specifications concerning what may or may not be used in a flux. The existing classifications are based on the mechanical properties (ultimate tensile strength and Charpy impact toughness) of the resulting weldment or the method of flux manufacture.

Table 4 gives the AWS flux classification system for mild and low alloy steels.[3] The prefix "F" designates a flux and is followed by two digits which represent the tensile strength (in k.s.i.) and toughness requirements of the finished weld. Following that are four digits which designate the wire to be used.

AWS Flux Classification	Tensile Strength (ksi)	Yield Strength (ksi)	Elongation in 2 in. min. %	Charpy V-notch Impact Strength
F60xxxx	60			not required
F61xxxx	to	45	25	20 ft-lb at 0°F
F62xxxx	80			20 ft-lb at 20°F
F70xxxx	70			not required
F71xxxx	to	50	22	20 ft-lb at 0°F
F72xxxx	95			20 ft-lb at 20°F

Note: xxxx refers to wire classification.

TABLE 4 - Mechanical property requirements for flux classification[4].

Fluxes are manufactured by either fusion or solid-state bonding processes. Fused fluxes are characterized by good chemical homogeneity and non-hygroscopic tendencies. Drawbacks to this type of flux are that it is impossible to add metallic alloying or deoxidizing agents to them (due to gross density differences) and their production requires costly energy-consuming electrical furnaces. On the other hand, bonded fluxes will accept additions of powdered metals, and their manufacture is less energy-intensive. However, chemical homogeneity is sometimes a problem with these fluxes, and a binder must be added in order to encourage particle formation.

Covered electrodes are classified according to specifications established by the AWS and the ASTM.[4] Table 5 shows some characteristics of mild and low alloy steel electrodes. The electrode class number begins with "E." The first two digits following stand for the minimum tensile strength requirements of the deposited metal. The third digit indicates the welding position (e.g., horizontal) for which the electrode can be used, and the last digit tells the performance characteristics (e.g., low-hydrogen, high deposition, etc.) of the electrode.

D. Basicity of Fluxes

The basicity of fluxes and slags is a controversial subject. Much research has been done in this area, but most of it has been empirical in nature. Most of the controversy centers around the definition of basicity and how different components in a flux contribute to basic (or acid) flux behavior. This is understandable because high-temperature flux research is both expensive and difficult.

The most applicable definition of basicity is given by the Lewis Theory.[5] It defines an acid as an ion which can form covalent

Class No.	Work Position*	Current Supply +	Penetration	
All Position, Deep Penetrating - Good Properties				
EXX10 EXX11	All All	DC+ AC (DC+)	Digging Digging	Deep Deep
All Position, Light Penetrating				
EXX13 EXX14	All All	AC (DC-) AC (DC-)	Soft Soft	Medium Medium
Production Welding				
EXX12 EXX24	All HF-F	DC- AC AC (DC-)	Mild Mild	Medium Light
Deep Groove Heavy Section				
EXX20 EXX27 EXX30	HF-F HF-F F	DC- AC DC- AC DC- AC	Mild Mild Mild	Medium Deep Medium Medium
Low Hydrogen - Difficult to Weld				
EXX15 EXX16 EXX18 EXX28	ALL All HF-F HF-F	DC+ AC DC+ AC DC- DC- (AC)	Mild Mild Mild Mild	Medium Medium Medium Medium

HF = Horizontal fillet position
F = Flat
Current supply in parentheses indicates that, for production welding, some sacrifice in advantages must make using the designated supply.
DC+ = Direct current, reverse polarity
DC- = Direct current, straight polarity
AC = Alternating current

Table 5. Characteristics of covered electrodes.

bonds with unshared electron pairs and a base as an ion which can donate an unshared electron pair for bonding.[5] In other words, a flux component's basicity is a measure of its ability to surrender an electron pair to form covalent bonds with a neighbor species. Of course, its ability to do this depends on the nature of the neighbor species--so basicity is a relative term. There are some amphoteric oxides which can act either as acid or base depending on the acidity/basicity of its environment. This is especially true of some of the transition metal oxides. Table 6 shows a listing of the chemical behavior of some fluxes.

For practical purposes, flux basicity is usually defined as a ratio of the concentration of basic components to acid components; although these relationships are empirical they have been used to represent the chemical behavior of fluxes with some success. There are many such basicity formulae in existence. In fact, a search of literature on the subject may leave one with the impression that there are nearly as many basicity equations as there are investigators. Several such equations are given here as examples.

One of the most recently developed indices was put forth by Eagar[6] in 1978. His equation:

$$B.I. = \frac{[CaO+MgO+BaO+SrO+Na_2O+K_2O+Li_2O] + 1/2\ (MnO+FeO)}{SiO_2 + 1/2(Al_2O_3+TiO_2+Zro_2)}$$

Zaks and Zhorova[7] reported using an equation of this form:

$$B.I. = \frac{\Sigma a_i N_i}{wt.\%SiO_2}$$

Popular Description	Compositional ranges expressed as oxides								Basicity Index
	SiO_2	TiO_2	ZrO_2	Al_2O_3	MnO	CaO	MgO	CaF_2	
Acid Ca silicate High SIO_2	50-60	-	-	3-5	-	25-30	8-12	2	0.5-0.8
Neutral Ca silicate	30-40	-	-	10-15	0-5	25-30	10-15	5-10	0.8-1.2
Basic, Ca silicate Low SIO_2	30-40	-	-	3-5	-	35-45	0-5	10-15	1.2-1.7
Highly basic, Low SIO_2, Medium Al_2O_3	5-12	-	-	10-15	-	10-15	30-40	20-30	3-5
Acid Mn silicate	30-40	-	-	0-10	35-45	0-10	-	0-10	0.5-1.0
Neutral High Al_2O_3	10-20	5-15	0-10	20-50	10-20	0-5	-	5-15	0.5-2.0

Table 6 - Compositional ranges of some common submerged arc fluxes[5].

Where B.I. stands for basicity index, N_i is the weight percent of the i^{th} component in the flux and a_i is a coefficient expressing the different affinities of each component for silica.

Flux basicity is important because more basic compositions are able to refine tramp elements such as sulfur, phosphorous, and oxygen from the weld metal. In fact, attempts are being made to weld steels with more basic fluxes to obtain better weld metal toughness.[6] Several investigators[6,8,9,10] have reported finding that basic fluxes reduced the oxygen content of the weld metal. However, Eagar[6] reported that the oxygen level hit a minimum and leveled off despite further increases in flux basicity. This trend is shown in Figure 1.[6] He further states that more basic compositions may even contribute to increased oxygen levels in weld metal. The reason given for this is that highly basic fluxes are quite fluid and could flow away from the weld puddle too easily, thus, allowing oxygen from the atmosphere to enter the arc plasma.[6]

Ito et al.[8] also reported that weld metal oxygen content decreased with increasing flux basicity. Their results (see Figure 2) differ from those of Eagar in that the oxygen content of the weld metal drops continuously as flux basicity increases. However, Ito et al. used a somewhat different basicity index than Eagar. Also, Eagar did not report the welding parameters for his data (which came from other sources[9,10]); nor did he know the base metal compositions. Thus, it is difficult to compare these (and other researcher's) results. However, both men[6,8] agree that basicity is only one factor affecting the refining ability of a welding flux.

Many welding researchers[8,11,12,13] have reported that additions of CaF_2 to most fluxes (regardless of basicity) reduce weld metal oxygen levels. Figure 2 shows the results of Ito et al.[8] Additions of only 7% CaF_2 to even highly acidic fluxes resulted in

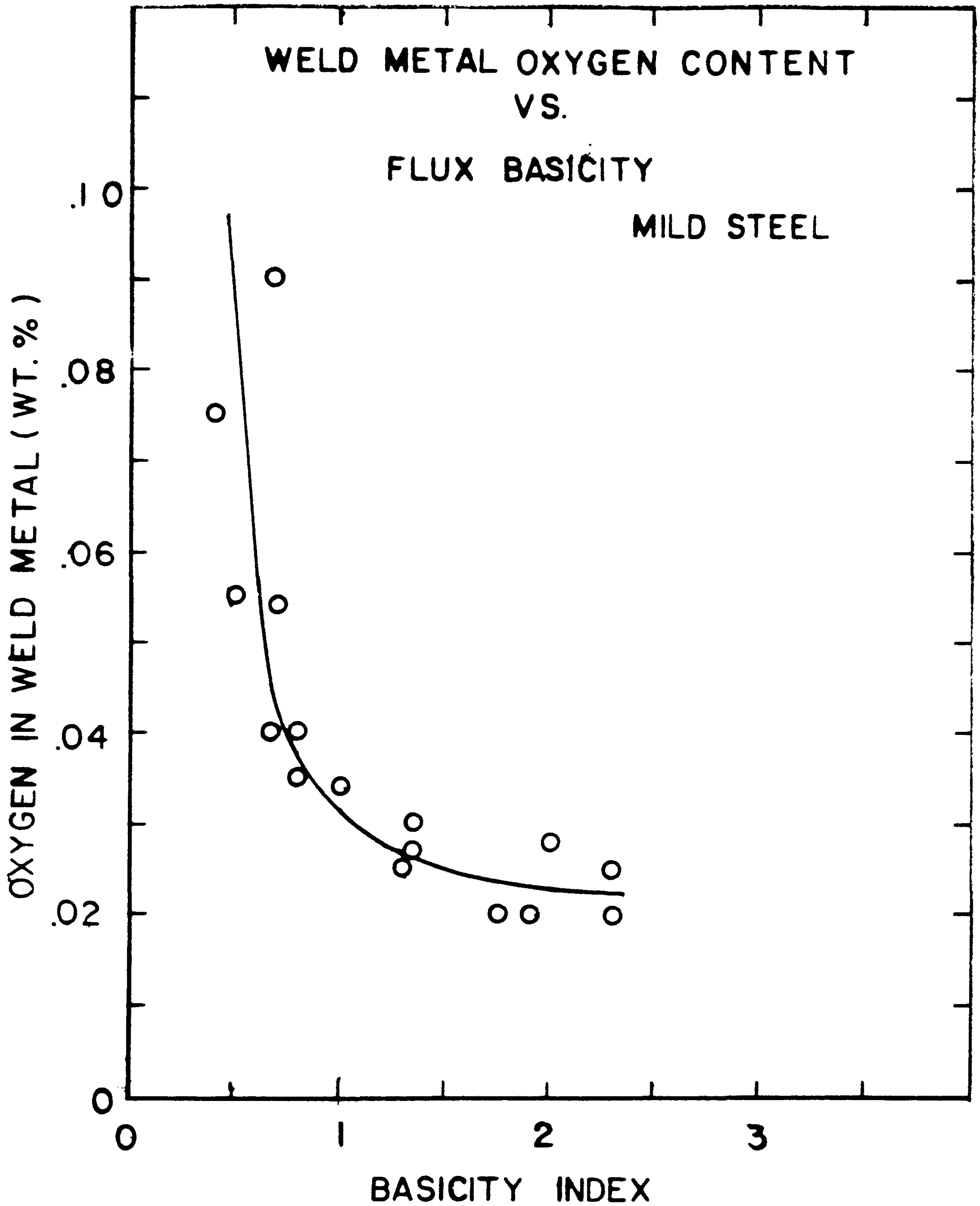

Fig. 1. Weld metal oxygen content as a function of flux basicity[6].

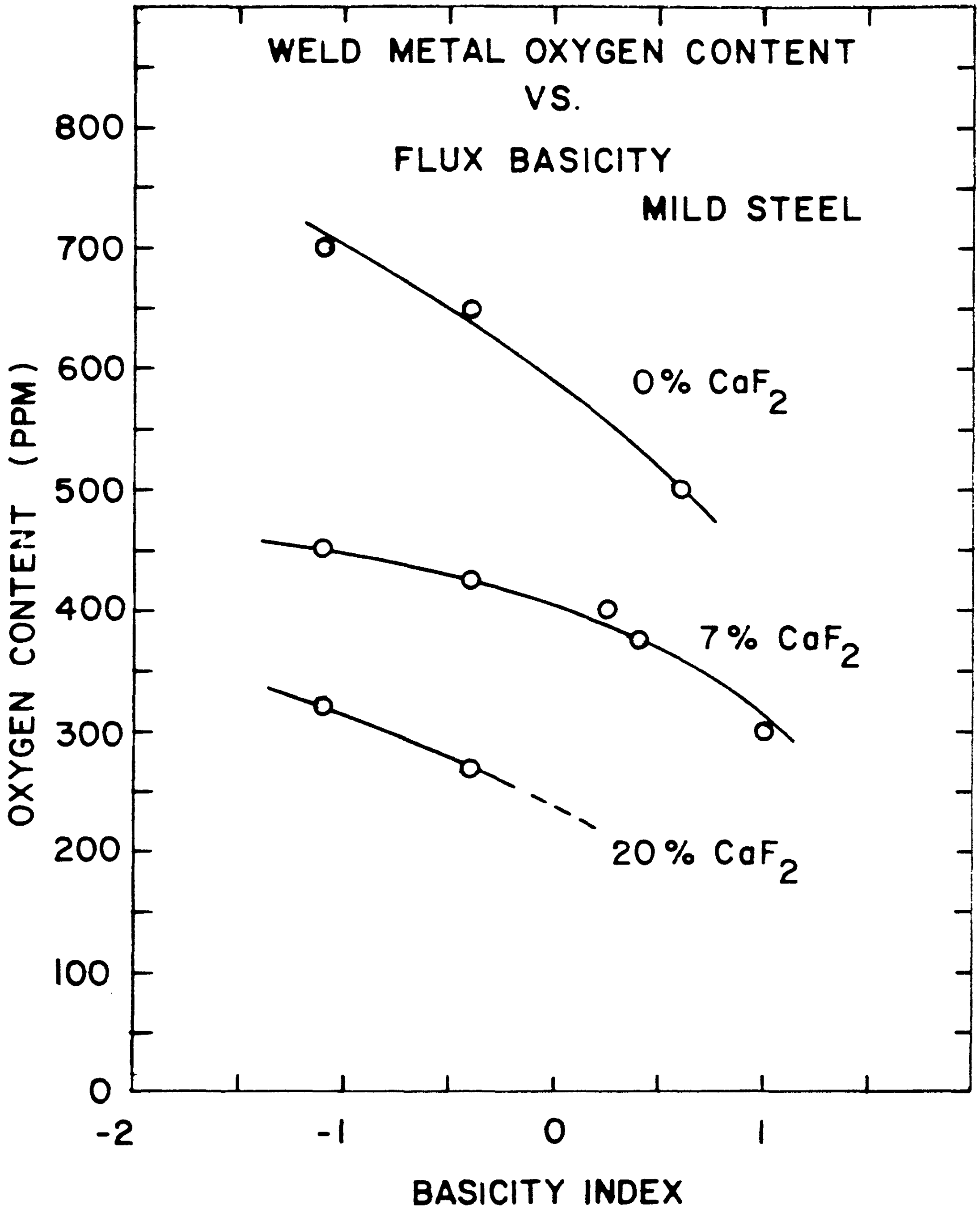

Fig. 2. Weld metal oxygen content as a function of flux basicity and CaF_2 flux content[8].

drastically reduced weld metal oxygen levels in welds made on mild steel. It was speculated[8] that CaF_2 generates gas in the arc region and lowers the partial pressure of impurity gases in the arc plasma, thereby lowering their concentrations in the weld metal. Figure 3 shows that CaF_2 is also effective in removing nitrogen and hydrogen from weld metal.[8]

Despite the considerable progress made so far, more work is needed to determine the factors and mechanics which control the refining ability of fluxes.

E. The Manganese Silicate Flux System

This system is commonly used as a submerged arc welding flux. It enjoys the advantages of a low melting eutectic (1245°C at 38 wt. % SiO_2) and the fact that its constituents are readily available. The $MnO-SiO_2$ phase diagram is shown in Figure 4, and Table 7 lists its prominent features.[14] This type of flux is considered acidic because of the amount of silica present. Welds made with manganese silicate fluxes generally have higher oxygen contents, and hence, lower impact properties, than welds made with more basic fluxes.[6,8] They also tend to contribute manganese and silicon to the weld metal.[6,8,12] Nonetheless, such fluxes are used for welding steels, especially in joining components where low temperature toughness is not needed.

F. The Design of Welding Flux Research at CSM

Early welding flux research provided much valuable information concerning the effects of flux components on weldment and arc properties. However, many of the early investigations were made with little or no thought of a long range goal. To avoid the pitfalls of such a lack of direction, a long-range goal has been

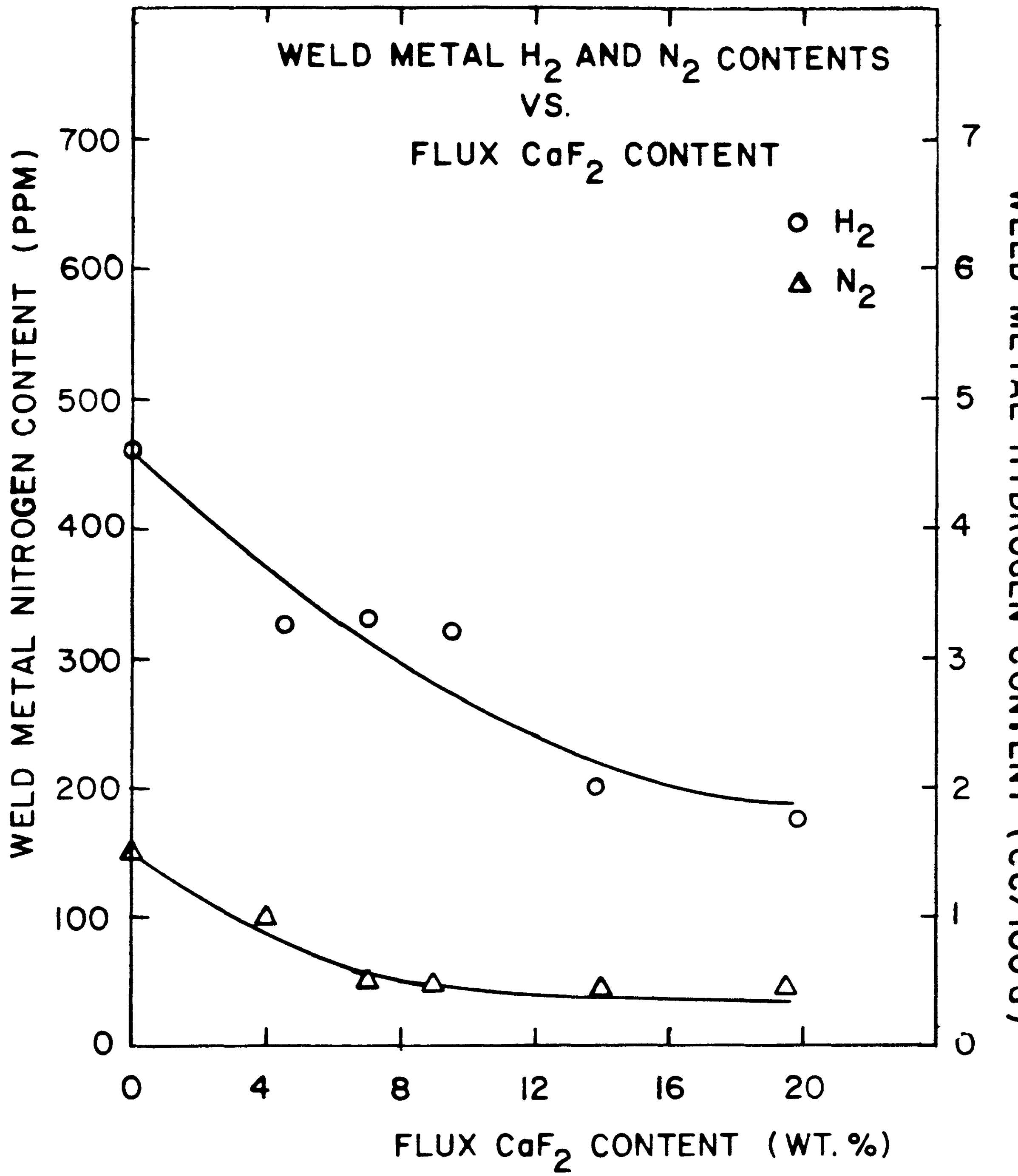

Fig. 3. Weld metal hydrogen and nitrogen as a function of % CaF_2 in the flux[8].

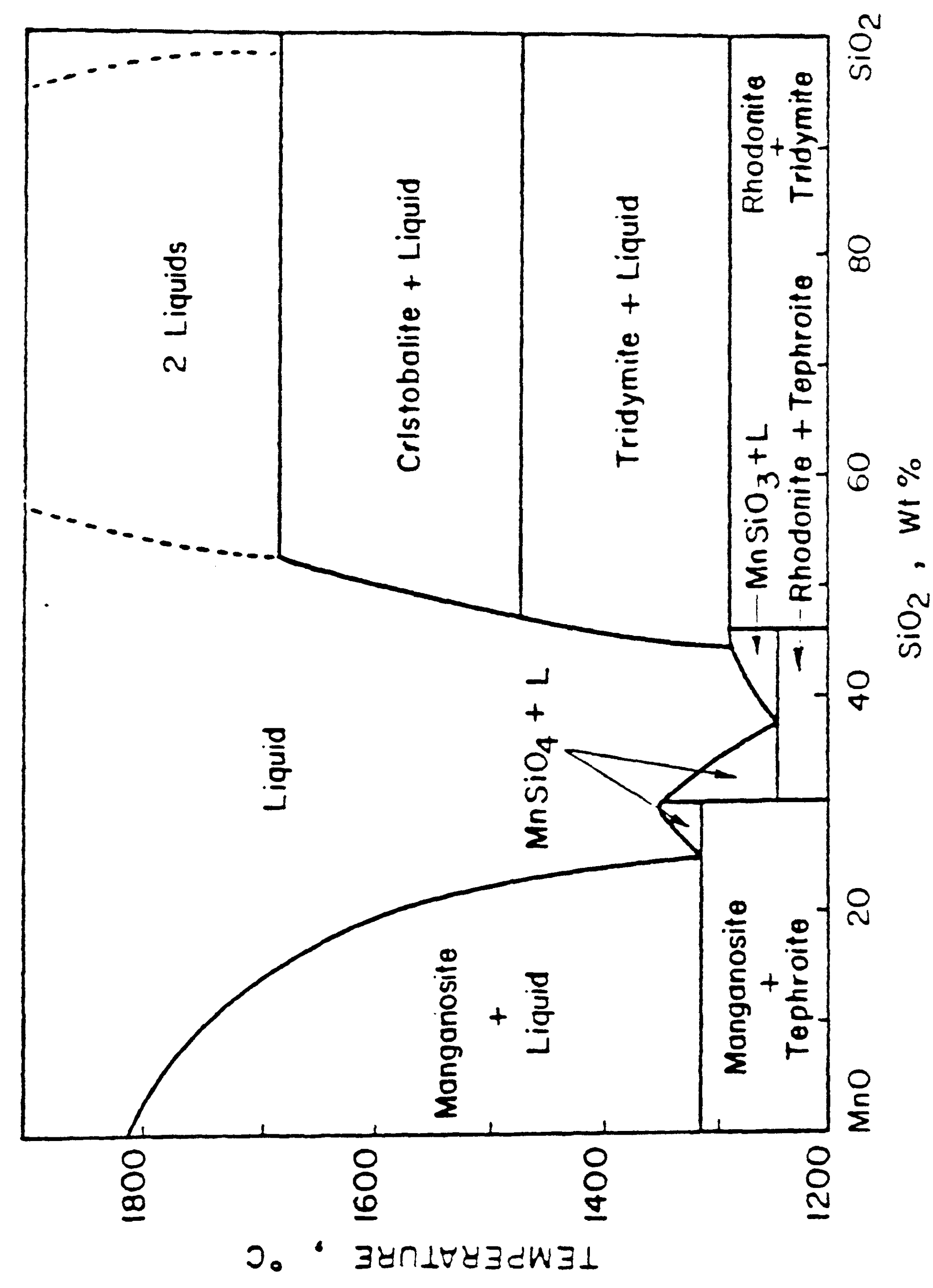

Fig. 4. $MnO-SiO_2$ equilibrium phase diagram[14].

MnO Wt. %	SiO_2 Wt. %	Temperature °C	Physical Phenomena
0	100	1,710	Melting point ....SiO_2
1	99	1,681	Limit of two liquid region
53	47	1,471	Tridymite -- Cristobalite inversion
54.2	45.8	1,286	Incongruent melting point Rhodonite
56	44.0	1,286	Peritectic: Rhodonite, Silica and Liquid
62	38	1,245	Eutectic: Rhodonite, Tephroite and Liquid
70.3	29.7	1,347	Congruent melting point: Tephroite + Liquid
74.5	25.5	1,315	Eutectic: Tephroite, MnO and Liquid
100	0	1,815	Melting point ....MnO

TABLE 7 - Salient features of the $MnO-SiO_2$ binary system[13].

set and a systematic plan to reach that goal has been developed. The aim of welding flux behavior which can be used to design welding flux systems with specific applications in mind. Presently, welding flux development is a long, drawn-out empirical process. A model based on the behavior of flux components would at least provide more direction for their development. It is felt that a thorough knowledge of the role of each component in a flux must be obtained before such a model can be developed. Table 8 shows an overview of the plan for CSM flux research. So far, most of the investigations have involved the physical effects of flux properties on welds, but mechanical and chemical investigations are also underway.

The manganese silicate flux system was chosen as a starting point for several reasons: it is commonly used for welding steels; it possesses a low-melting eutectic; also, its binary phase diagram and a number of its ternary diagrams, e.g., $MnO-SiO_2-CaO$, are well documented.

Flux research at CSM began with the $MnO-SiO_2-CaO$ systems. Ferrera and Olson[15] investigated the physical properties of these fluxes and their effects on arc stability and weld bead morphology. Alizo[16] investigated the mechanical properties of steel weldments made with these same flux systems. Janzen[17] conducted studies involving the $MnO-SiO_2-CaO/CaF_2$ systems. Schwemmer[18] studied the $MnO-SiO_2-FeO$ system. The most recently completed study is the work of Carmona.[19] He investigated the effects of alkaline earth and transition metal oxide additions to the $MnO-SiO_2$ system.

Beginning with Schwemmer's work, data has been reported in terms of atom percent metal ion (ionic percent) to form a more fundamental basis for the comparison of different flux systems. More details of these projects are given in Table 9.

FLUX SYSTEM	PHYSICAL	MECHANICAL	CHEMICAL
$MnO-SiO_2$	X		
" " - CaO	X	X	
" " - CaF_2	X		
" " - CaO/CaF_2	X		
" " - FeO	X		
" " - MgO	X		
" " - SrO	X		
" " - BaO	X		
" " - TiO_2	X		
" " - V_2O_3	X		
" " - Cr_2O_3	X		
" " - CaO	X		
" " - ZnO	X		
" " - Al_2O_3	X		
" " - Li_2O	X		
" " - Na_2O	X		
" " - K_2O	X		

Table 8. An overview of physical, chemical and mechanical investigations.

INVESTIGATOR	ADDITIONS TO THE $MnO-SiO_2$ SYSTEM	STEEL PLATE WELDED	PROPERTIES STUDIED
Ferrera[15]	CaO	1020	Viscosity Arc Stability Bead Morphology Capillarity
Alizo[16]	CaO	1020	Mechanical Properties of the Weld Metal
Janzen[17]	CaF_2, CaO/CaF_2	1020, 4340	Viscosity Arc Stability Bead Morphology Capillarity
Schwemmer[18]	FeO	1020, 4340	Viscosity Arc Stability Bead Morphology Capillarity Mossbauer Analysis - Fe^{+2} ion
Carmona[19]	Alkaline Earths, Transition Elements	1020	Viscosity Arc Stability Bead Morphology Capillarity

Table 9. Welding flux research carried out as CSM.

G. Objective of This Investigation

The objective of this investigation is the observation of the effects of alkali additions on the physical behavior (changes in flux viscosity, arc stability, and capillarity effects) of $MnO-SiO_2$ base fluxes. These behavioral changes are then related to changes in weld bead morphology.

Compounds containing alkali elements are frequently found in welding fluxes as impurities and occasionally as additives. Sodium and potassium silicates are often added to covered electrode coatings to act as binders. For these reasons it is desirable to know what effects the alkali elements have on the $MnO-SiO_2$ flux system.

II. EXPERIMENTAL MATERIALS

A. Flux Preparation

All fluxes were made from reagent grade chemicals to eliminate unwanted compositional variables. Calculated amounts of SiO_2, MnO_2, and alkali hydroxides were mixed together to give the desired compositions. The silica content of all fluxes was kept constant at 38 wt.%, and hydroxides were added at the expense of calculated amounts of MnO_2. Hydroxides were used rather than alkali oxides because the latter are more difficult to handle, and MnO_2 was used because MnO is unstable at room temperatures. The hydroxides lose their water of hydration at low temperatures, and MnO_2 decomposes into MnO and oxygen at 847°C. Thus, the hydroxides and MnO_2 both decompose during melting to form the desired components.

B. Materials Used in Welding

The experimental fluxes were used to make single pass, bead-on-plate submerged arc welds on 1020 and 4340 steels. All plates were 1/2" × 3" × 8" in size. AWS type E70S-3 mild steel filler wire was used for welding 1020 steel, and Linde 71 alloy steel wire was used for 4340 steel. Tables 10 and 11 give the base metal and filler wire compositions for 1020 and 4340 steels, respectively.

III. FLUX VISCOSITY

A. Background

The viscosity of fluxes has long been viewed as one of the more critical requirements for producing good welds. For this reason, components for fluxes have been chosen from systems possessing fairly low-melting eutectics (usually around 1300°C according to Jackson[20]). Proper flux viscosity for a given welding application is a compromise dictated by a number of requirements. For example, weld metal refining is expedited by a very fluid flux, as greater fluidity promotes flux-metal refining. Also, a more fluid flux allows gases in the weld puddle to escape more easily. On the other hand, a more viscous flux tends to contain the weld puddle and thus encourages deeper penetration. A more viscous flux is obviously needed for overhead and vertical welding. However, if the flux viscosity is too great, undercutting of the weld bead can occur. This results in decreased weldment fatigue and toughness properties and is undersirable. The point of this discussion is to illustrate the complexity of the problem of flux viscosity.

TABLE 10

COMPOSITION OF BASE METAL AND
WELDING WIRE FOR 1020 WELDS (WT%)

ELEMENTS	1020 BASE METAL	E70S-3 FILLER WIRE
%C	0.18 - 0.23	0.06 - 0.15
%Mn	0.3 - 0.6	0.025
%P Max	0.040	0.035
%S Max	0.050	0.09 - 0.14
%Fe	Balance	Balance

TABLE 11

COMPOSITION OF BASE METAL AND WELDING WIRE FOR 4340 WELDS (WT%)

ELEMENTS	4340 BASE METAL	LINDE 71 FILLER WIRE
%C	0.38 - 0.43	0.31
%Mn	0.6 - 0.8	0.55
%P	0.040	0.01
%S	0.040	0.01
%Si	0.2 - 0.35	0.65
%Ni	1.65 - 2.0	--
%Cr	0.7 - 0.9	1.25
%Mo	0.2 - 0.3	0.5
%V	--	0.25
%Fe	Balance	Balance

The viscosity of a fluid is a measure of its resistance to flow. It results from intermolecular bonds and the necessity of momentum transfer from one particle to the next; both of these factors contribute to a fluid's resistance to shear stress brought on by flow.[21]

Viscosity can be expressed by Newton's law which states that the shear stresses produced by flow are proportional to the velocity gradient between two shearing layers of fluid.[22] In equation form this is:

$$\tau - \eta \frac{dv}{dy}$$

where η is the coefficient of viscosity, τ is the shear stress of flow, and dv/dy is the velocity gradient between moving layers of fluid. Fluids obeying this relationship are known as Newtonian fluids.

The effect of flux viscosity on weld penetration has been well documented by CSM investigators.[15,17-19] All of them reported that an increase in flux viscosity caused increased weld penetration. For example, Figure 5 shows penetration as a function of flux viscosity (at 1723°K) for welds made on 1020 and 4340 steels using MnO-SiO_2-FeO fluxes (from Schwemmer[18]).

B. The Effect of Temperature on Flux Viscosity

The viscosity of any fluid depends on its temperature and composition. Both of these factors affect the strength of the intermolecular bonds which resist flow. Richardson[23] reported that the viscosity-temperature relation for silicate melts is exponential; the equation given for this relation is

$$\eta = \eta_o \exp\left[(E_\eta)_p/RT\right]$$

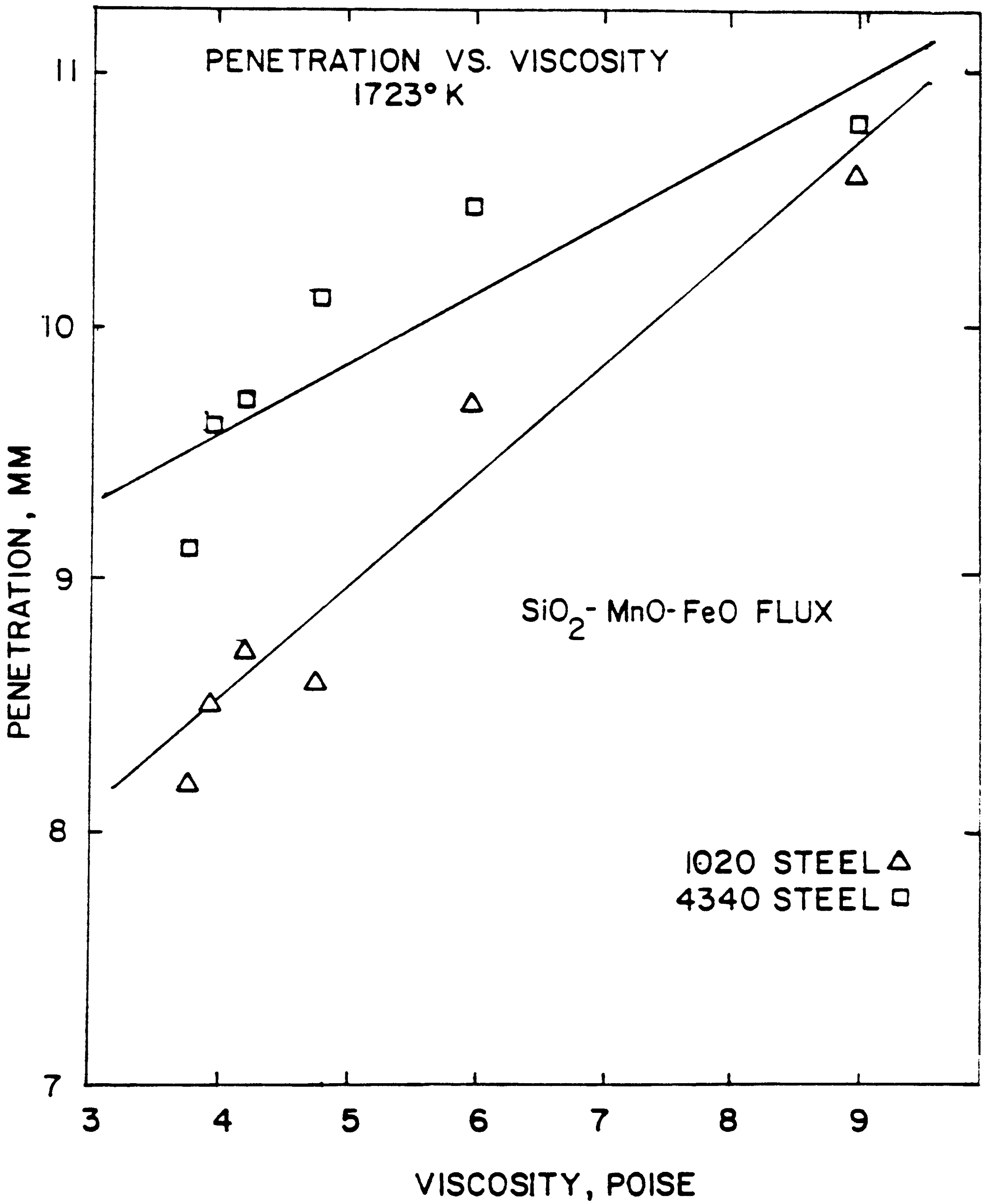

Fig. 5. Weld penetration vs. flux viscosity at 1723°K, 1020 and 4340 steels, $MnO-SiO_2-FeO$ flux system[18].

where $(E_n)_p$ is an activation energy term. As the temperature is increased, the bonds between silicate units are weakened, and flux viscosity is decreased.

C. Compositional Effects

Flux composition is the second factor controlling viscosity. A considerable amount of work on this subject has been published. Interest in this area stems not only from the welding industry but also from the steel and glass making industries.

The effects of composition on flux viscosity can be better understood if one knows something about the structure of the flux. The structures of crystalline molten, and amorphous (glassy) silicates are well-known from x-ray diffraction studies.[24] These studies showed that the SiO_4 tetrahedron is the building block for both glassy and molten silica; further studies showed this tetrahedron to be intact even in NaO/SiO_2 glasses.[25,26] Electrical conductance tests on silica melts give very low values, indicating that the structural bonding is covalent.[23] Also, the fact that molten silica is very viscous (about 10^{12} poise at 1400°C[26]) indicates the tetrahedra are essentially unchanged even after melting.[23] Figure 6 shows schematic diagrams of crystalline and molten silica structures. The difference between the two is the lack of long-range ordering in the molten state, i.e., a number of the SiO_4 tetrahedra corners are unshared.

When a molten oxide is introduced into the silica network, some of the oxygen bridges between the tetrahedra are broken. This is termed network modification. Such a reaction for addition of a divalent oxide, e.g., MnO can be represented by an equation[23]:

$$(\vdots Si-O-Si \vdots) + MO = 2(\vdots Si-O^-) + M^{2+}$$

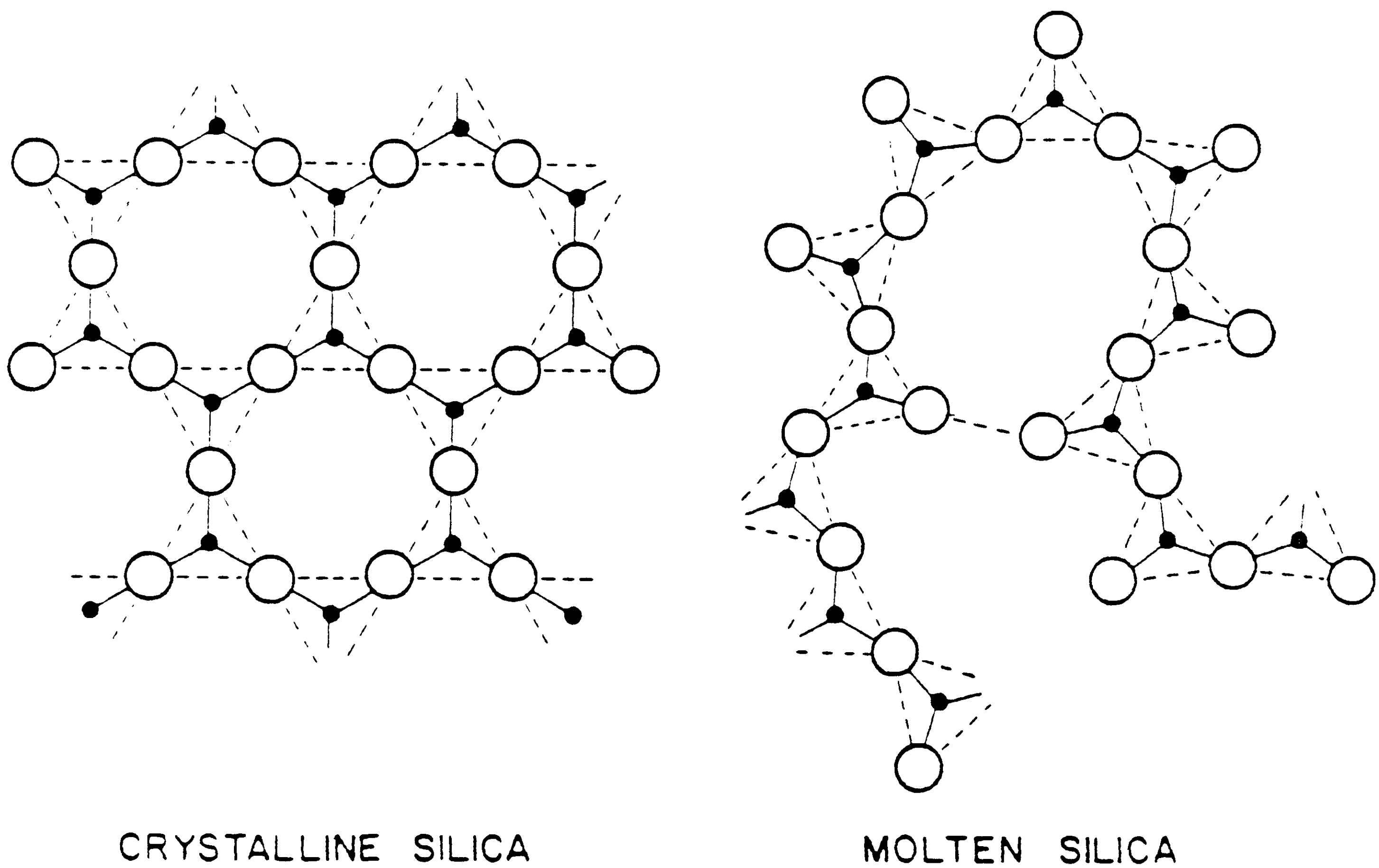

Fig. 6. Schematic drawings of crystalline and molten silica structures.

When bonds between tetrahedra are broken, unshared negatively charged corners are produced, and the metal cations are attracted by these corners. Note that each cation can be associated with more than one negatively charged corner. The disruption of bonds between the tetrahedra and their replacement with the much weaker attraction of the metal cations results in a viscosity decrease. A schematic of this situation is shown in Figure 7.

The above reaction equation must be altered for the case of alkali (monovalent) oxide additions:

$$(\vdots Si-O-Si) + M_2O = 2(\vdots Si-O^-) + 2M^+$$

Again, Si-O-Si bonds between tetrahedra are broken and the cations are attracted to the unshared corners. However, because of the cations' monovalence, the network modification scheme must be somewhat different than that for divalent metal ions. Because of the alkali ions' lesser charges, each is probably associated with fewer (and perhaps only one) negatively charged tetrahedron corner. This would provide even less attractive force between the tetrahedra than the divalent metal ions. Following this reasoning, it would seem that the alkali ions must be stronger network modifiers than those with greater valences. In fact, viscosity measurements on alumino-silicate slags suggest that aluminum ions (with valence of +3) can actually become part of the silicate network.[23] Thus, on a mole-per-mole basis, additions of alkali ions should bring about a greater viscosity decrease in molten silica than ions with greater valence numbers.

Figure 8 shows viscosity-composition curves for three binary silicates. The temperature for each curve is different, but the important thing to note is that the silicate viscosity decreases continuously with increasing oxide additions.

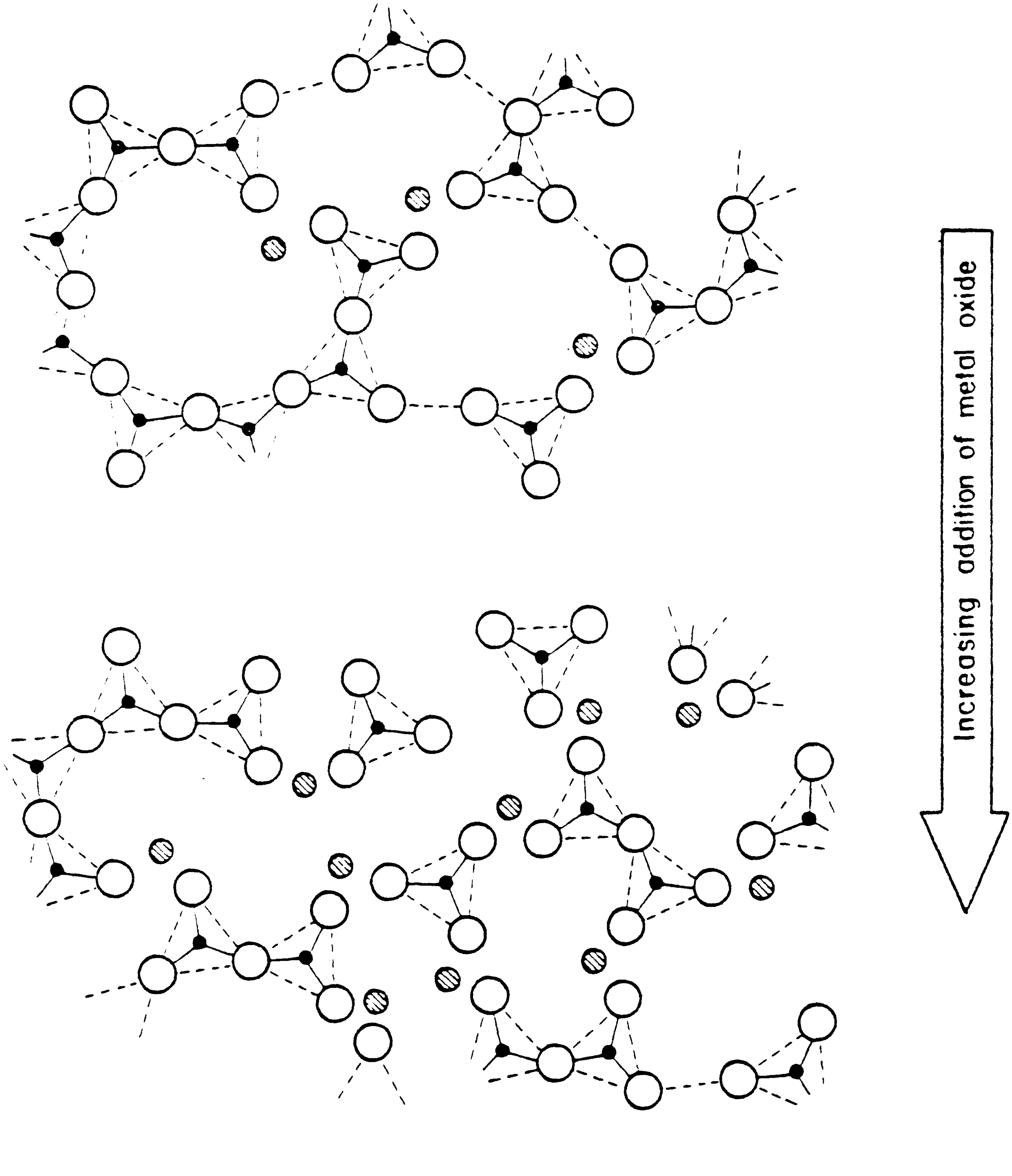

Fig. 7. Schematic drawings showing modification of the silica network[23].

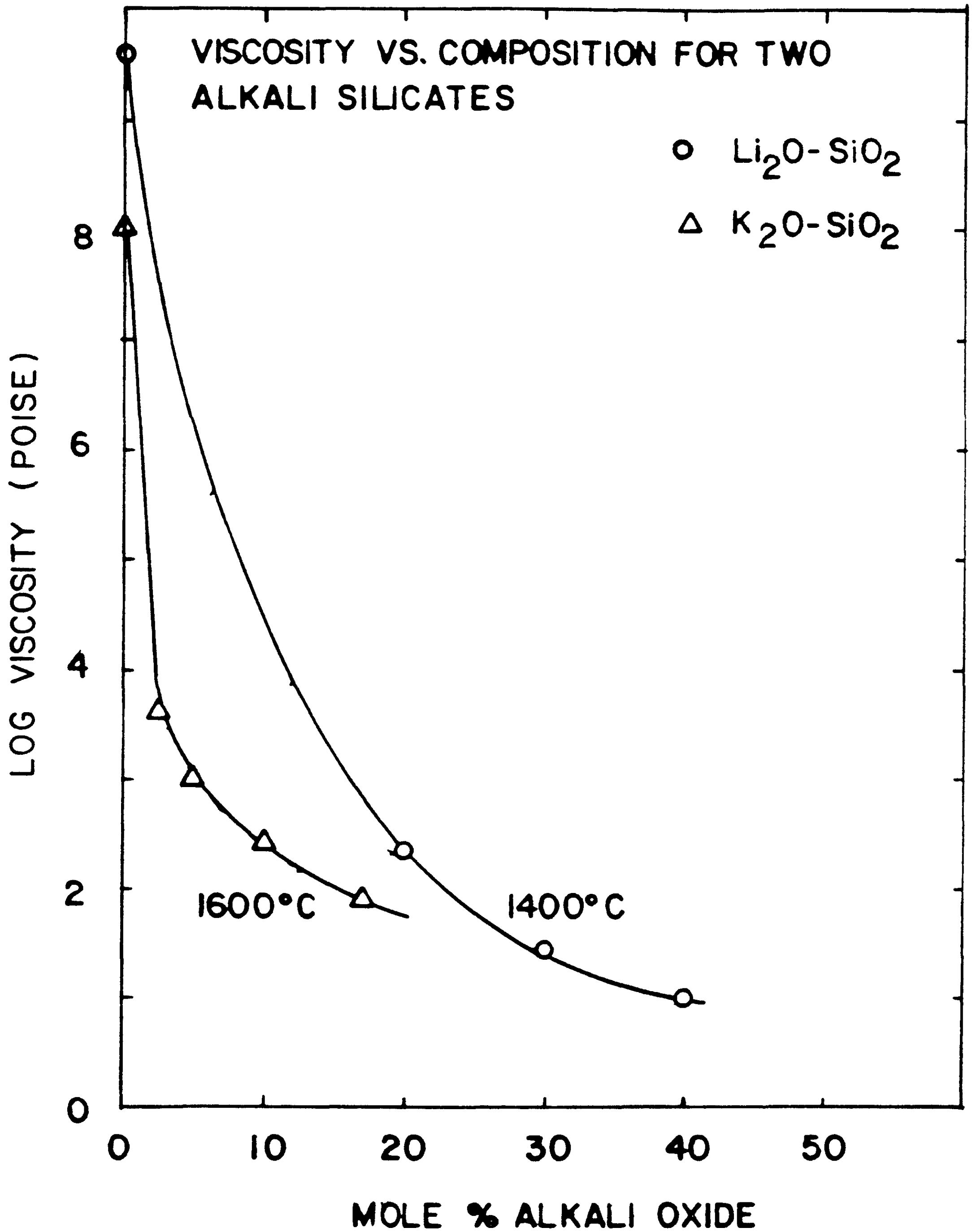

Fig. 8. Viscosity-composition curves for two binary silicates[23].

So far, the discussion of compositional effects has been limited to silica and binary silicates. However, in order to consider more complicated systems, it is necessary to first consider simpler ones.

The flux compositions studied in this investigation were ternary systems. They all contained only 38 wt. % silica, so the structure was already heavily modified before the ternary additions were made. In fact, Bockris et al.[27] have inferred from thermal expansivity tests on silicates that additions of up to 12 mole % metal oxide cause the network to break down in a random manner. At higher concentrations the network degenerates more or less into large anions surrounded by metal cations and O^{2-} ions. Figure 9 shows drawings of the types of anions which are thought to exist in such silicate melts. Little is known about the distributions of anions in these melts because existing chemical analysis techniques tend to break down and/or polymerize the anions.[23] However, analyses of phosphate glasses (phosphate and silicate compounds possess similar network structures) have confirmed the existence of definite anion size distributions.[23] The shapes of these distributions are temperature and composition dependent. Generally, as the temperature and/or metal oxide content of the network increase, the sizes and charges of the silicate anions decrease.[23]

D. Experimental Procedures

All fluxes were melted in a graphite-lined induction furnace. Futhermore, each composition was melted in its own graphite crucible to avoid cross-contamination. The molten bath temperature was raised to at least 1500°C, and a Brookfield torque viscometer was used to measure the flux viscosity as the bath cooled to 1450°C. Temperatures were measured with a two-color pyrometer.

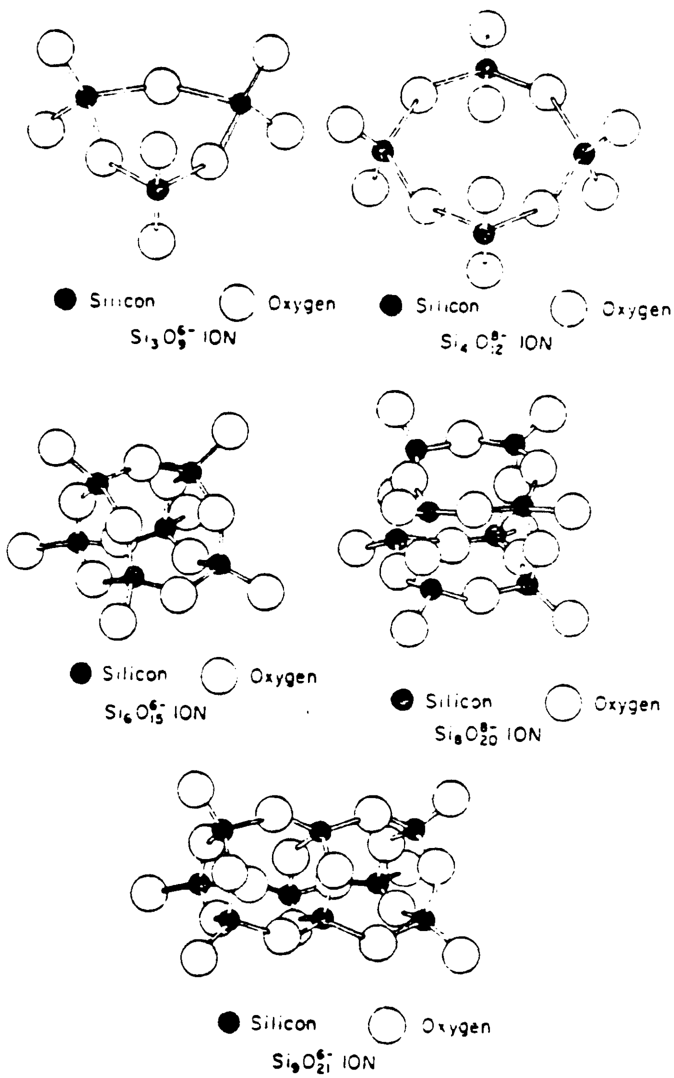

Fig. 9. Schematic drawings of anions thought to exist in silicate melts[23].

Figure 10 shows photographs of the melting equipment, the pyrometer and the viscometer.

The viscosities of other manganese silicate fluxes have been reported to be nearly constant in the 1400-1500°C range,[5,20] so it is felt that representative viscosity measurements were obtained even though the readings were taken over a range of temperatures.

After these measurements were taken, the molten fluxes were poured onto a metal chill to obtain a solid glassy structure. This solid was then ground and screened (only particles between 14-100 mesh were used in welding). The granular fluxes were then baked in air at 700°C for several hours to remove moisture and graphite which may have been picked up during melting. Figure 11 is an illustrative flow chart showing all the flux preparation steps.

The fluxes were also chemically analyzed to determined post-melt compositions. Fine particles (<100 mesh) from the grinding stage were used to insure that a representative sample was taken from each flux. The samples were boiled in nitric acid to leach out the alkali elements, and appropriate dilutions were made to obtain proper concentrations for atomic absorption analysis.[28]

E. Experimental Results

1. Chemical Analysis

The initial and post-melt compositions of all fluxes are given in Table 12. The fluxes were analyzed only for alkali content, as it was felt that very little silicon or manganese were lost during melting. The results show that considerable alkali vapor losses occurred. Fluxes containing lithium suffered the greatest

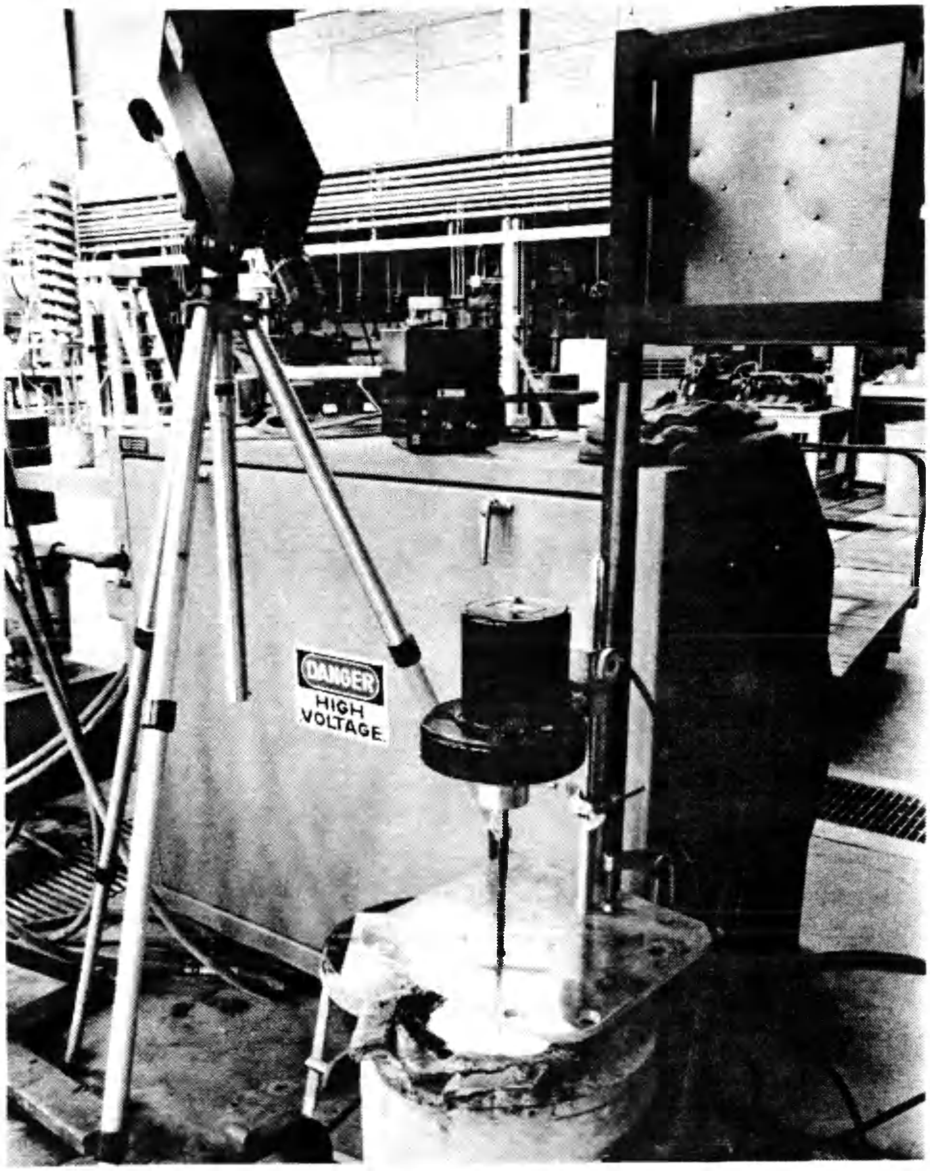

Fig. 10. Photograph showing flux melting equipment.

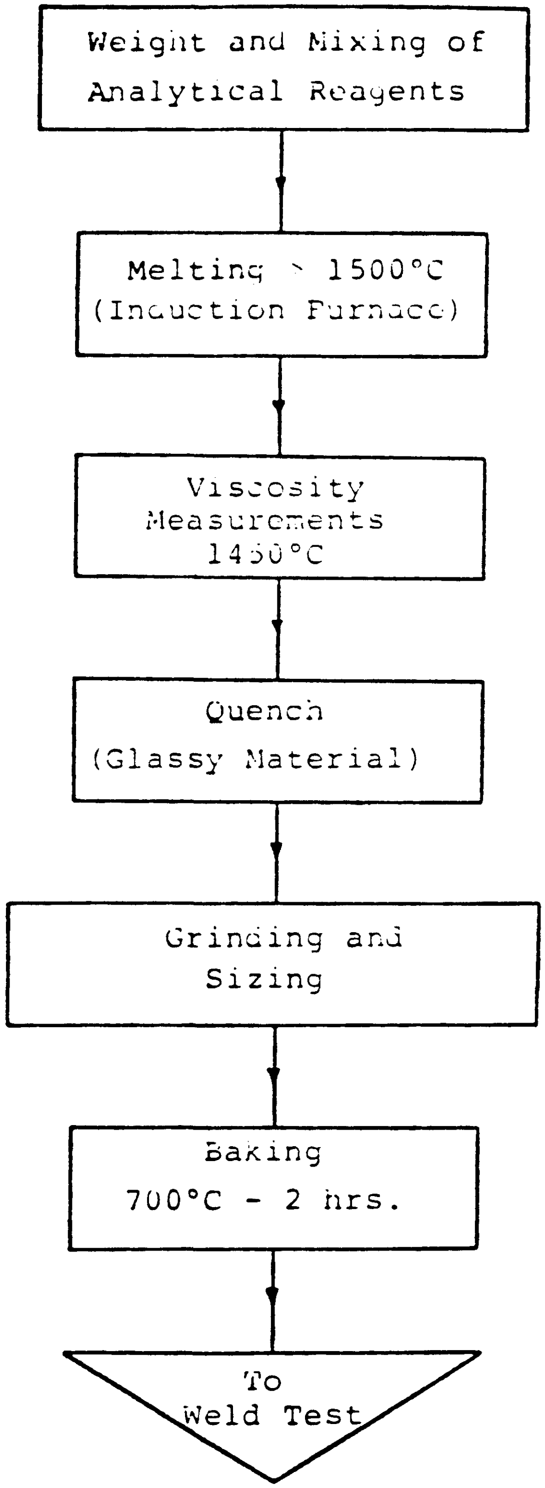

Fig. 11. Flow chart showing steps in the flux preparation process.

#	Alkali Addition	Original Alkali Content Ionic %	Post-Melt Alkali Content Ionic %	Percent Loss	Remarks	
1	-	-	-	-	Eutectic	
2	Sodium	1	0.7	30		
2a	"	1	0.9	10		
"	"	1	0.9	10	Repeat	
3	"	3	1.4	53.3		
4	"	5	4.6	8		
4a	"	5	4.45	11		
5	"	7	5.8	17.1		
5a	"	7	6.35	9.3		
6	"	9	8.05	10.6		
6a	"	9	8.15	9.4		
6b	"	9	8.2	8.9		
"	"	9	8.1	10	Repeat	
7	Potassium	1	0.2	80		
8	"	3	1.8	40		
8a	"	3	2.0	33.3		
8b	"	3	2.3	23.3		
"	"	3	2.3	23.3	Repeat	
9	"	5	4.2	16		
10	"	7	5.9	15.7		
11	"	9	7.5	16.7		
12	Lithium	1	0.3	70		
13	"	3	1.1	63.3		
13a	"	3	1.1	63.3		
14	"	5	1.6	68		
15	"	7	3.15	55		
15a	"	7	3.3	52.9		
15b	"	7	3.4	51.4		
16	"	9	4.0	55.6		
16a	"	9	7.9	12.2		
16b	"	9	7.3	18.9		
"	"	9	7.3	18.9	Repeat	

TABLE 12 - CHEMICAL ANALYSES OF FLUXES.

losses. It is impossible to tell whether this reflects variations in melting practice or a high vapor pressure for lithium relative to the other alkalis.

Thirty-four analyses were made, and six of these were duplicate tests made to check precision. Comparision of the duplicates shows the precision of the tests to be quite good.

2. Viscosity Results

Figures 12, 13, and 14 show the effects of lithium, sodium, and potassium on flux viscosity. In each case the viscosity decreases to a minimum at a relatively low alkali content and then increases. The curve for sodium-bearing fluxes (Figure 13) is displaced to the right relative to the other curves, i.e., its minimum occurs at a higher alkali content than that for either lithium- or potassium-bearing fluxes. The reasons for this is not presently known.

These figures all confirm the contention that the alkali elements are stronger network modifiers than manganese (which has a valence of +2 in the melt). But the reasons for viscosity increases at greater alkali levels are not certain.

Welding flux research at CSM has reached a point at which it is possible to make some general observations concerning compositional effects on the viscosity of $MnO-SiO_2$ fluxes. Figure 15 shows flux viscosity as a function of added metal valence for 1 ionic % concentrations. With the exception of strontium, it is apparent that the alkali metals are the strongest network modifiers. That this plot does not show a continuous, smooth trend is not surprising. It does not take into account such factors as ionic radius and electro-negativity.

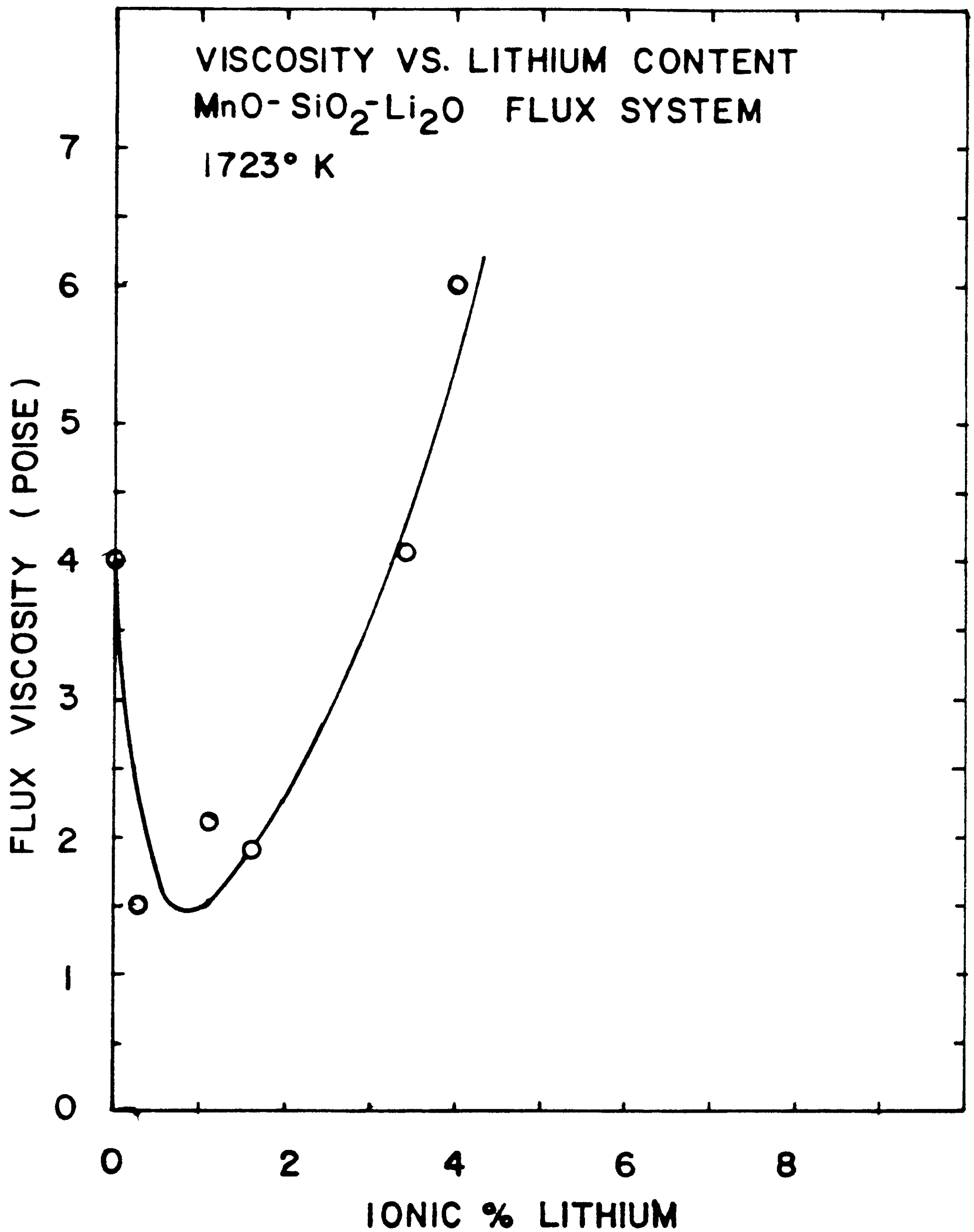

Fig. 12. MnO-SiO_2 flux viscosity at 1723°K vs. lithium content.

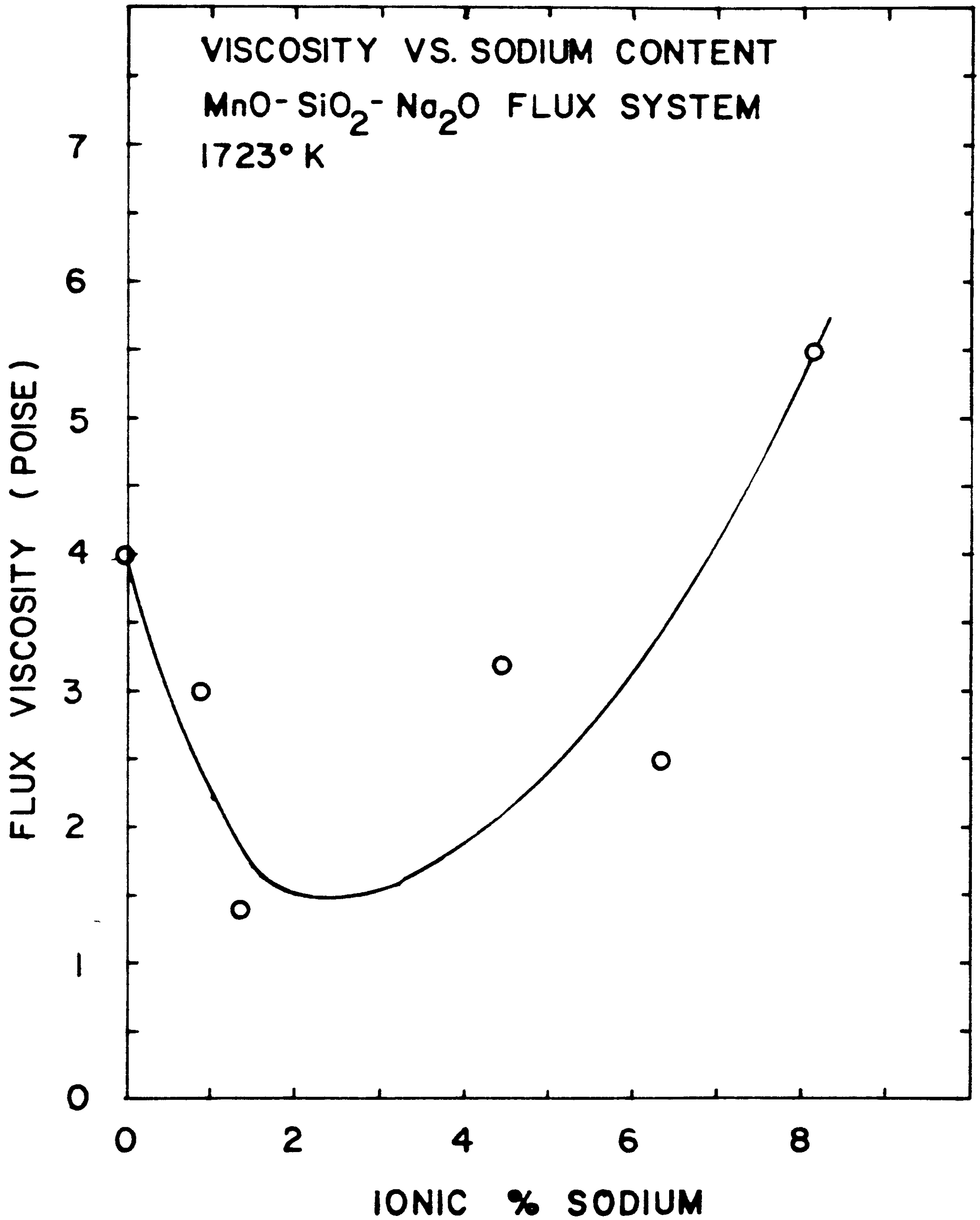

Fig. 13. $MnO-SiO_2$ flux viscosity at 1723°K vs. sodium content.

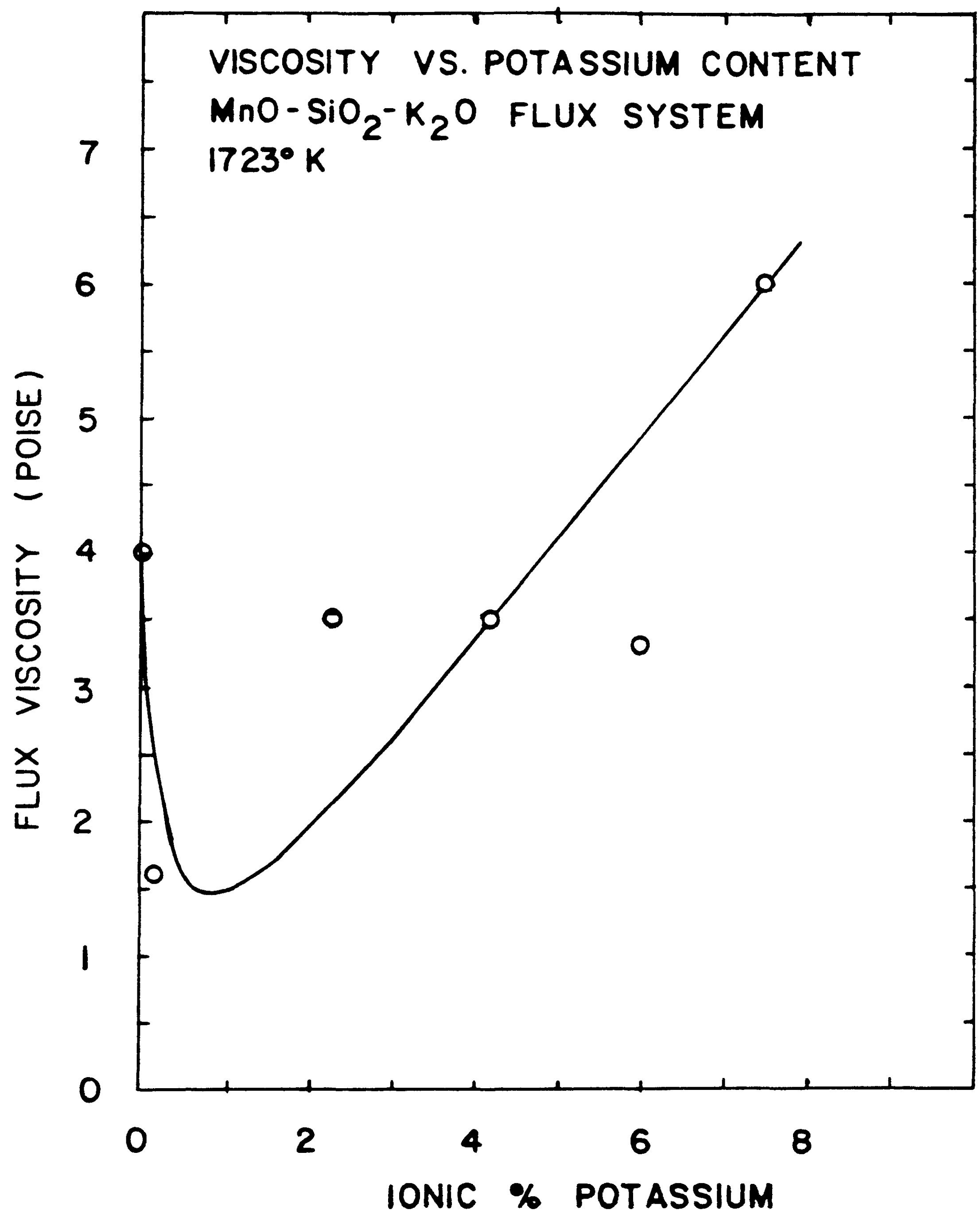

Fig. 14. $MnO\text{-}SiO_2$ flux viscosity at 1723°K vs. potassium content.

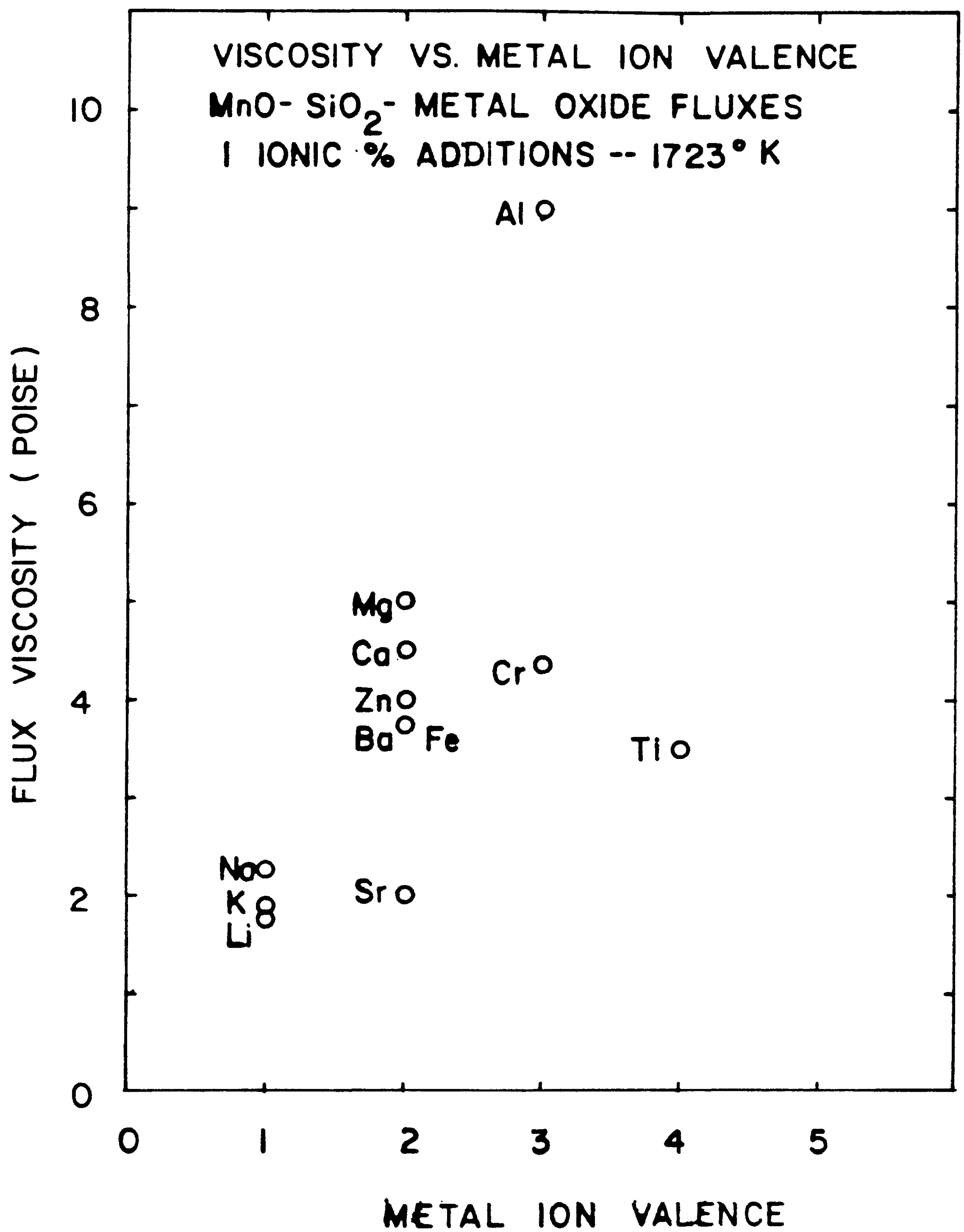

Fig. 15. Flux viscosity at 1723°K vs. valence of the added metal ion for 1 ionic % additions.

The valence of a metal cation reflects to some extent its attraction for the negatively charged, unshared silicate tetrahedra corners. This attraction appears to increase as the valence goes from +1 to +2 and is reflected by increased flux viscosity. But this scheme breaks down at higher valence numbers. Additions of only 1 ionic % aluminum increased flux viscosity tremendously, but the same additions of chromium and titanium had little effect. The effect of aluminum additions is not surprising since this element is known to act as a network former in some slags and minerals.[23]

Figures 16 and 17 show the same plot as Figure 15 at 3 and 5 ionic % addition levels. The trends for 1 and 3% are quite similar, but the scene changes at the 5% level. Viscosities of fluxes containing alkalis have begun to increase, and the viscosities of other fluxes have also changed. At this time, it is not certain why the viscosities of many of the fluxes increase after a certain metal ion addition level, but it is possible that complicated ionic interactions take place which begin to rebuild the network system.

IV. ARC STABILITY

A. Characteristics of the Welding Arc

The physics of welding arcs is quite complex. This is especially so in the case of submerged arc welding, since the arc cannot be directly observed.

A good general definition of welding arc was stated by Jackson.[29]

> "A welding arc consists of a sustained electrical discharge through a high temperature conducting plasma,

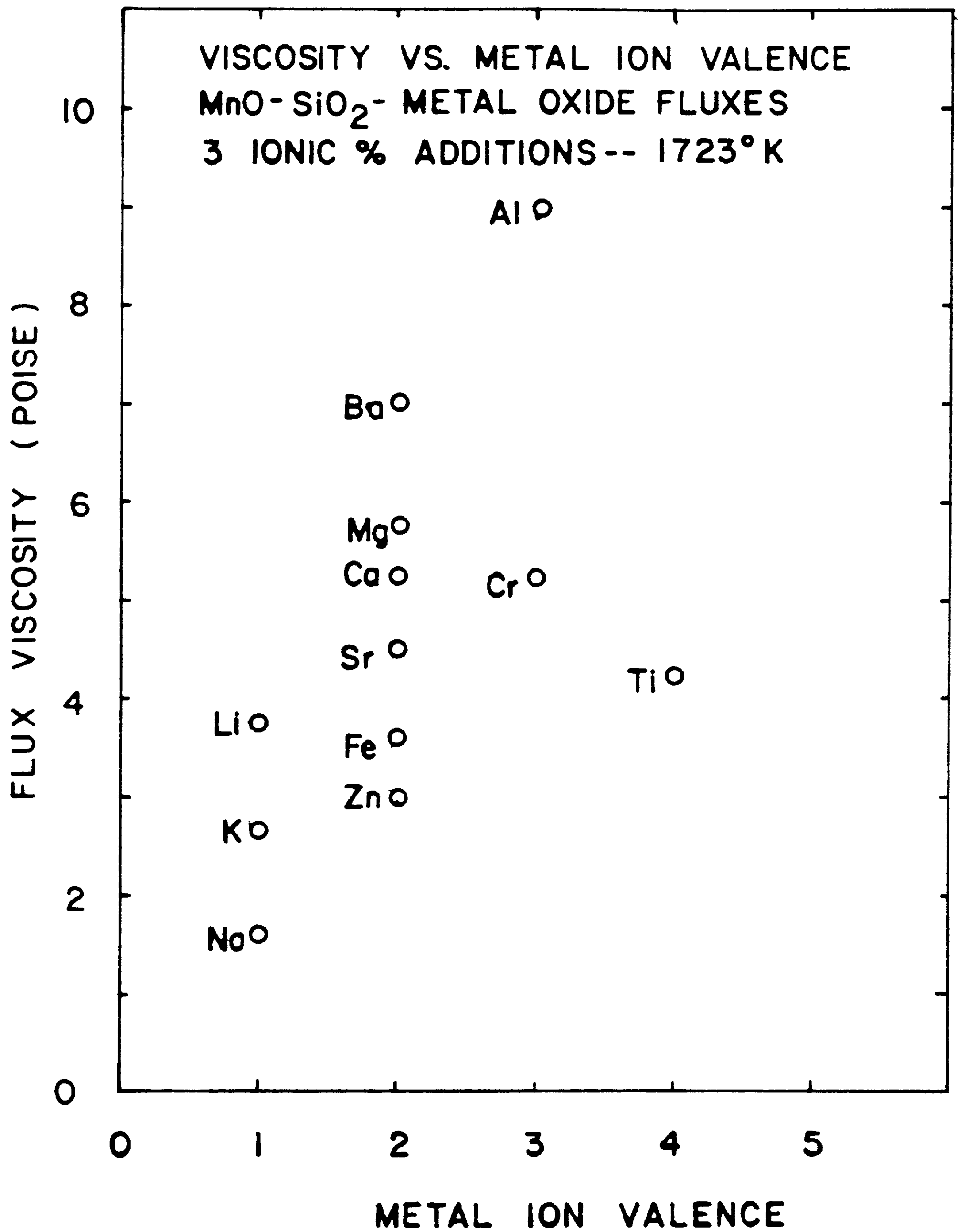

Fig. 16. Flux viscosity at 1723°K vs. valence of the added metal ion for 3 ionic % additions.

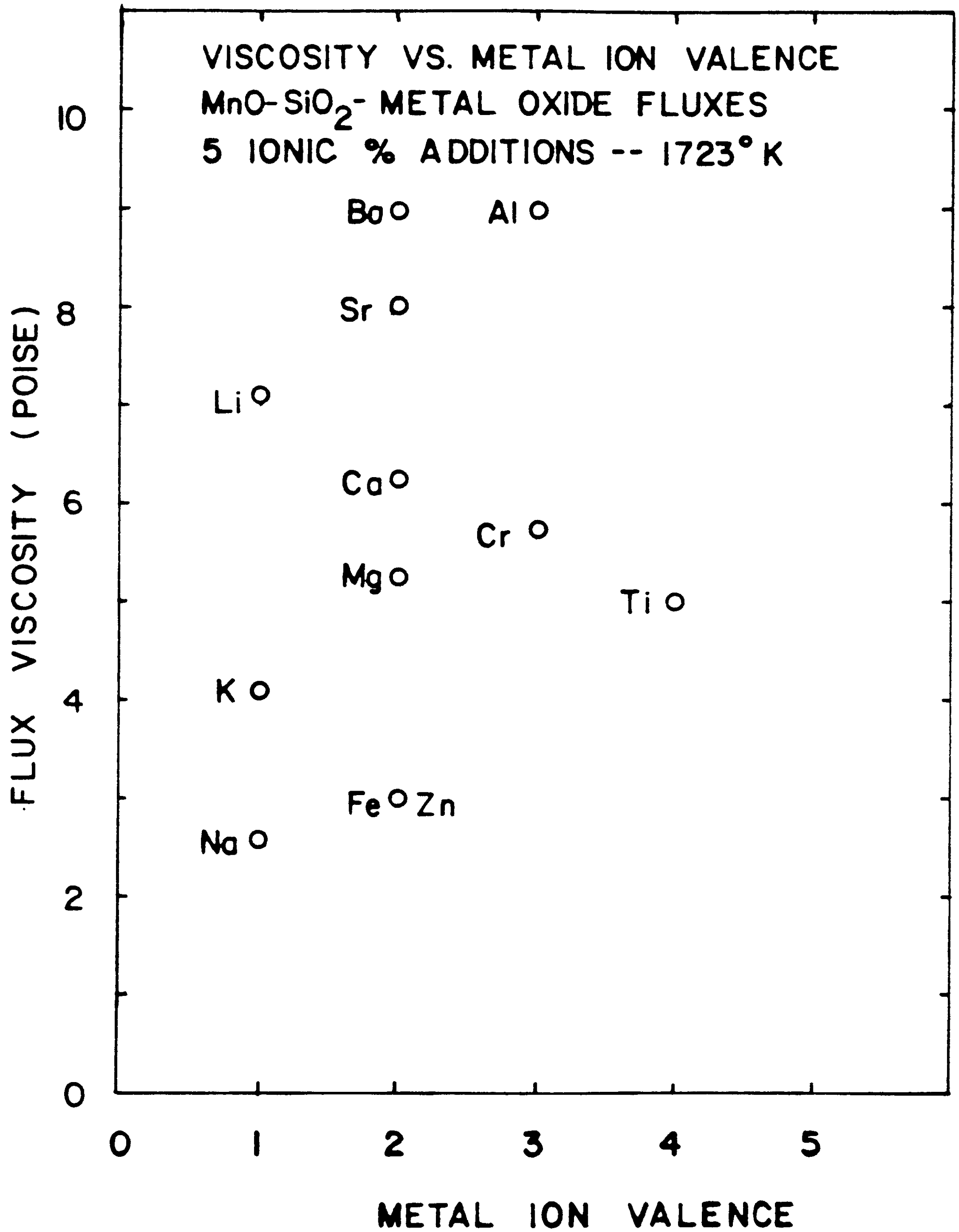

Fig. 17. Flux viscosity at 1723°K vs. valence of the added metal ion for 5 ionic % additions.

producing sufficient thermal energy so as to be useful for the joining of metals by fusion."

Welding arcs are high-current, low-voltage electrical discharges. They may be separated into several types according to the welding process: consumable electrode arcs such as those in gas-metal arc welding (GMAW), shielded-metal arc ("stick") welding, and submerged arc welding (SAW); or non-consumable electrode arcs such as are found in gas-tungsten arc welding (GTAW). Arcs also vary with regard to polarity and current type: some are run with straight polarity (the electrode is made the cathode). Both AC and DC current are used in welding--in multiple-wire submerged arc welding both are often used simultaneously. Polarity setting and current type are dictated by the welding process and the desired results.[30] Direct current and reverse polarity were used to make the welds for this investigation.

The arc itself (often called the plasma) contains ions from the flux, the atmosphere, the electrode and the base metal, and electrons from these ions as well as from the cathode. There are also flux and metal droplets and vapors to be found as well as highly excited gas atoms and molecules.[31] The electrons, which flow from cathode to anode, are responsible for current conduction. They are much more mobile than larger ions and are thus much better charge conductors.

The arc can be divided into several zones: the cathode region where electrons enter the arc; the plasma region; and the anode region, where electrons leave the arc. There are voltage drops associated with each of these zones. Figure 18 shows a schematic of the zones of an arc and their associated voltage drops. The anode and cathode regions of the arc are about 10^{-2} mm in length, and the plasma region may vary between 1-3 mm in length.[31] Concentrations of charge carriers are greater in the anode and cathode regions. The thermal and voltage gradients are also greater

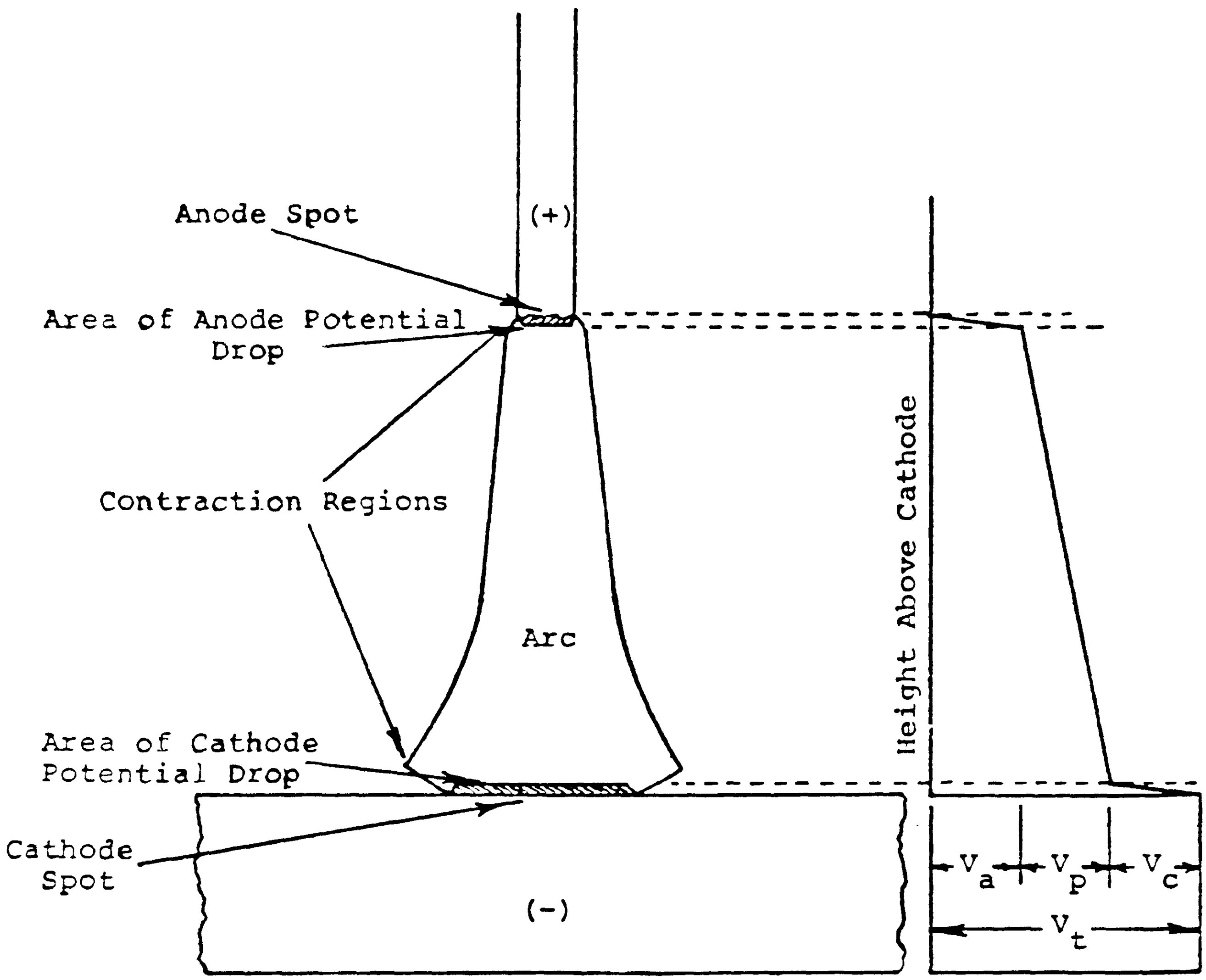

Fig. 18. Typical zones of a welding arc with the associated voltage distributions.

in these zones. These gradients dictate the energy given off in any one region of the arc.[32] Thus, most of the heat of the arc is generated in these two zones. The relative energy levels of these two zones vary with the welding process. In submerged arc welding more heat is generated at the cathode.[30] For this reason, deeper penetration can be achieved using reverse polarity (cathode workpiece) with this process. Interestingly enough, in the GTAW process, more heat is generated at the anode.[30]

The areas where the arc column contacts the workpiece and the electrode are known as the cathode and anode spots (for reverse polarity), respectively. These areas affect the shape of the arc. The cathode spot is especially important because it determines the current density, and thus, the heat input, at the work surface. A small cathode spot will give a greater current density and heat input to the work which will result in deeper weld penetration. This means that any factor, e.g., impurity element concentrations, which increases the cathode spot size will result in a loss of penetration. Such an effect has been observed by several investigators.[33,34] Bennett and Mills,[33] in a study of the weldability of high-manganese stainless steels, linked a decrease in weld penetration to very slight increases (on the order of parts per million) in the aluminum content of the base alloy.

B. Arc Stability

The term arc stability (or instability) has been used in several ways. Spraragen and Claussen[42] defined it as a ratio of a given arc length to the maximum distance over which an arc can be supported. This definition may be useful in processes where the arc can be directly observed, but its applicability to the submerged arc process is limited. A more pertinent measure of this stability has been used in all CSM flux research. Arc stability, for our purposes, is the average voltage fluctuation of the arc from the set machine voltage. This fluctuation is greater in less stable arcs.

Proper arc stability is important to weld quality. A decrease in stability lowers the average heat input to the work which in turn results in decresed and often irregular weld penetration. This effect has been observed by CSM investigators.[15,17-19] Figure 19 shows the effect of arc stability on penetration in welds made on 4340 steel using MnO-SiO_2-CaF_2 flux.

This stability also affects the ease of arc ignition and maintenance during moderate changes in gap length.

C. Factors Influencing Arc Stability

The stability of any welding arc is strongly affected by the components found in the plasma. Some work on the effects of different compounds on arc stability has been done[15,17-19,35,36] but until recently most of it was done using single component fluxes[35,36] so that the results are not always applicable to present work. The early workers[35,36] reported that compounds of easily ionized elements, e.g., alkali and alkaline earth oxides, provided better arc stability than did compounds ionized with greater difficulty, e.g., SiO_2, $A\ell_2O_3$, etc. They also found that compounds with ionization energies similar to that of the base metal such as FeO and MnO has little effect on the arc. Table 13 gives the ionization potentials for some elements commonly associated with steels.

From the early results it appears as though the ionization potentials of species around the arc control its stability. More recent investigators have found similar results for more complex ternary fluxes. Ferrera and Olson[15] found that calcium (ionization potential 6.11 volts) oxide additions to manganese silicate

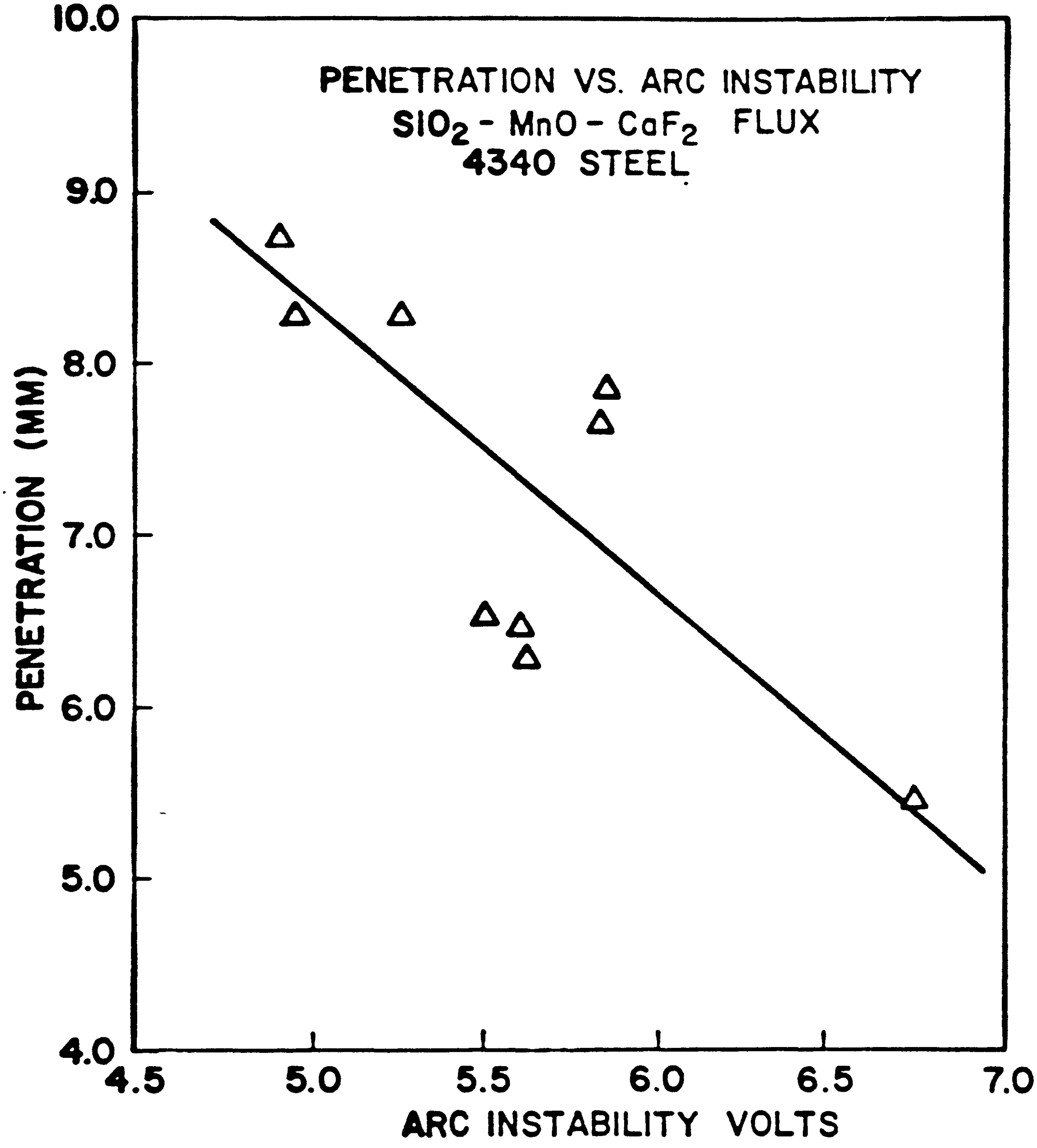

Fig. 19. Penetration vs. arc stability, MnO-SiO_2-CaF_2 flux, 4340 steel[17].

TABLE 13

FIRST IONIZATION POTENTIALS FOR SOME COMMON ELEMENTS[34]

Element	Ionization Potential, eV
Iron	7.87
Carbon	11.265
Manganese	7.432
Silicon	8.149
Chromium	6.74
Nickel	7.633
Molydenium	7.10
Vanadium	6.74
Phosphorus	10.487
Sulphur	10.375

fluxes had a strong stabilizing effect on the welding arc. This is shown in Figure 20 for 1020 steel. Schwemmer[18] observed a similar but much milder stabilizing effect from FeO additions to $MnO-SiO_2$ fluxes when welding 1020 steel. But he obtained very surprising results when such fluxes were used to weld 4340 steel. Additions of up to 10% FeO disrupted arc stability; further additions then stabilized the arc. Figure 21 shows these results. The arc stability function for 4340 steel is presumably complicated by the presence of the alloying agents Cr, Mo, and Ni.

The above examples support the findings of early workers, i.e., that ionization, potential determines a flux component's effect on arc stability. But recent work by Carmona[19] has shown that the situation is not that simple. Figure 22 shows arc stability as a function of the ionization potential of alkaline earth and transition element additions to $MnO-SiO_2$ fluxes. Not only does the arc become more stable as the ionization potentials of additions increase, but even zinc, which has a potential of 9.39 volts (greater than that of the base metal iron) stabilizes the arc. Also, barium and strontium additions to the flux made the arc less stable, even though their ionization potentials are less than that of iron.

In his studies on the effects of CaO and CaF_2 additions to $MnO-SiO_2$ fluxes, Janzen[17] found that welding arcs on 4340 steel were more stable than those on 1020 steel. Figure 23 shows arc stability for these steels as a function of flux calcium content. The difference between the two is due to the alloying agents in the 4340 steel. The reason for this behavior is not certain, it is quite possible that the alloying agents lower the thermionic work function of the base metal and make electrical conduction through the arc less difficult, thereby stabilizing it.

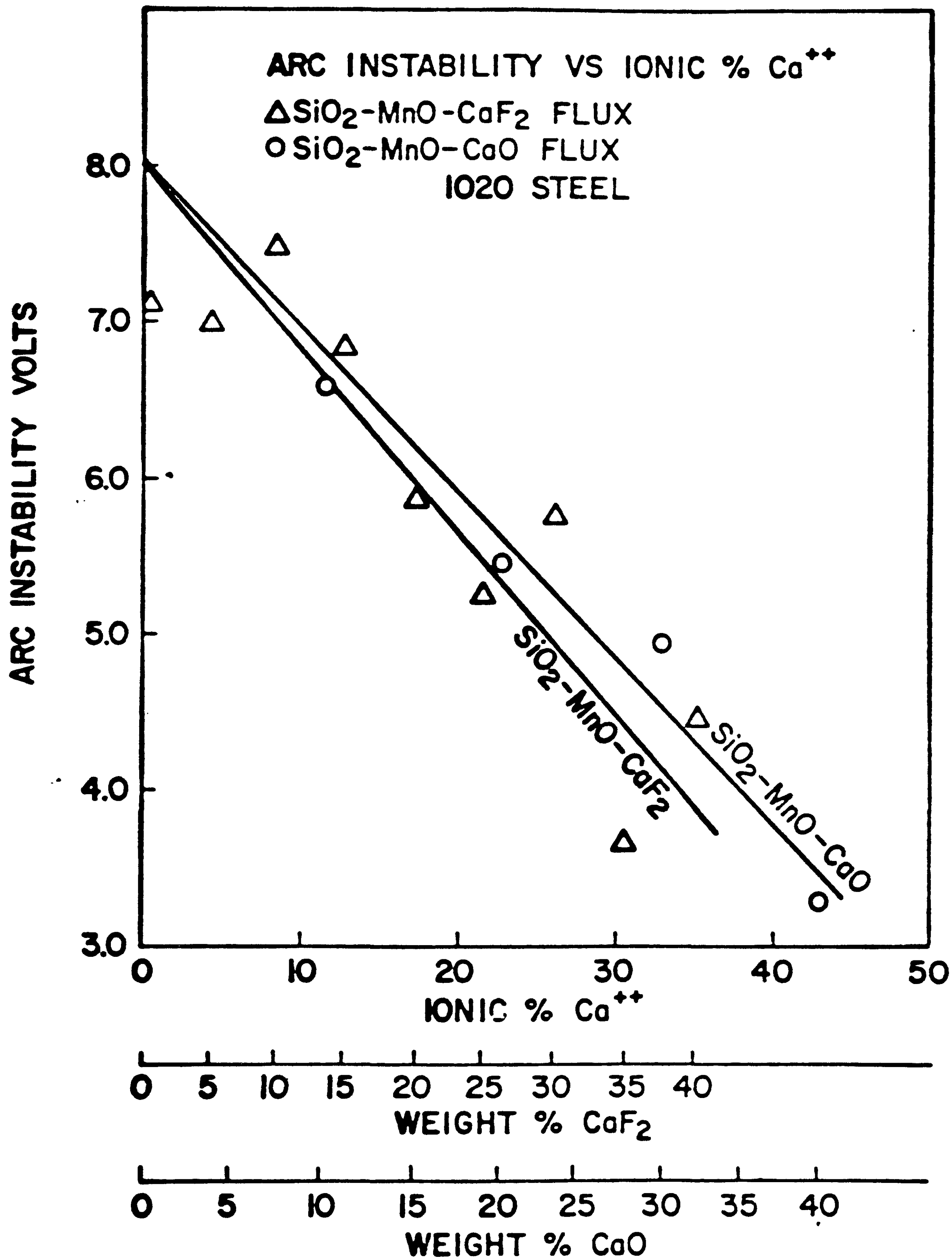

Fig. 20. Arc stability vs. calcium content of $MnO-SiO_2-CaO$ and $MnO-SiO_2-CaF_2$ fluxes, 1020 steel[15].

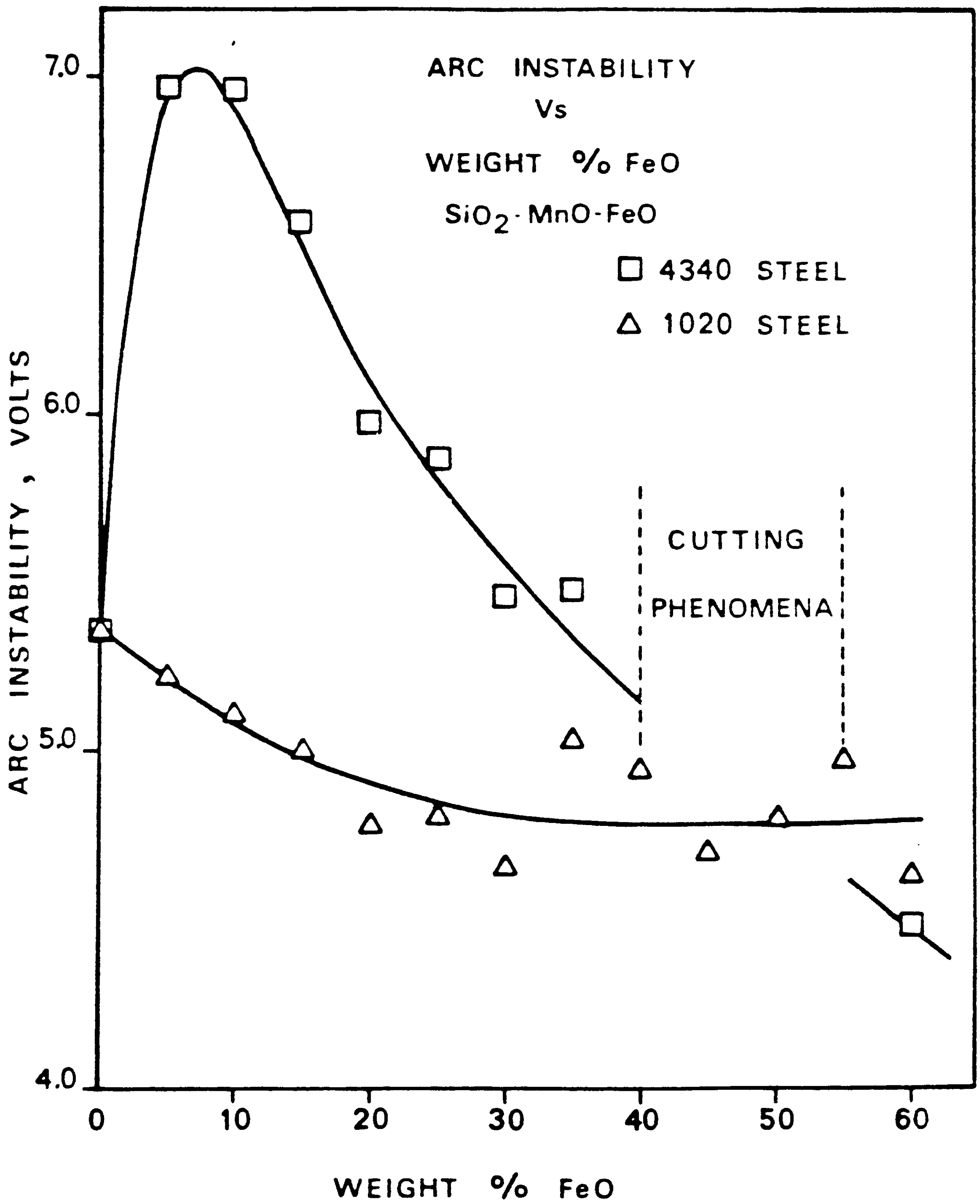

Fig. 21. Arc stability vs. wt. % FeO in $MnO-SiO_2-FeO$ fluxes, 1020 and 4340 steels[18].

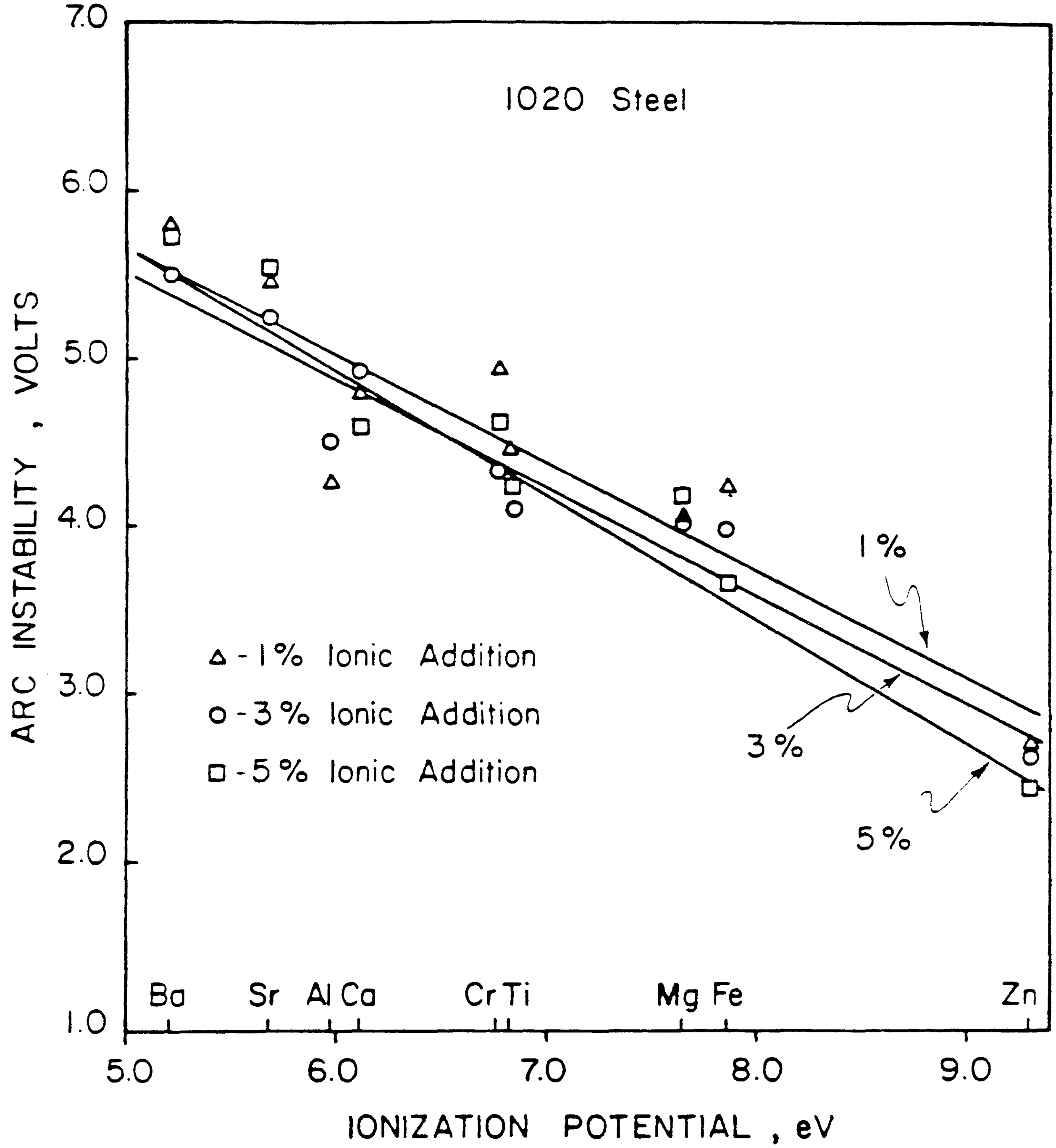

Fig. 22. Arc stability as a function of ionization potential of the alkaline earth and transition metal ionic additions to a $MnO-SiO_2$ welding flux system[19].

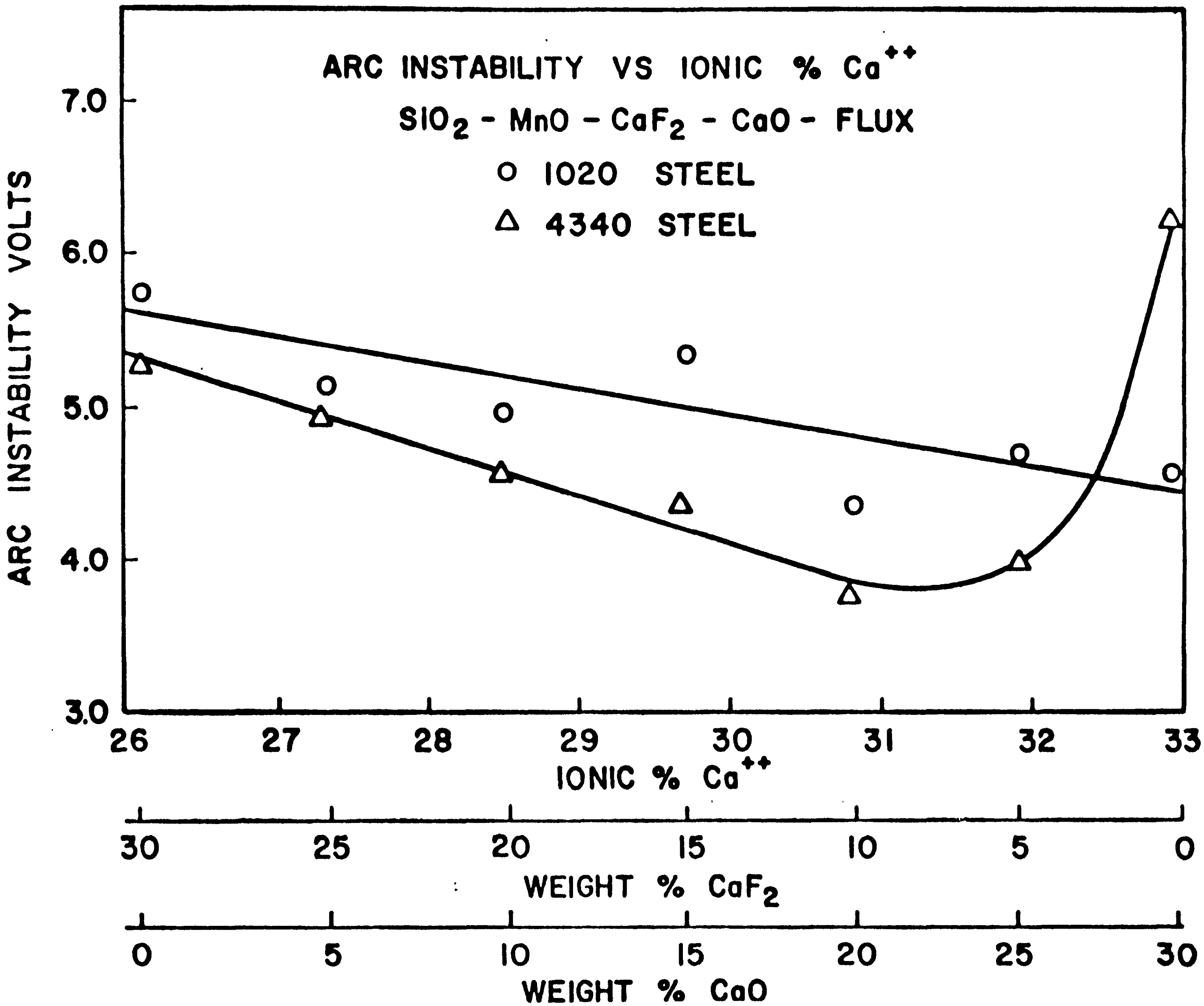

Fig. 23. Arc instability vs. ionic % Ca^{++} in SiO-MnO-CaO-CaF_2 flux for both 1020 and 4340 steel[17].

D. Experimental Procedures

1. Submerged Arc Welding

This process is one in which an arc is struck between the workpiece and a continuously-fed filler wire. Its distinctive feature is the fact that the arc is covered with a layer of protective granular flux. Wire fed down through the flux is melted by heat from the arc. Flux granules surrounding the arc are also melted, and this forms a molten flux layer which covers the weld puddle and protects it from the atmosphere. Figure 24 is a schematic cutaway of the submerged arc process.

Submerged arc welding is an automatic process; all the operator does is adjust the machine controls. A constant voltage power supply is employed, and current is controlled by the wire feed rate. The wire feeder and flux hopper ride on a stationary track. These arrangements make it possible to maintain constant arc length, flux depth, horizontal travel speed, electrode melting rate, voltage current, etc. Weld reproducibility is thus much improved since most operator-related variables are eliminated. This makes the submerged arc process a good research tool. Figure 25 shows a photograph of the welding equipment used in this investigation.

All welds were made using reverse polarity direct current set at 30 volts. The wire speed was adjusted to maintain the current at 500 amps, and the horizontal travel speed was 18.9 inches per minute. These parameters are also listed in Table 14.

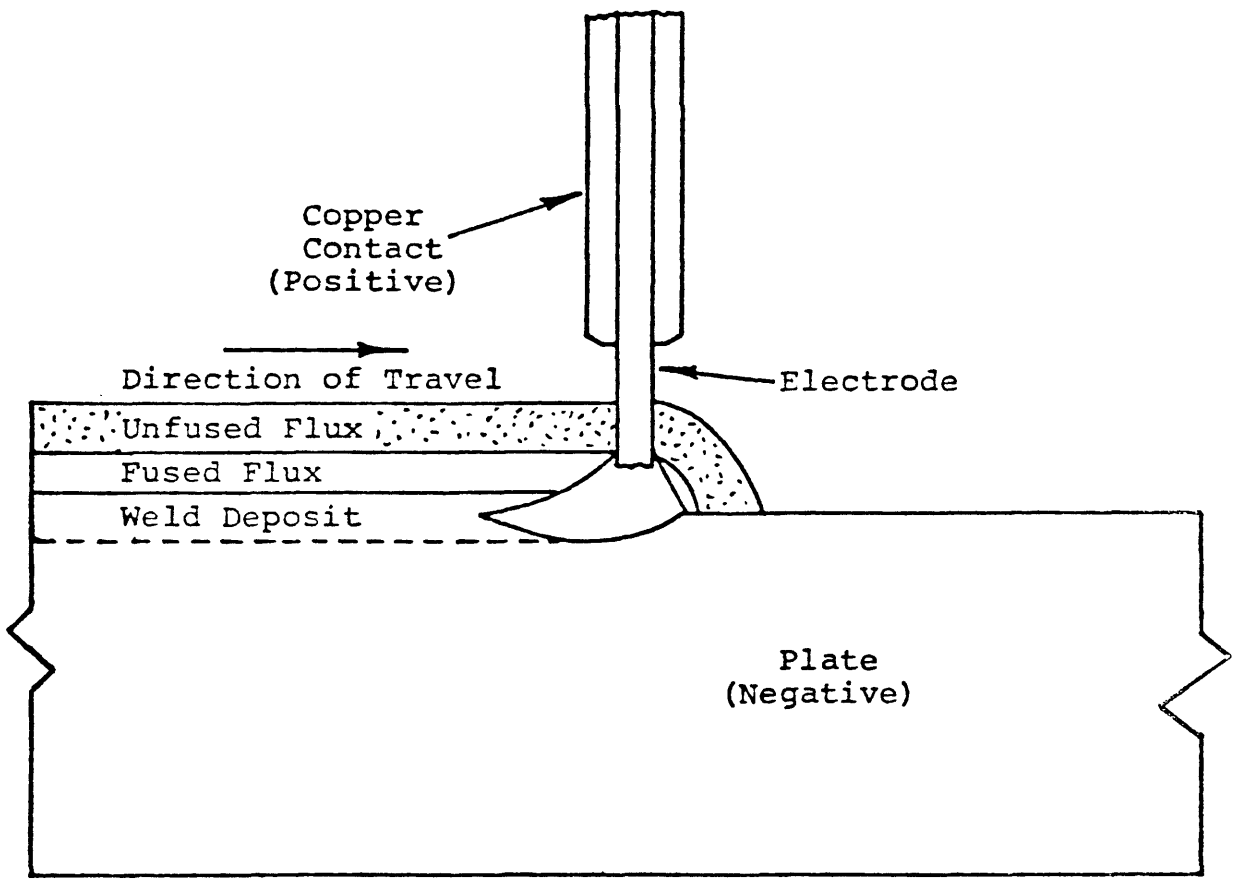

Fig. 24. Schematic cutaway drawing of the submerged arc welding process.

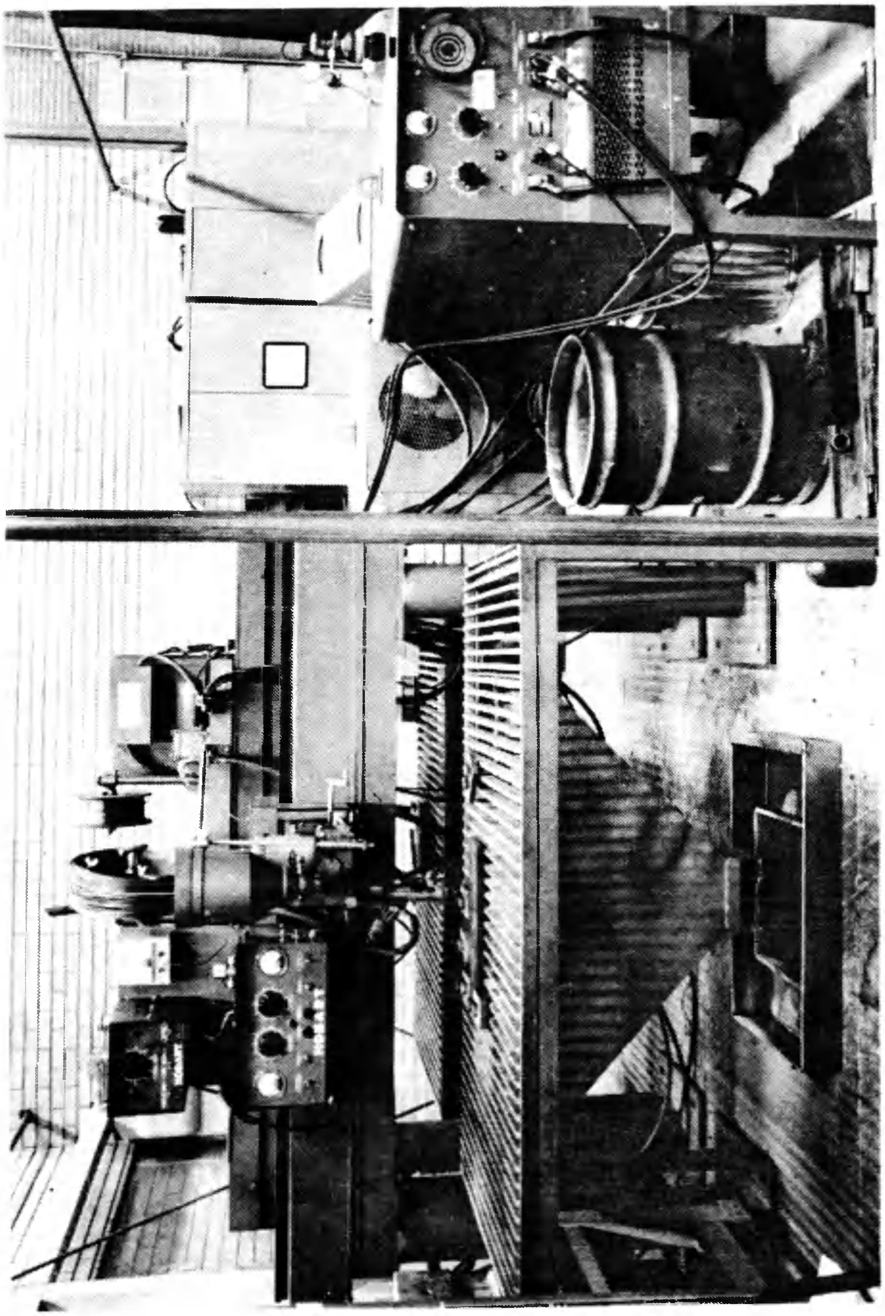

Fig. 25. Photograph of submerged arc welding equipment.

Voltage	30 Volts
Current	500 Amps
Travel Speed	0.48 m/min (18.9 in/min)
Wire Speed	Variable to Maintain 500 Amps
Heat Input	18.7×10^6 Joules/m (4.76×10^4 Joules/in)

TABLE 14 - Welding parameters used in this investigation.

2. Arc Stability Measurements

A Tektronix oscilloscope was used to maintain the arc voltage during welding. The instrument was set in the single sweep mode and a camera attached to the CRT screen recorded the voltage fluctuations used to measure arc stability. Figure 26 shows photographs of two such voltage traces. The vertical axis in the photos is voltage and the horizontal is time (seconds). The mean voltage fluctuaction was obtained by measuring the area of the voltage trace, converting this measurement from units of area to volt-seconds, and then dividing this number by the oscilloscope sweep time.[28] This mean fluctuation is used as a measure of arc stability. Two such oscillographs were taken during each weld and averaged together to get a more representative measure.

E. The Effects of Alkali Additions on Arc Stability

Figures 27 and 28 show the effect of alkali additions to the flux on the stability of welding arcs on 1020 and 4340 steels, respectively. Note that the stabilizing effect is more pronounced for 1020 steel. This indicates that the effects of the alloying agents in 4340 steel play such a dominant role in stabilizing the arc that the alkali ions have less effect. A close scrutiny of Figures 27 and 28 also reveal that arc on 4340 steel are more stable--in agreement with the results of Janzen[17] for the MnO-SiO_2-CaO/CaF_2 flux systems (see Figure 23).

Figures 29 and 30 show how the alkali ionization potentials affect arc stability for welds on 1020 and 4340 steels, respectively. The results for 1020 steel are not all consistent. For 1 and 3 ionic % additions the arc grows less stable with increasing ionization potential; greater additions increase stability. The reason for this trend reversal is not apparent, but Figure 27 may provide an answer. It shows that arc from welds made with low

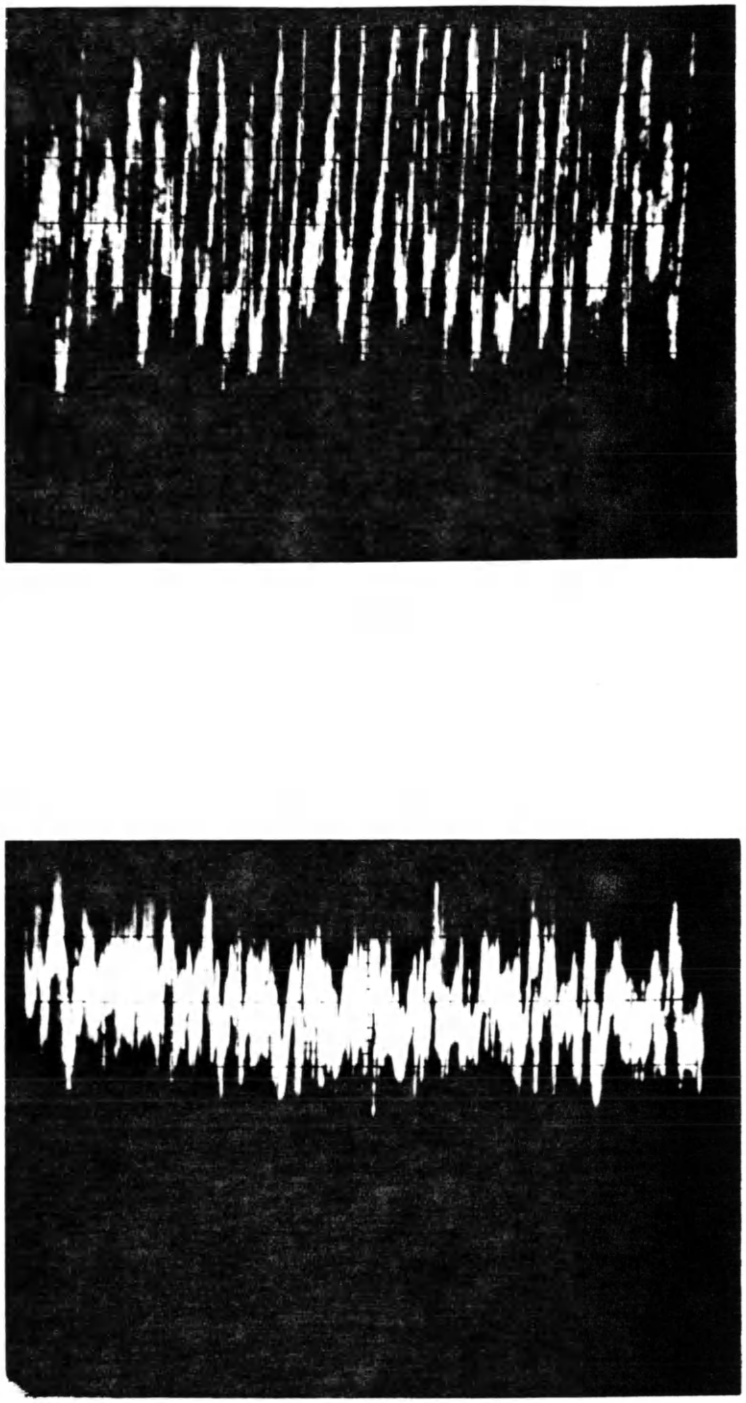

Fig. 26. Two arc voltage oscillographs used to measure arc stability.

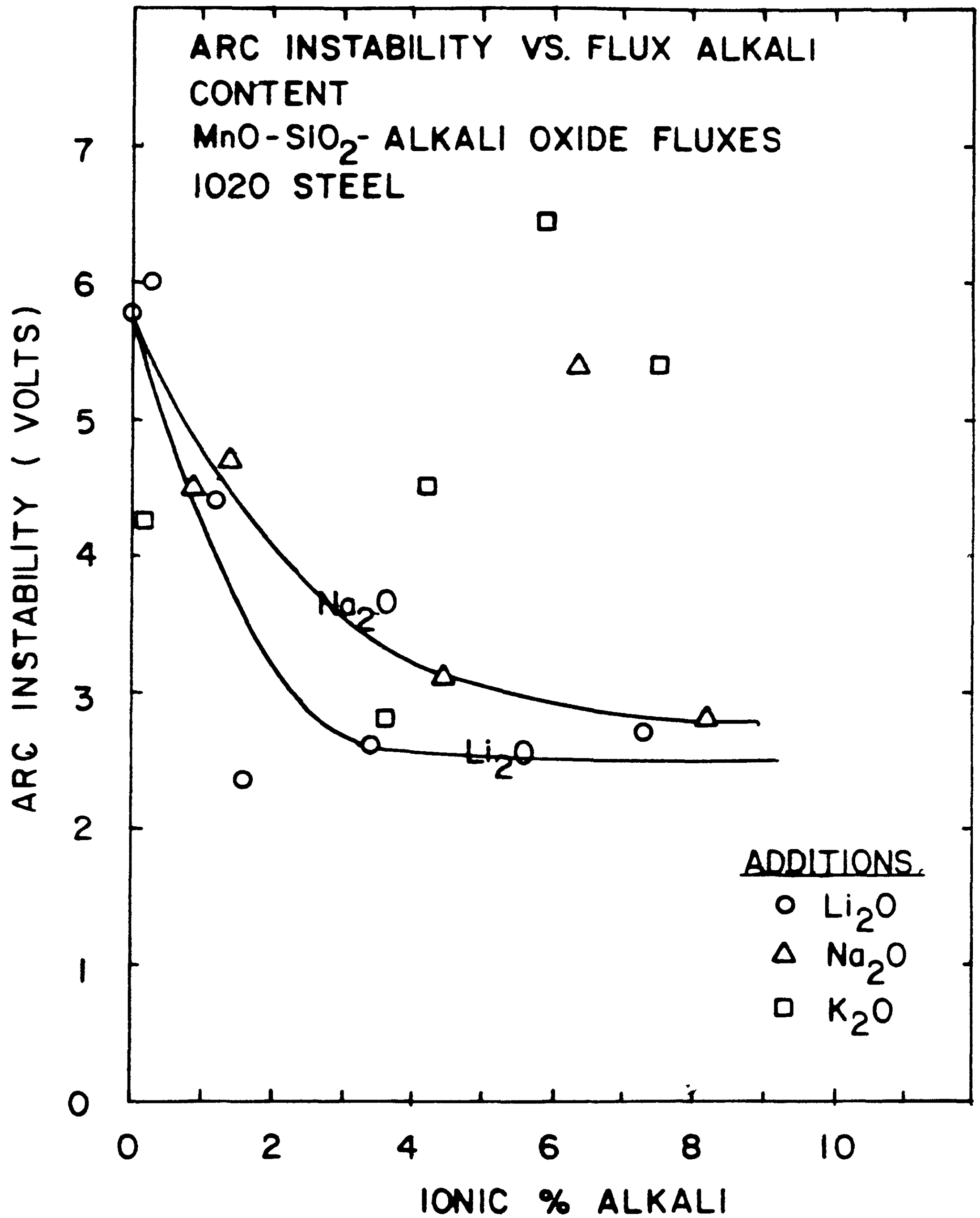

Fig. 27. Arc stability vs. $MnO-SiO_2$ flux alkali content, 1020 steel.

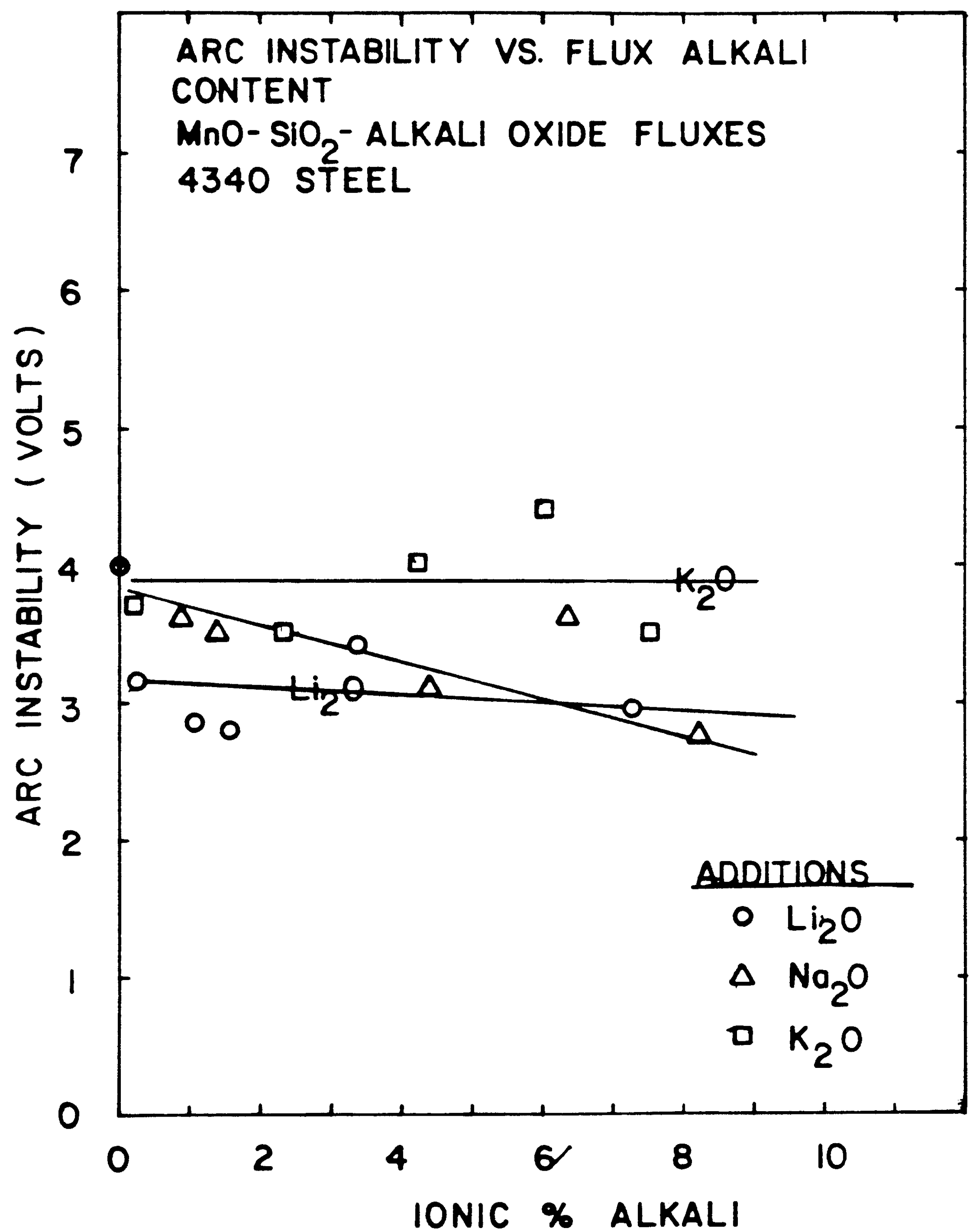

Fig. 28. Arc stability vs. $MnO-SiO_2$ flux alkali content, 4340 steel.

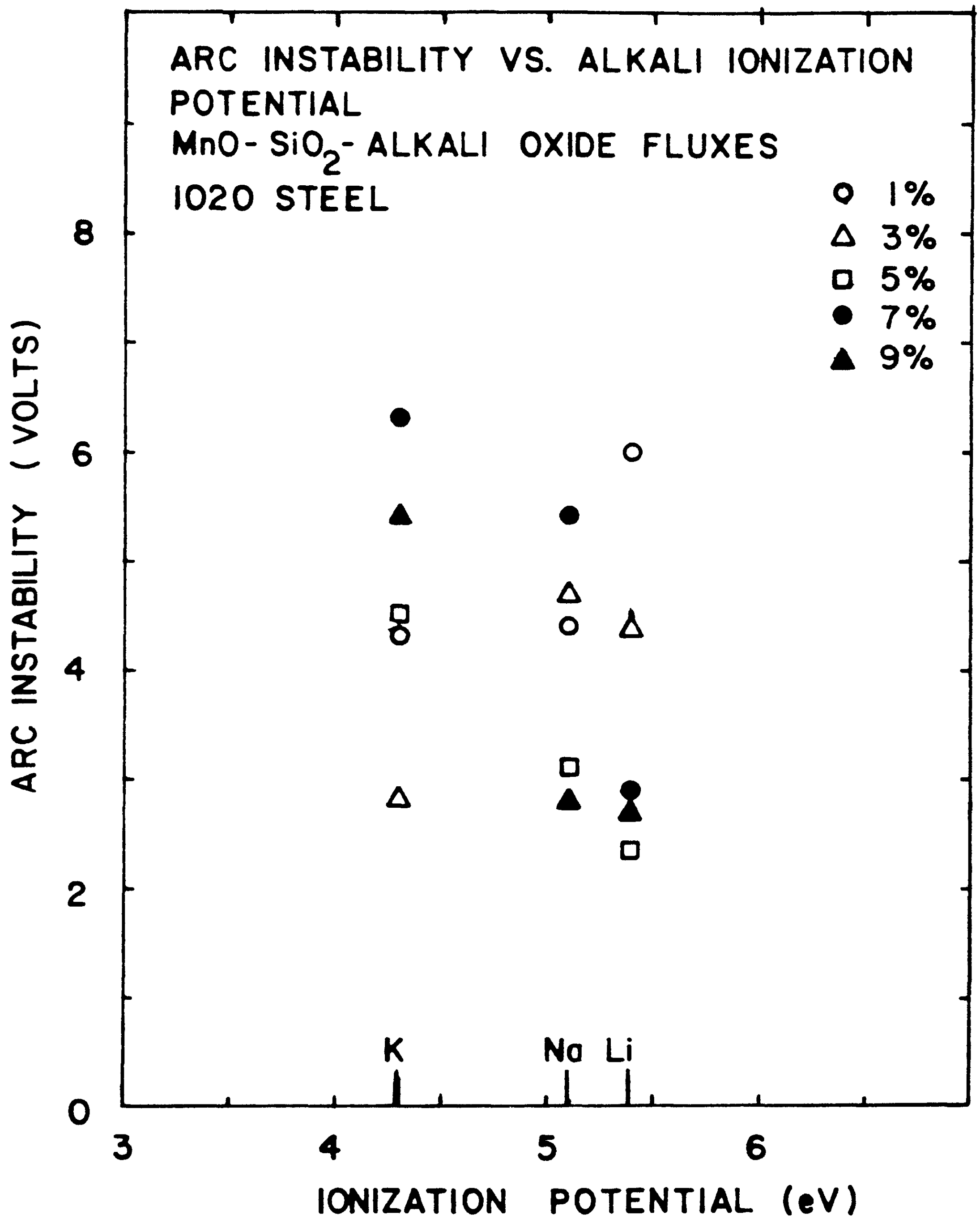

Fig. 29. Arc stability vs. alkali ionization potential, 1020 steel.

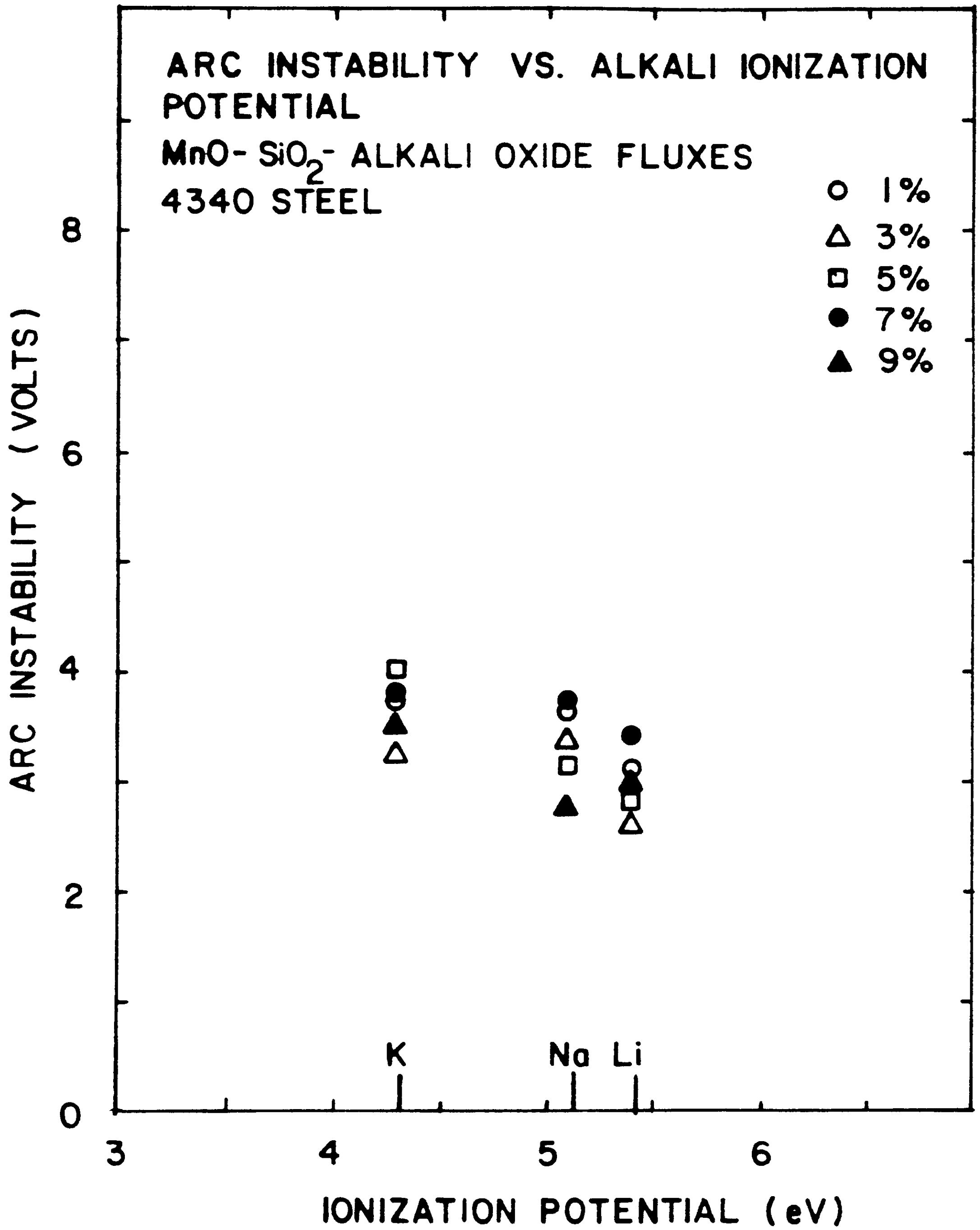

Fig. 30. Arc stability vs. alkali ionization potential, 4340 steel.

alkali fluxes are relatively unstable. Data scatter tends to be greater for less stable welding arcs (compare Figures 27 and 28), so it can be argued that low arc stability may be masking the effect of ionization potential. In the case of 4340 steel, the arc stability increases slightly with increasing alkali ionization potential. This result agrees with the results of Carmona.[19]

V. THE EFFECTS OF CAPILLARITY ON WELD BEAD MORPHOLOGY

A. Background

Three phases exist in a submerged arc weld while it is in progress: solid parent metal, molten weld metal, and molten flux. There is a surface tension associated with each interface, and these tensions can have a powerful effect on the shape of the weld bead.

The morphology of a weld bead refers to its physical shape. Certain dimensions are usually measured to describe the shape of a bead. Figure 31a is a schematic cross-section of a bead-on-plate weld showing the important dimensions--the bead width, the depth of penetration, and the interfacial angles α and β. The depth of penetration is measured from the plate surface to the lowest point in the fusion zone. The width-to-depth ratio (W/D) is a popular means of describing the overall shape of a weld bead. A low ratio indicates a narrow bead with deep penetration, and a high ratio indicates a relatively wide, shallow bead. The two angles α and β are useful if one is interested in determining the relative strengths of the interfacial tensions.

There are many factors which can affect weld bead morphology. Some are related to the welding machine parameters and other to the flux. Still other factors can be brought in if one considers

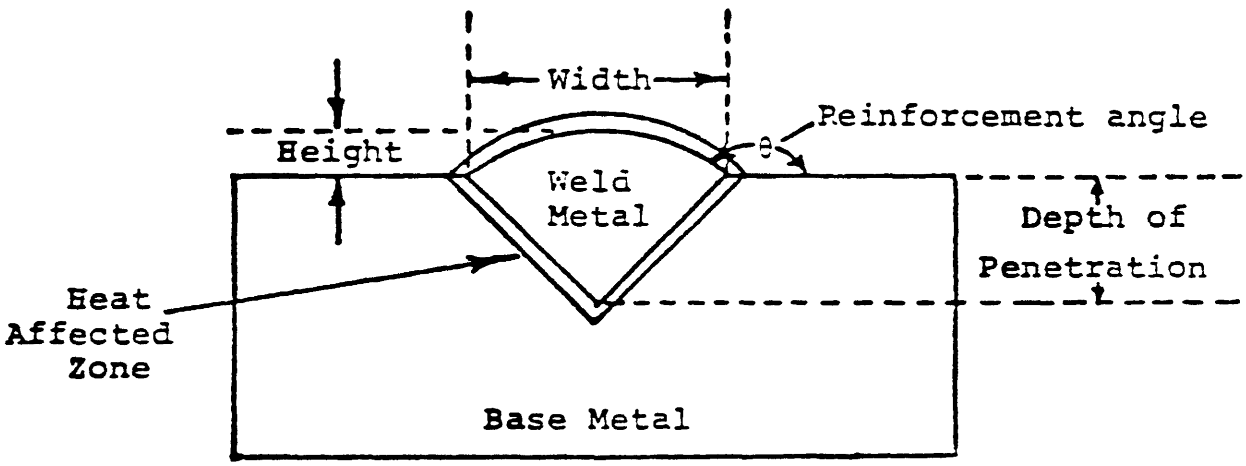

Fig. 31a. Schematic drawing of cross-section of a bead-on-plate weld.

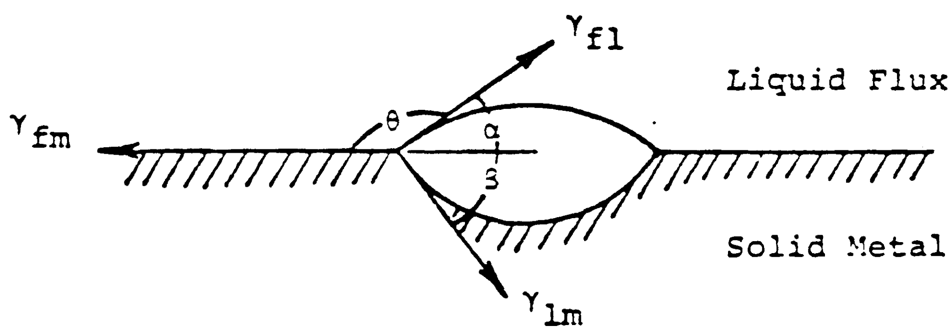

Fig. 31b. Schematic drawing of the interfacial tension balance at the toe of a weld bead.

the thickness and geometry of the workpiece and the type of alloy being welded, but these will not be discussed here.

Welding machine parameters--especially current, voltage and travel speed--are among the most important factors which influence bead morphology. Welding current is controlled by wire feed rate in the submerged arc process. Current thus controls the electrode melting rate, the depth of penetration, and the amount of parent metal melted.[37] Welding voltage, on the other hand, has less effect on the deposition rate, but it affects the heat distribution at the workpiece and thus affects bead shape and penetration. Excessive voltage results in a wider, flatter weld bead with shallow penetration. Weld travel speed affects heat input and the quantity of metal deposited per unit length of weld; penetration decreases with increasing travel speed.

An equation relating weld penetration to these three machine parameters has been developed by Jackson and Shrubsall.[38]

$$\text{Penetration} = K(I^4/SE^2)^{1/3}$$

where K is a constant related to the flux and base metal composition and the welding process, I is current, S is travel speed, and E is the welding voltage. This equation agrees with the general observations made in this section concerning the effect of machine parameters on weld penetration.

Flux composition also affects weld bead morphology since it controls viscosity, arc stability and capillarity. The effects of viscosity and arc stability on penetration have already been discussed; the effects of interfacial tensions will be discussed shortly.

B. The Role of Interfacial Tensions

Several authorities, notably Wassink[39] and Hazlett,[40] have proposed that welding can be treated as a wetting phenomenon which is controlled by interfacial tensions. Hazlett[40] proposed the use of an equilibrium force balance at the triple point phase boundary (at the weld toe) to explain how surface tensions affect bead morphology. Figure 31b shows a shematic of such a force balance. The three controlling tensions are the flux-liquid metal interfacial tension γ_{FL}, the flux solid metal tension γ_{FM}, and the solid metal-liquid metal (fusion line) tension γ_{LM}. Thus, we have a situation involving three variables and two equations, the horizontal and vertical force balances. If we assume the fusion line tension term γ_{LM} to be constant, then the relative strengths of the other two terms γ_{FL} and γ_{FM} can be calculated. The horizontal and vertical balances, respectively, for the schematic weld in Figure 31 are:

horizontal direction: $$\gamma_{FM} = \gamma_{FL} \cos \alpha + \gamma_{LM} \cos \beta \ . \ . \ . \qquad \text{(Eq. 1)}$$

vertical direction: $$\gamma_{FL} \sin \alpha = \gamma_{LM} \sin \beta \ . \ . \ . \qquad \text{(Eq. 2)}$$

Solving Eq. 2 for γ_{FL}, substituting this expression into Eq. 1, and dividing through by γ_{LM}, gives

$$\frac{\gamma_{FM}}{\gamma_{LM}} = \frac{\sin \beta \cos \alpha}{\sin \beta} + \cos \beta \ . \ . \ . \qquad \text{(Eq. 3)}$$

From Eq. 2 we can also see that

$$\frac{\gamma_{FL}}{\gamma_{LM}} = \frac{\sin \beta}{\sin \alpha} \ . \ . \ . \qquad \text{(Eq. 4)}$$

Eqs. 3 and 4 are useful in that the relative values for γ_{FM} and γ_{FL} can be calculated from measurements of the angles α and β taken from cross-sectional weld bead specimens. The measurement of absolute surface tensions for molten slags and fluxes on solid and liquid metals is extremely difficult work, and for our purposes the relative values are sufficient.

The assumption that γ_{LM} is constant is a valid one if the filler and base metal compositions do not change and if variations in flux composition have no effect on γ_{LM}.

As was mentioned, welding can be treated as a wetting process. If molten weld metal wets the solid plate, the bead will spread out over it. Wetting will occur if γ_{FM} is relatively large (refer to Figure 31). From Eq. 1 we can see that wetting will occur if

$$\gamma_{FM} > \gamma_{FL} \cos \alpha + \gamma_{LM} \cos \beta$$

Since much of the heat of the weld pool is transfereed to the solid plate, the contact area between the two has an effect on penetration. Heat will be more widely distributed if this contact area is increased by wetting, and this will decrease penetration. Thus, weld penetration should decrease as the value of γ_{FM} increases.

On the other hand, if γ_{FL} is relatively strong, wetting will occur to a lesser degree because of the tendency for the flux-liquid metal interface to minimize its area. As a result, the solid plate-weld pool contact area will be smaller and the concentration of heat in a smaller volume of metal will give greater penetration. So, weld penetration should increase with increasing values of γ_{FL} if all other factors are held constant.

C. Compositional Effects on Interfacial Tensions

Interfacial tensions are the result of imbalances of molecular forces at a boundary between two phases. These imbalances create excess energy at such an interface. This energy is called the specific surface energy and can be expressed by the equation[32]

$$\sigma = \gamma + \Sigma\, u_i \Gamma_i$$

where γ is the surface tension, u_i is the chemical potential of the i^{th} species, and Γ_i is the excess surface quantity of the i^{th} species. Surface tension is defined as the amount of work necessary to create a unit of surface area. The second term in the above expression is the contribution of solutes toward reducing the surface energy σ.

The compositional dependence of an interfacial tension between two phases can be expressed by differentiating the above equation to obtain

$$\frac{\partial \gamma}{\partial u_{i_T}} = \Gamma_i$$

This can be integrated and rearranged to give[32]

$$\Delta\gamma = RT \int \Gamma_i \; d \; \ell n \; a;$$

This last expression indicates that changes in surface tensions can be related to changes in the activities of different components in a system.

Work done on the surface tensions of molten metals has shown that very small compositional variations can cause large changes in the surface tension of iron.[41] Figure 32 shows the affects of

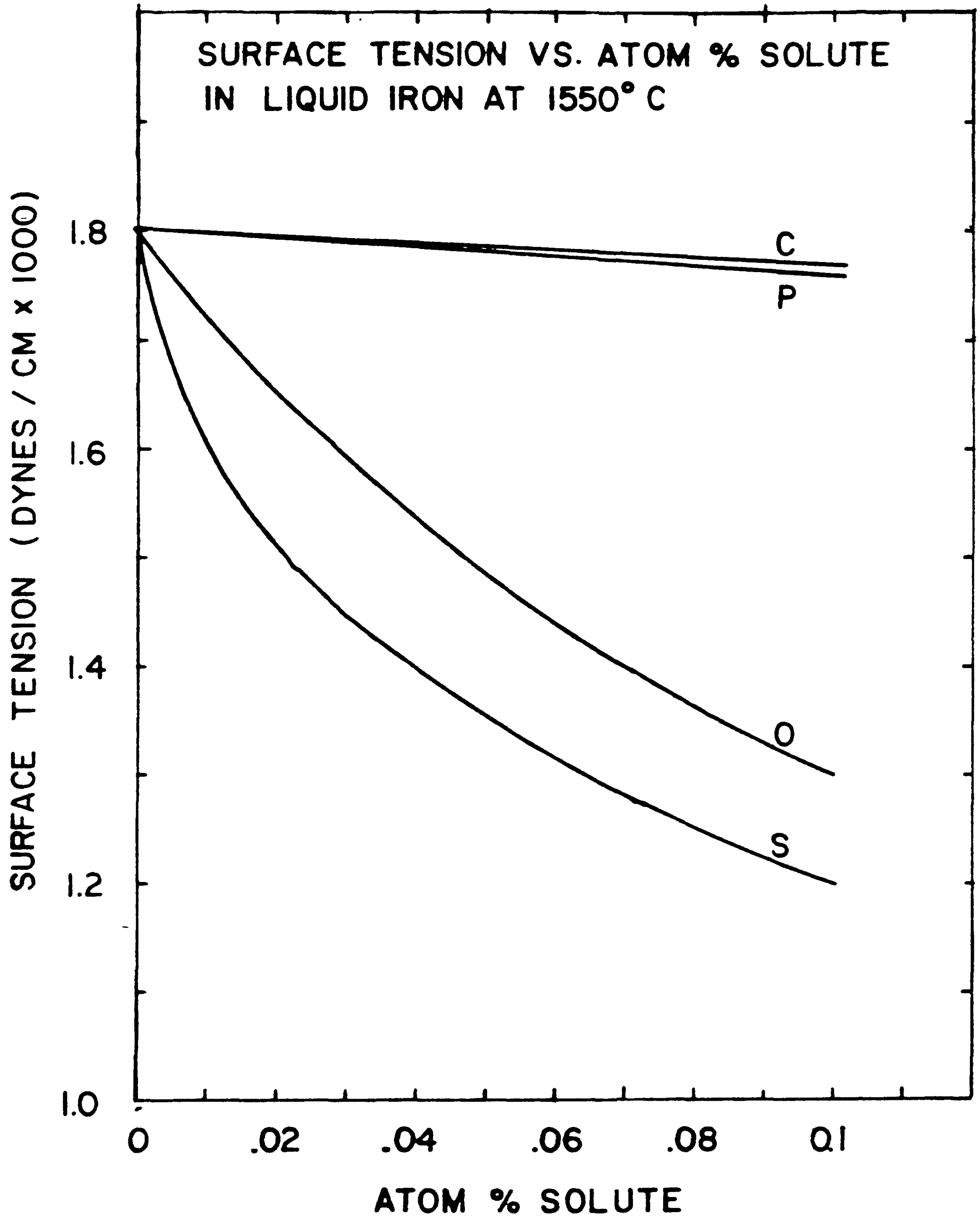

Fig. 32. Surface tensions for solutions of C, P, O, and S in liquid iron at 1550°C.

some solutes on the surface tension of iron at 1550°C.[41] Note that oxygen and sulfur have a stronger effect than carbon phosphorous. The former tow elements are said to segregate to surfaces and interfaces. For this reason it takes but a few hundredths of one percent of such elements to bring about drastic changes in surface tension. The latter two elements are not as prone to surface activity and thus have less effect. Similar observations have been made for solutes in other liquid metals.[23]

The surface tensions of slags and fluxes exhibit behavior similar to those of liquid metals, i.e., some species in solution tend to be more surface active than others. Figure 33 shows surface tensions of some liquid binary silicates as a function of silica content.[41] It has been reported that sulfur and some fluoride compounds lower the surface tensions of some silicates, especially those containing alkaline earths.[23]

Relatively little is known about surface tensions at slag-metal interfaces, largely due to the very difficult nature of such experimental work. Some data has been published for silicate slags on liquid iron-carbon solutions, and the interfacial tension values were found to lie below those for molten metal and above those for the slag measured separately.[23]

D. Procedures for Measuring Interfacial Tensions

Weld specimens were cross-sectioned in at least two locations to obtain representative bead morphology measurements. All specimens were polished to 0.05-micron alumina fineness and etched in 2% nital. Low magnification (approx. 2x) photographs were taken of each weld bead to measure widths and depths of penetration. It was necessary to take higher magnification (35x) photomicrographs of the weld bead toe regions in order to obtain accurate

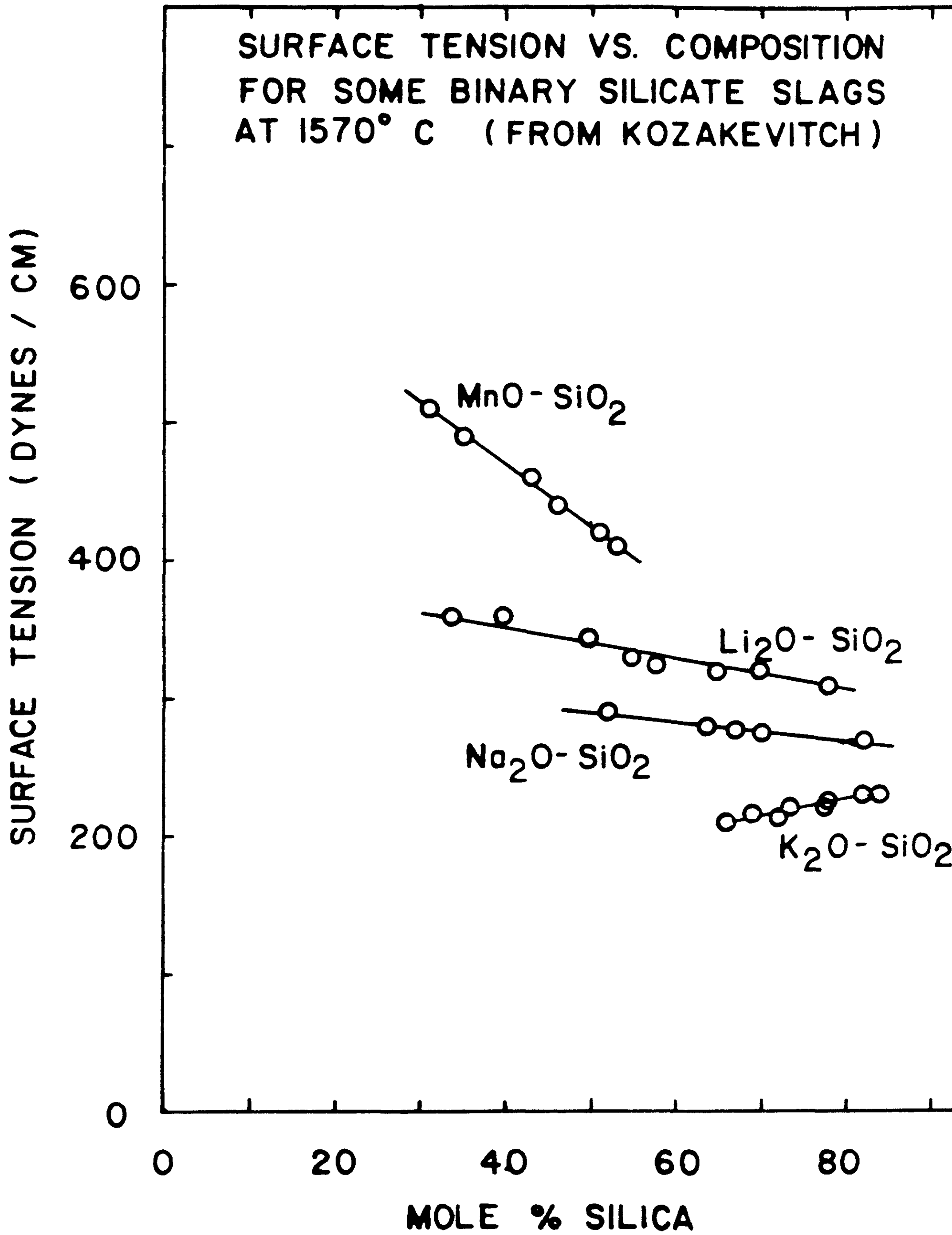

Fig. 33. Surface tensions of two binary silicates as a function of silica content[41].

measurements of the angles α and β. Values for the relative interfacial tensions γ_{FL} and γ_{FM} were then calculated from these measurements using Eqs. 3 and 4 found in Section B of this chapter. Figure 34 shows a photograph used to measure the weld bead contact angles α and β.

E. Experimental Results

Figures 35-37 are plots of penetration for 1020 steel welds as a function of the relative values of γ_{FM} and γ_{FL}. All three plots show that penetration increases with increasing γ_{FL} and decreases with increasing γ_{FM} in agreement with the work of Schwemmer.[18] It is interesing to note that the dependence of penetration on these interfacial tensions becomes sharper as the atomic number of the alkali addition increases. The reason for this trend is not known.

Figures 38-40 show the same plots for 4340 steel. In this case, only penetration in welds made with sodium-bearing fluxes shows the predicted behavior (see Figure 39). In Figure 38, penetration decreases with increasing γ_{FL}, exactly the opposite of the expected behavior. The results for welds made using potassium-bearing fluxes are similarly contrary.

The effect of flux composition on γ_{FL} and γ_{FM} for 1020 steel welds is shown in Figures 41-43. The value of γ_{FM} is not changed much except in the case of sodium-bearing fluxes which cause it to decrease considerably. The value of γ_{FL} increases slightly as the alkali content of lithium and sodium-bearing fluxes increases, but for potassium-bearing fluxes γ_{FL} appears to decrease to a minimum at about 3% potassium and then increase.

Figures 44-46 show the effects of flux composition on interfacial tensions for 4340 steel. The value of γ_{FM} appears to decrease

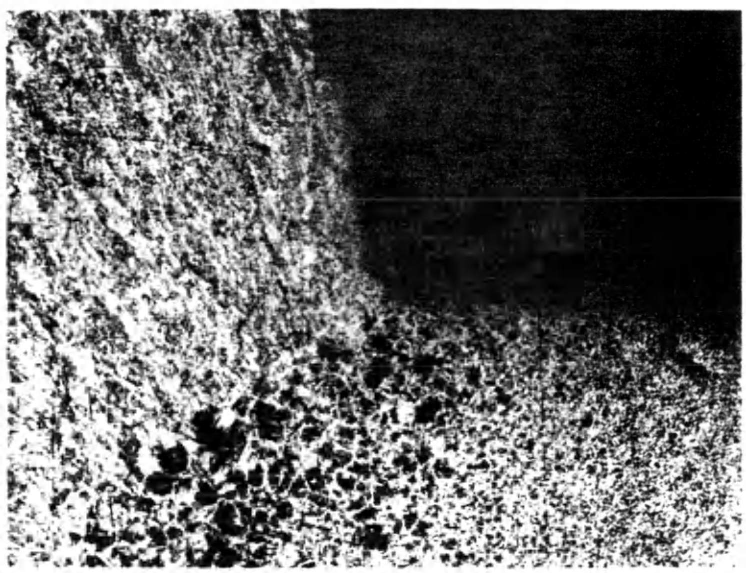

Fig. 34. Photomicrograph of a weld bead toe region used to measure the angles α and β.

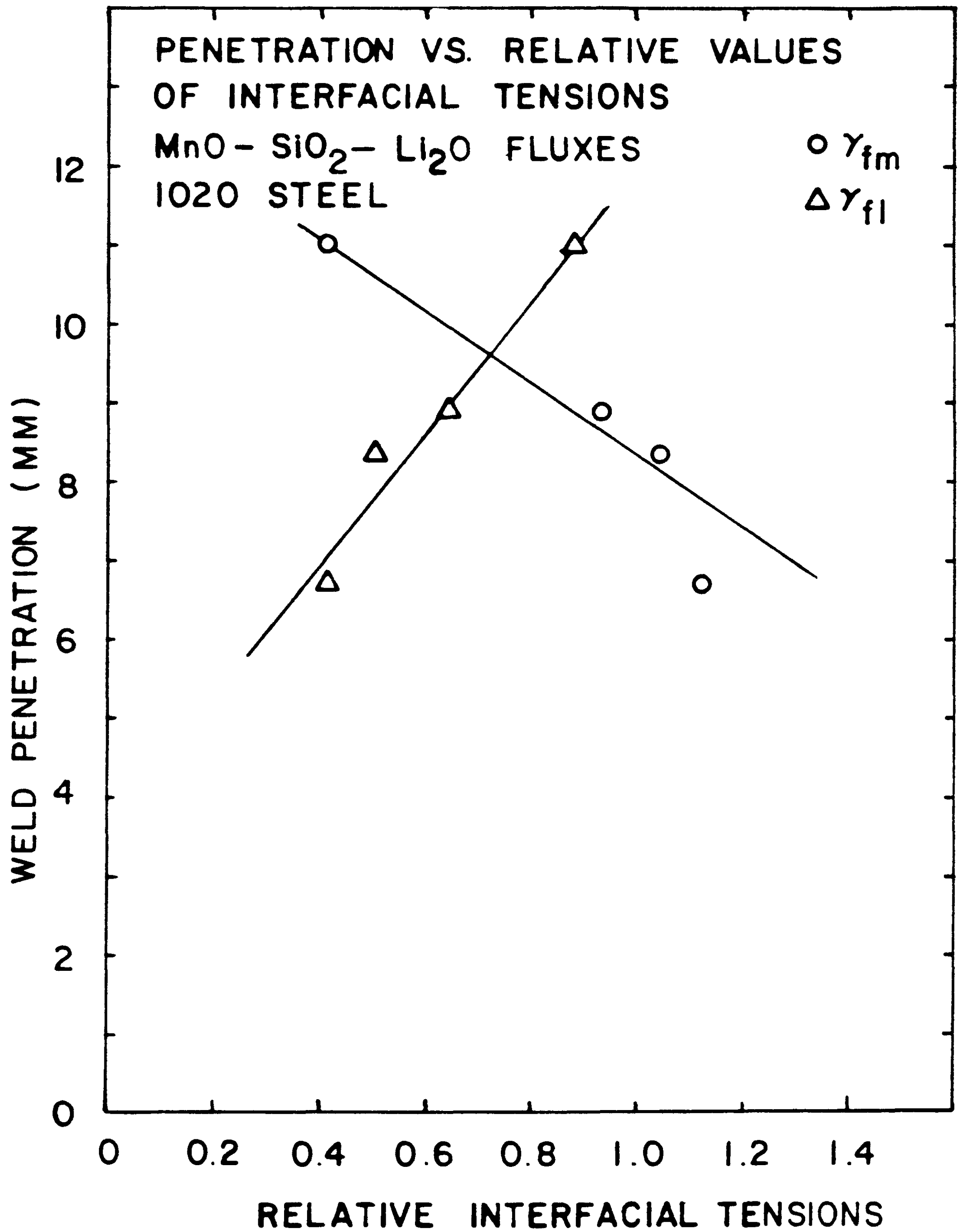

Fig. 35. Penetration vs. relative γ_{FL} and γ_{FM}, lithium additions to flux, 1020 steel.

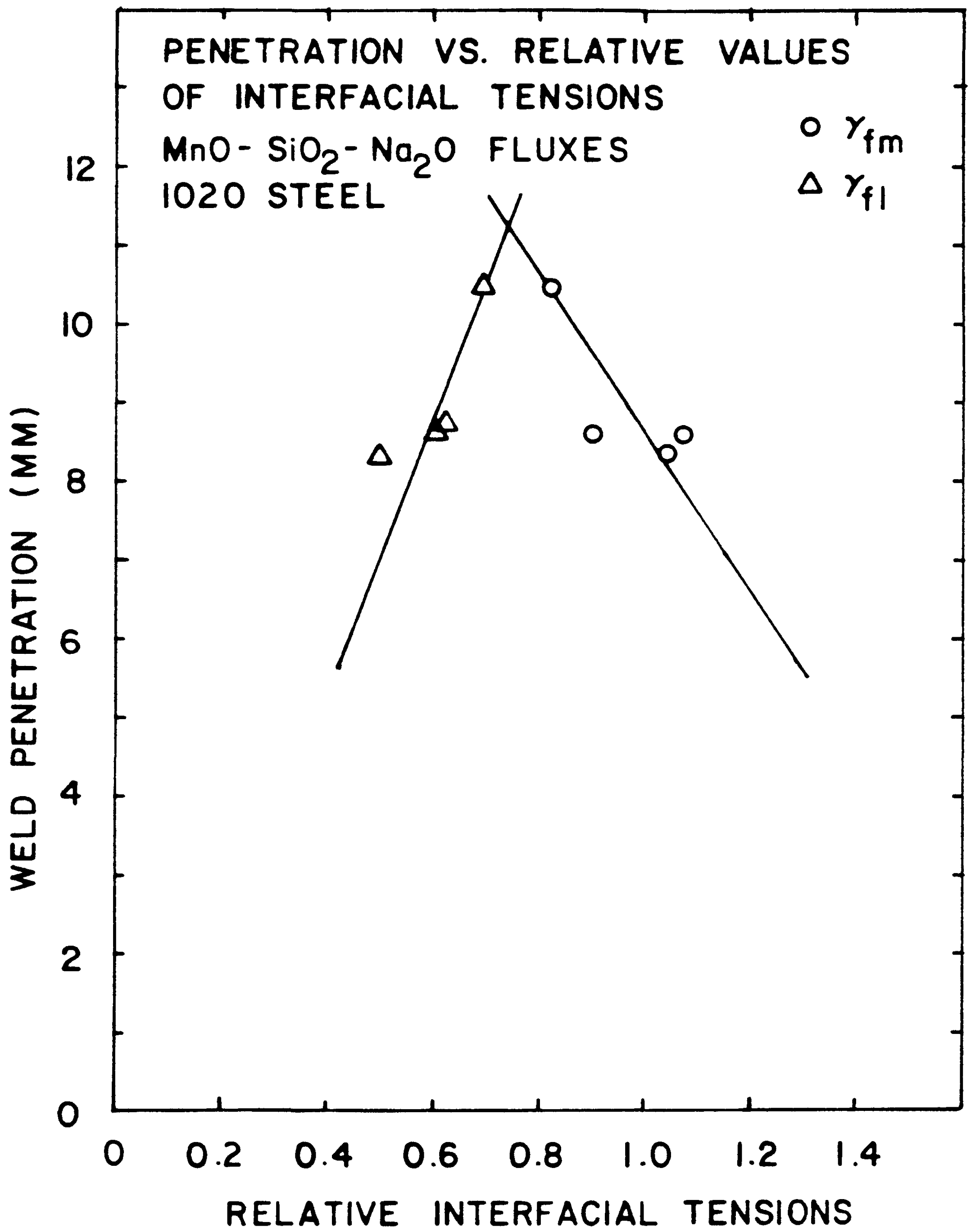

Fig. 36. Penetration vs. relative γ_{FL} and γ_{FM}, sodium additions to flux, 1020 steel.

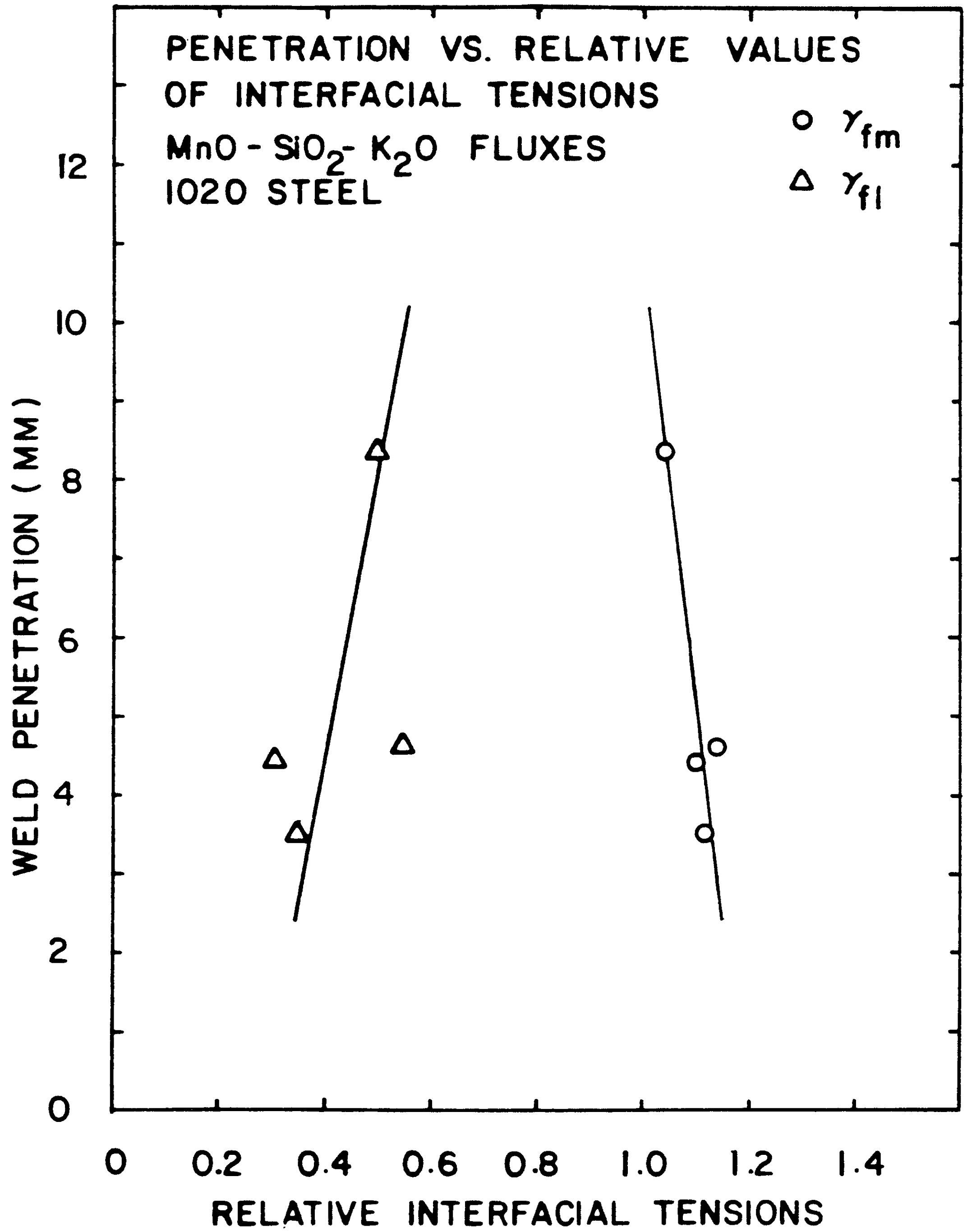

Fig. 37. Penetration vs. relative γ_{FL} and γ_{FM}, potassium additions to flux, 1020 steel.

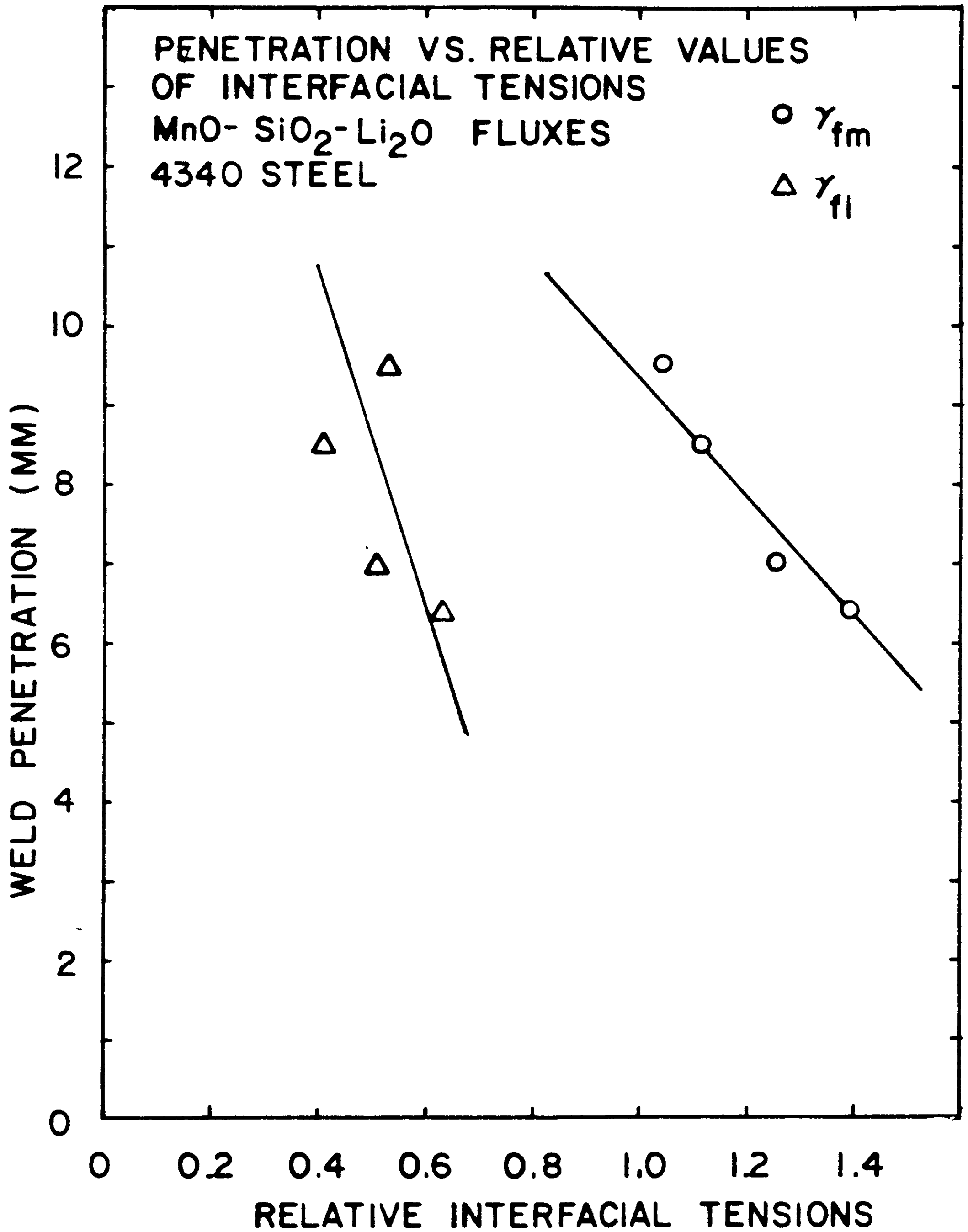

Fig. 38. Penetration vs. relative γ_{FL} and γ_{FM}, lithium additions to flux, 4340 steel.

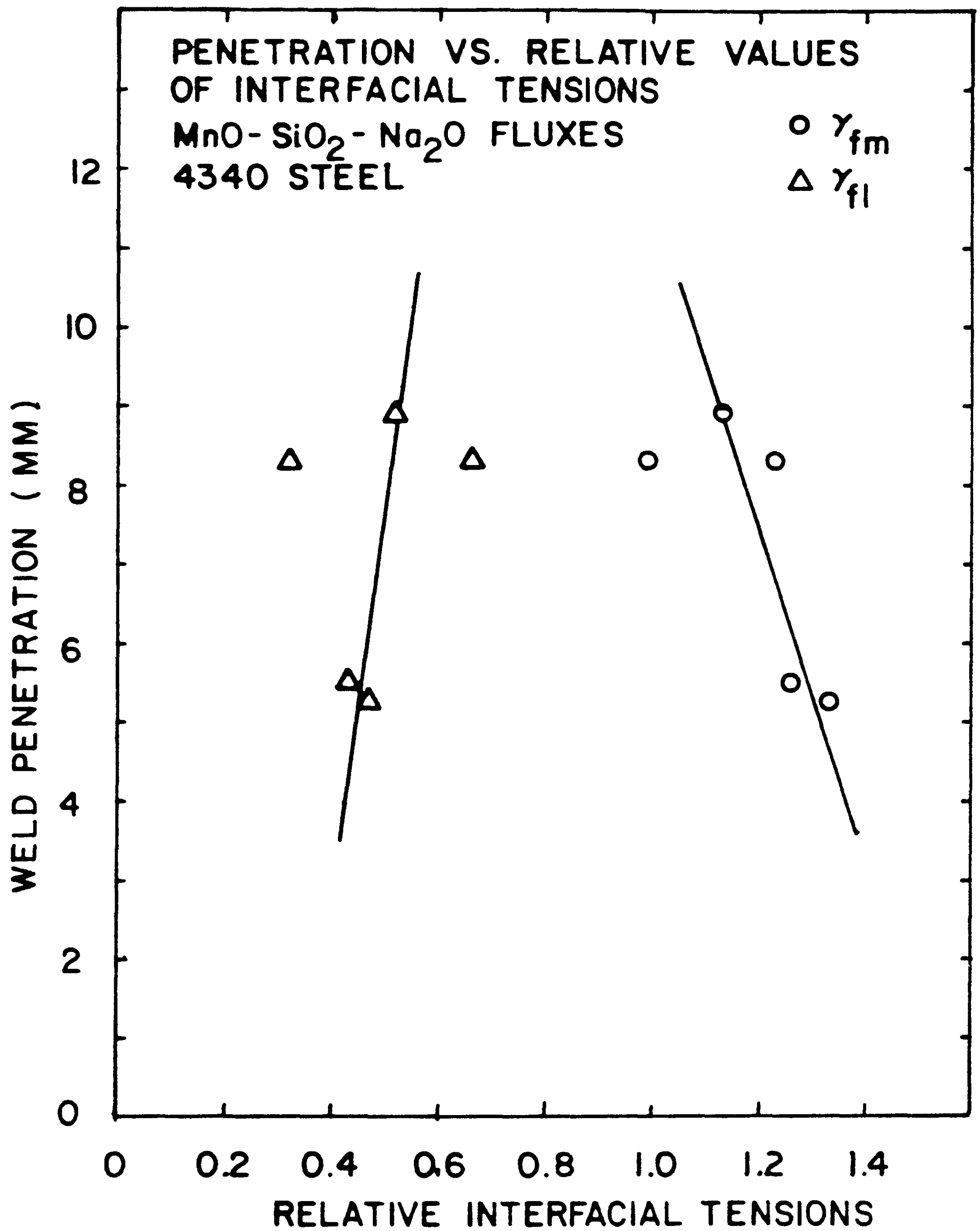

Fig. 39. Penetration vs. relative γ_{FL} and γ_{FM}, sodium additions to flux, 4340 steel.

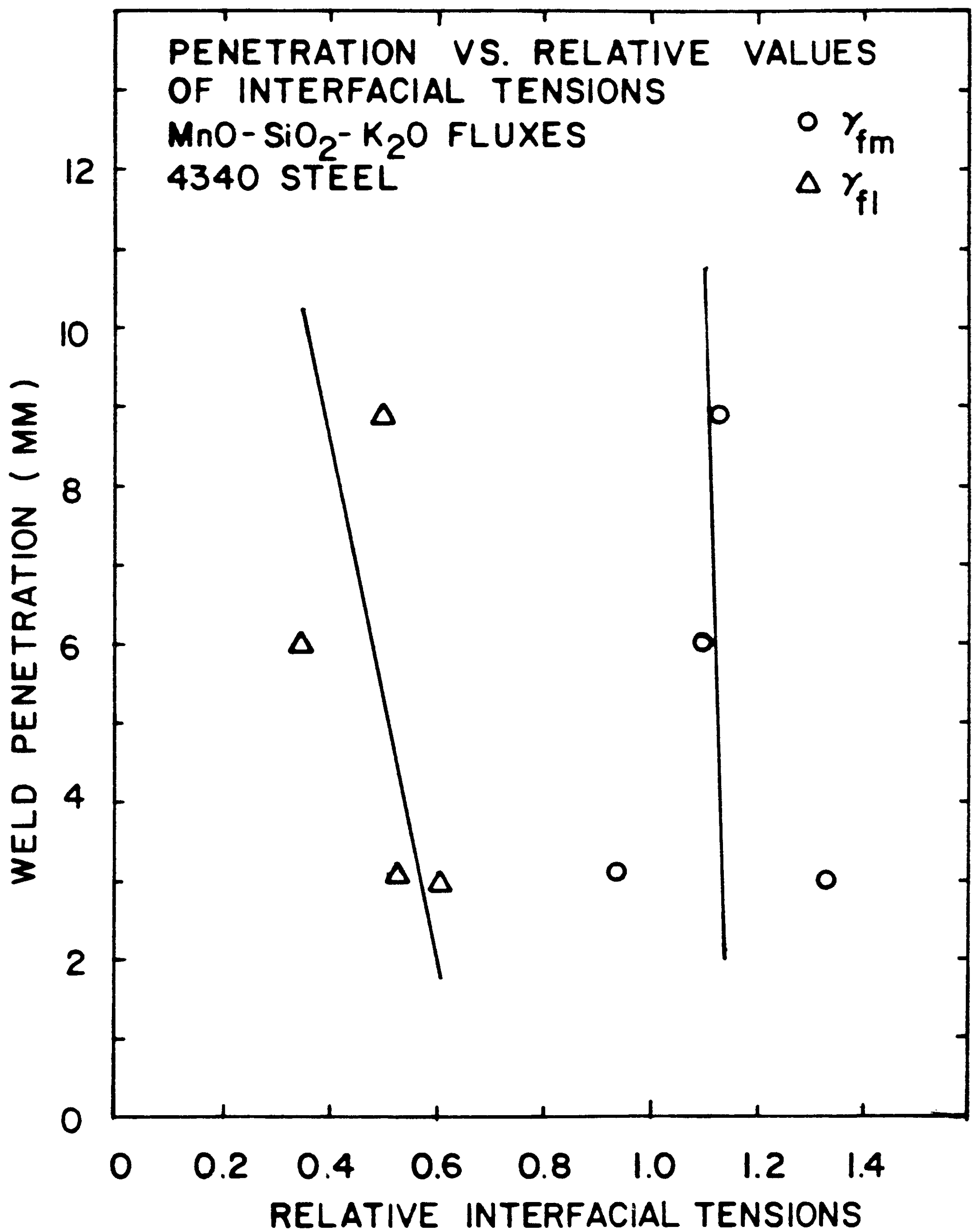

Fig. 40. Penetration vs. relative γ_{FL} and γ_{FM}, potassium additions to flux, 4340 steel.

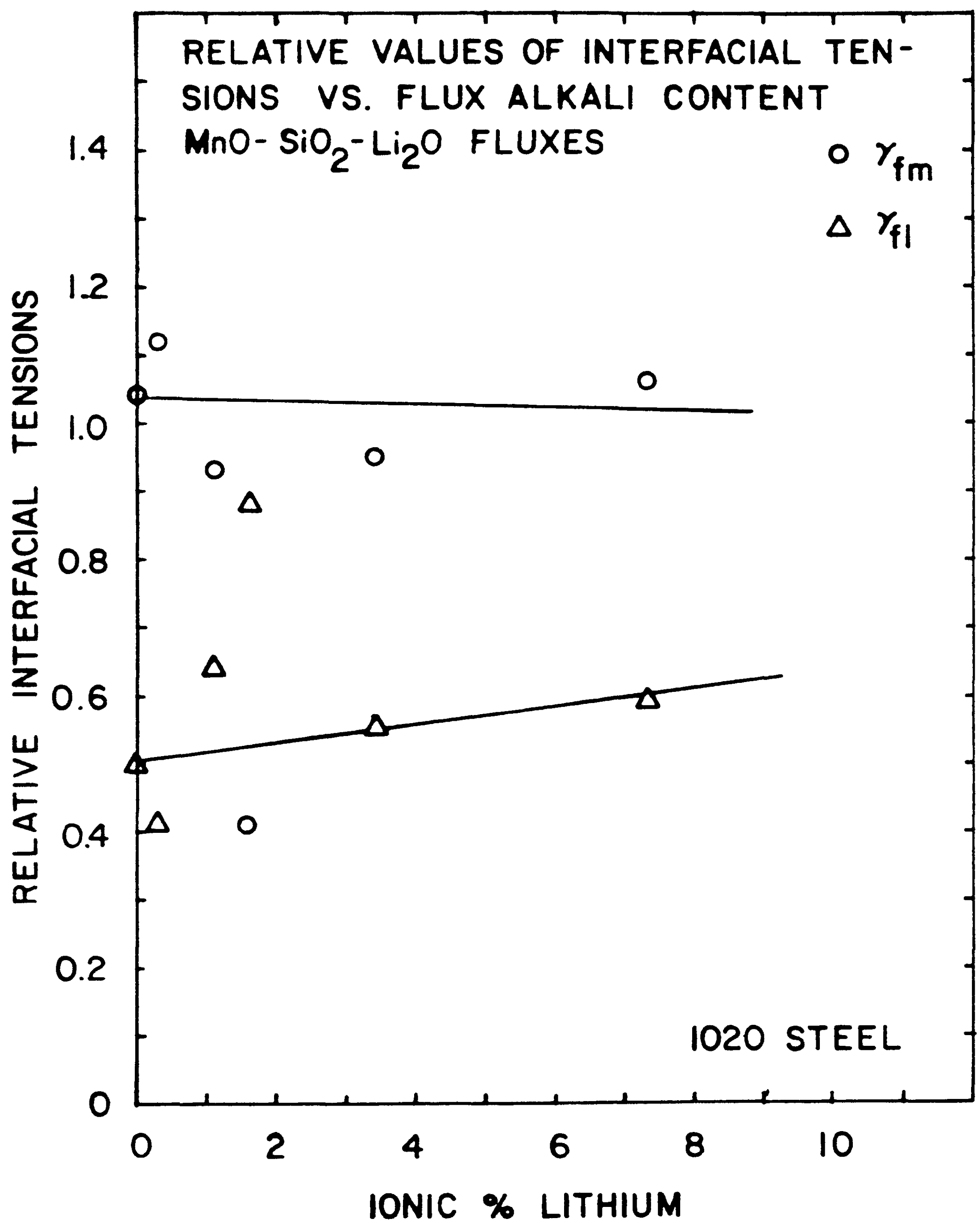

Fig. 41. Relative γ_{FL} and γ_{FM} vs. lithium content of flux, 1020 steel.

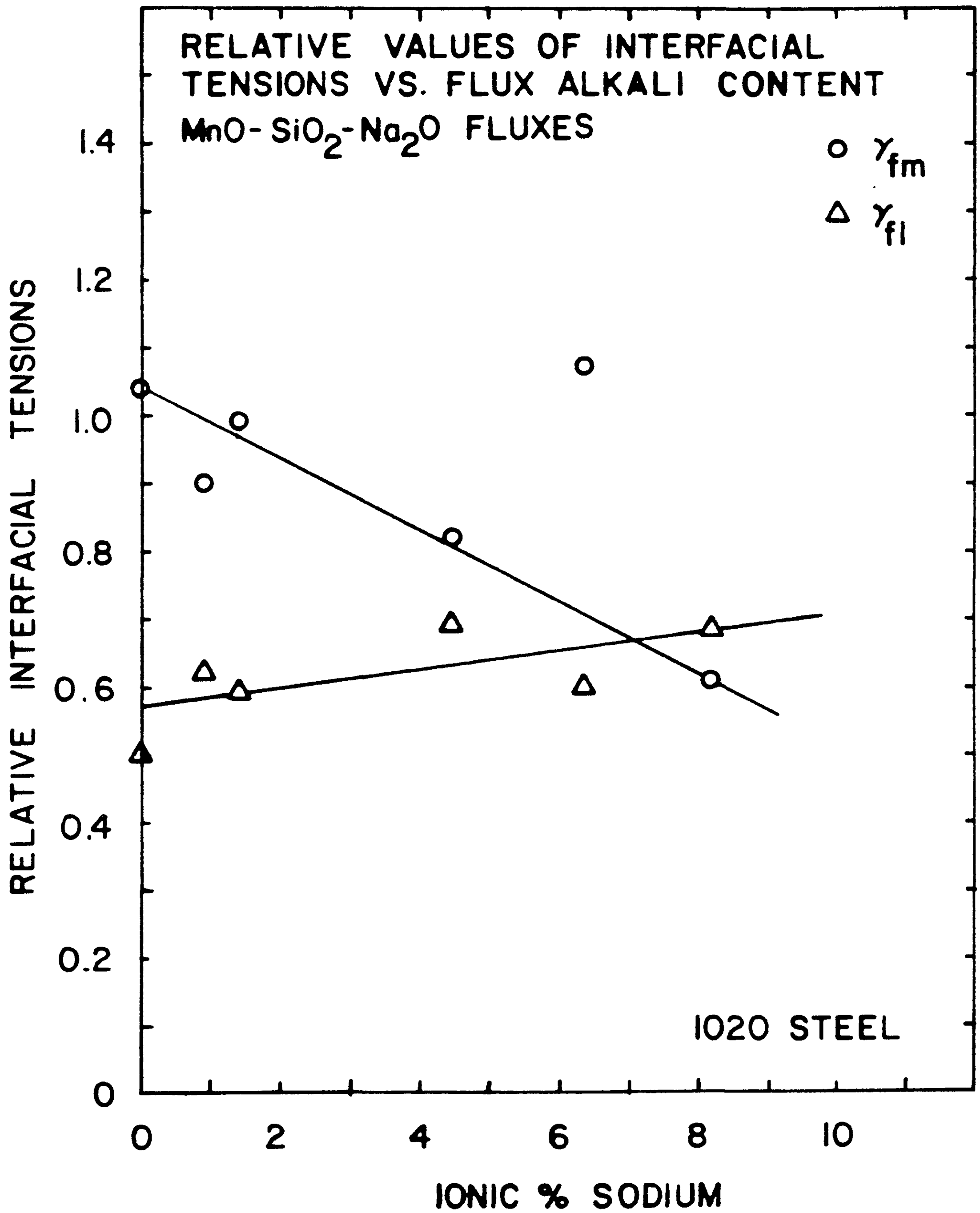

Fig. 42. Relative γ_{FL} and γ_{FM} vs. sodium content of flux, 1020 steel.

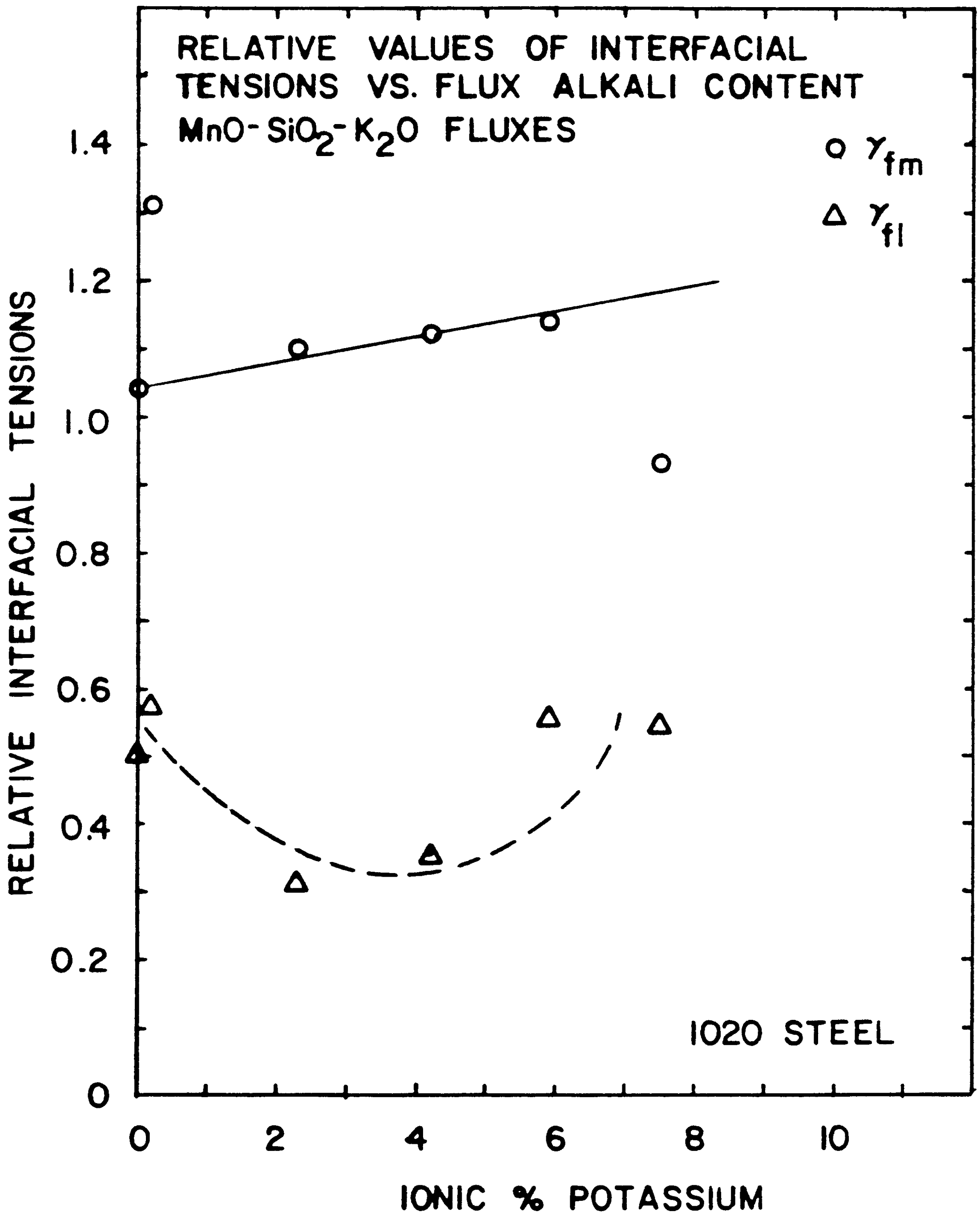

Fig. 43. Relative γ_{FL} and γ_{FM} vs. potassium content of flux, 1020 steel.

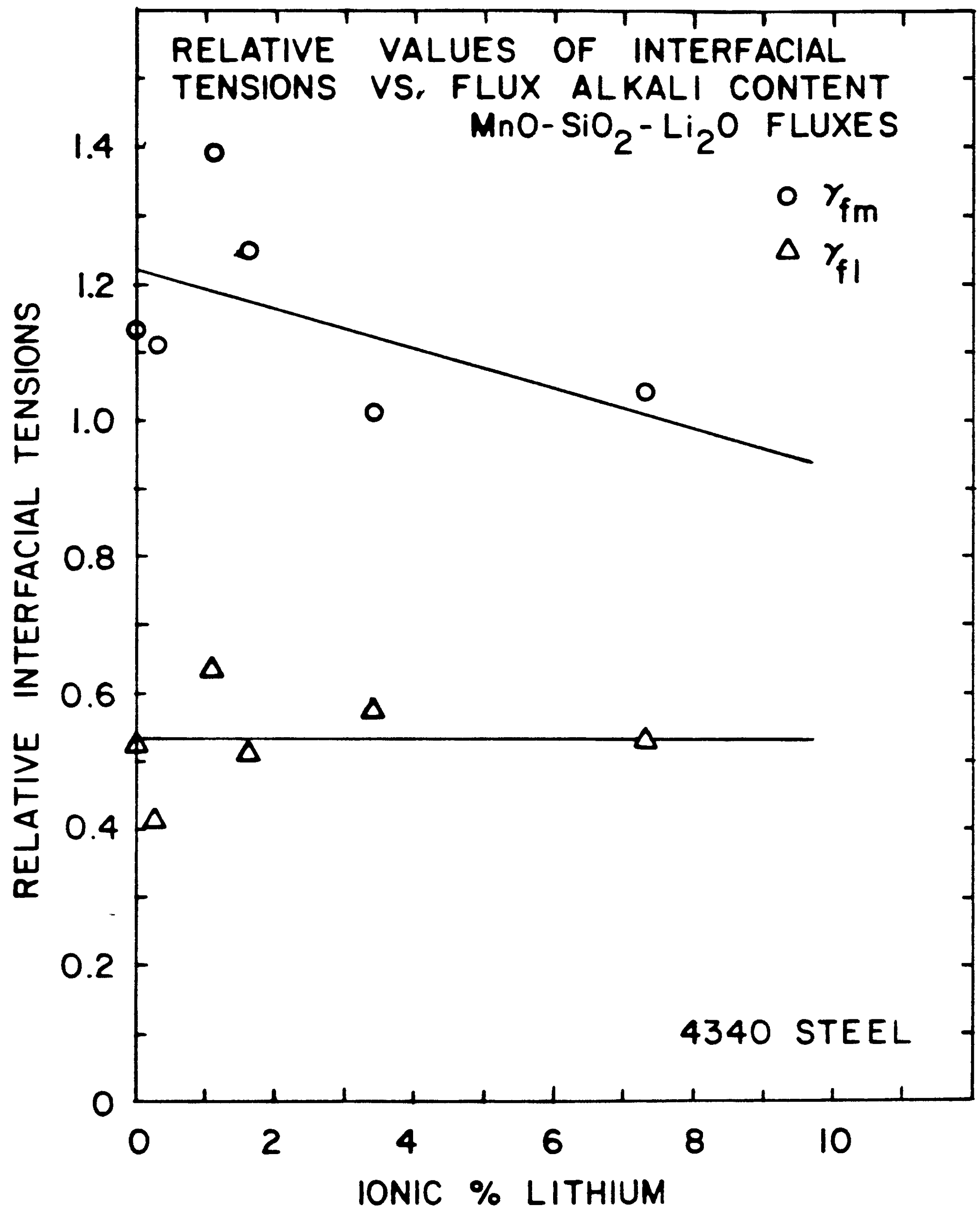

Fig. 44. Relative γ_{FL} and γ_{FM} vs. lithium content of flux, 4340 steel.

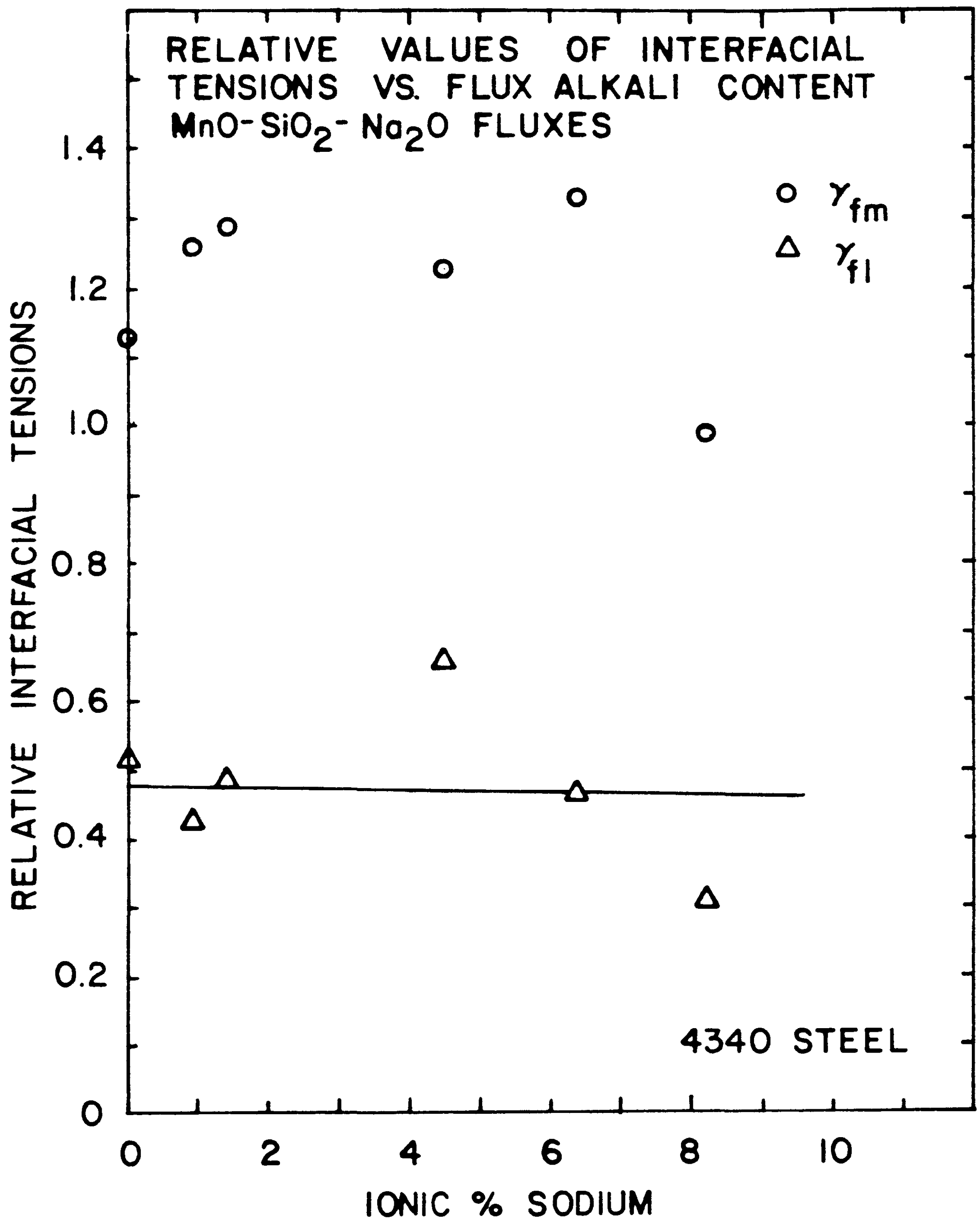

Fig. 45. Relative γ_{FL} and γ_{FM} vs. sodium content of flux, 4340 steel.

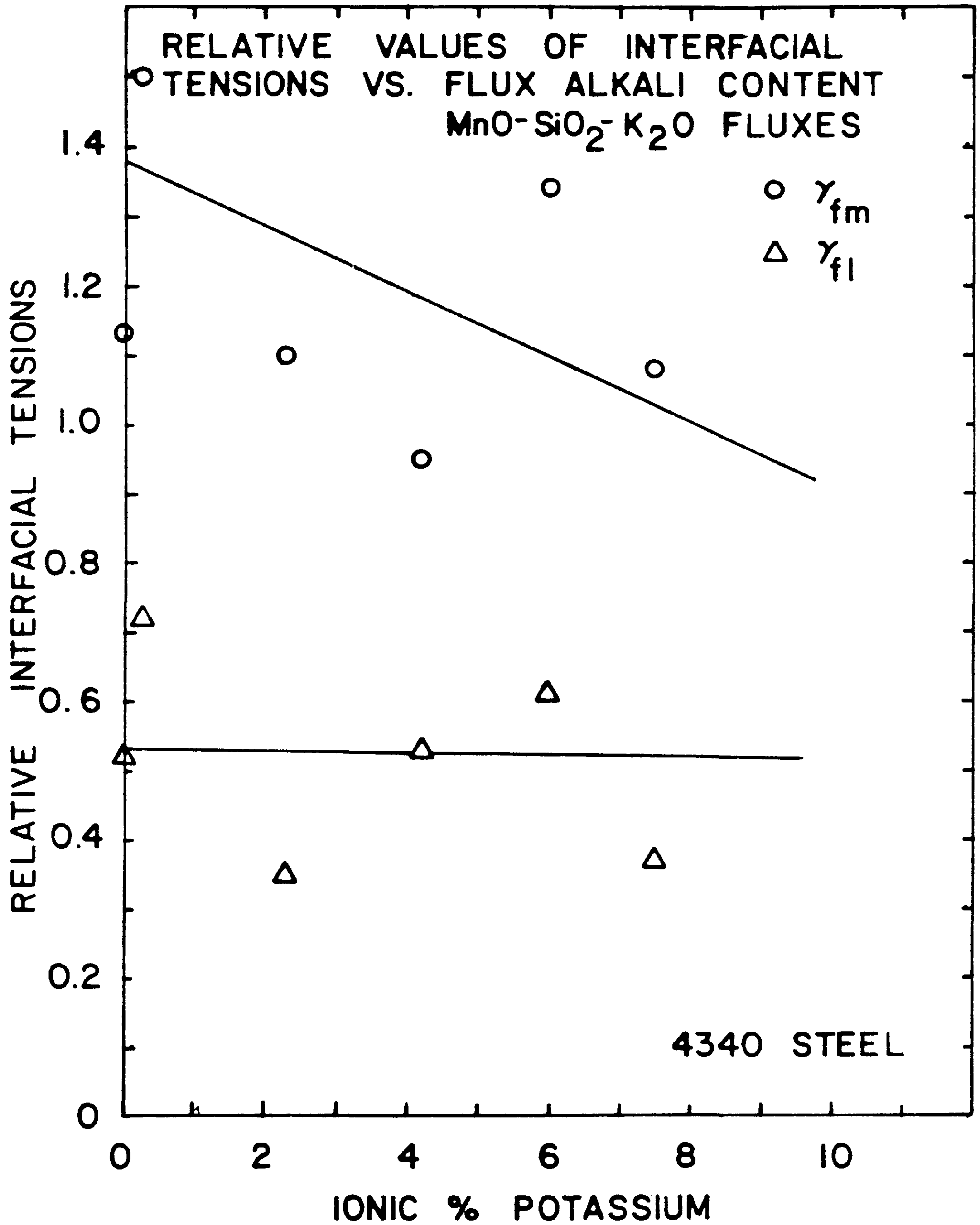

Fig. 46. Relative γ_{FL} and γ_{FM} vs. potassium content of flux, 4340 steel.

with increasing alkali flux levels, but the relatively wide scatter of data makes it difficult to be certain. The value of γ_{FL} is unaffected by flux composition.

VI. THE EFFECT OF FLUX BEHAVIOR ON WELD PENETRATION: RESULTS

A. The Effect of Flux Viscosity

Flux viscosity has a marked effect on penetration. For a given set of welding parameters, more viscous fluxes will give greater penetration, all other factors being equal.

Figure 47 shows this to be true for welds made on 1020 steel. In general, fluxes containing sodium gave the deepest penetration and potassium-bearing fluxes the least.

Penetration also increased with flux viscosity in welds made on 4340 steel with fluxes containing lithium and sodium but not with those containing potassium (see Figure 48). Penetration decreased with increasing viscosity of potassium-bearing fluxes. The reason behind this behavior is not known.

B. The Effect of Arc Stability

Figures 49 and 50 show that penetration in both 1020 and 4340 steel welds decreases as the arc becomes less stable. Note that penetration in 4340 steel is more sensitive to changes in arc stability than in 1020 steel. Schwemmer[18] observed the opposite to be true for welds made with $MnO-SiO_2-FeO$ fluxes.

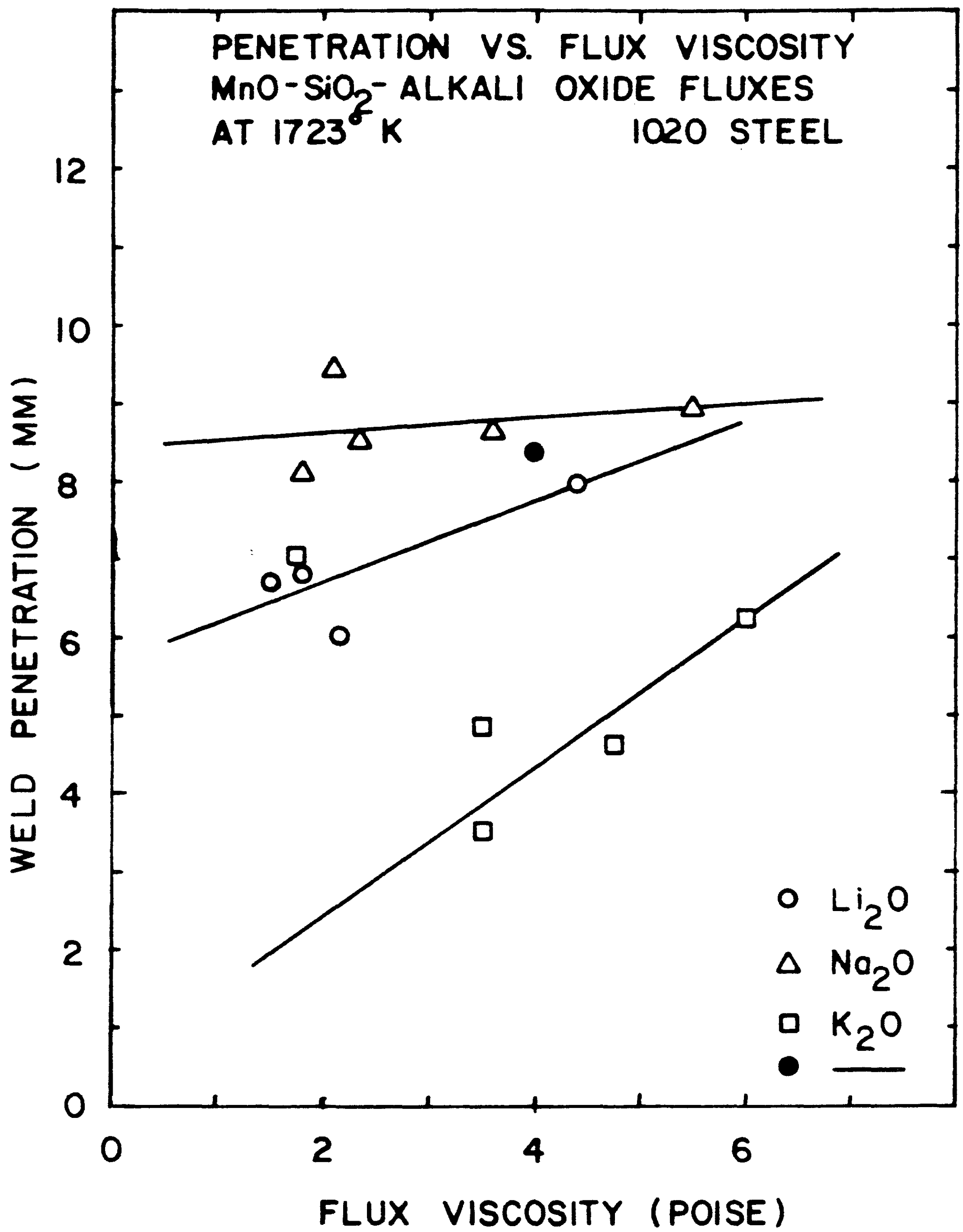

Fig. 47. Penetration vs. flux viscosity, 1020 steel.

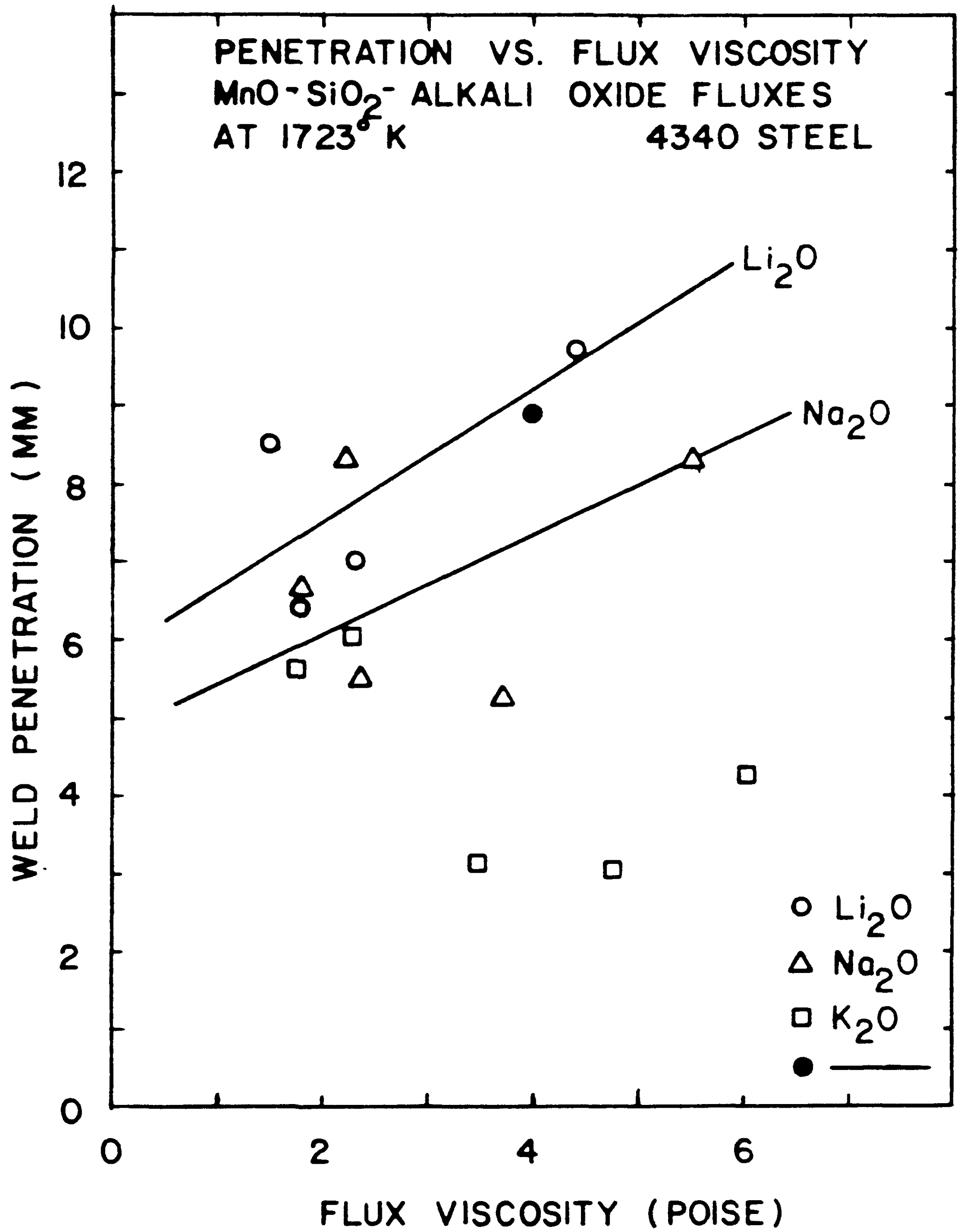

Fig. 48. Penetration vs. flux viscosity, 4340 steel.

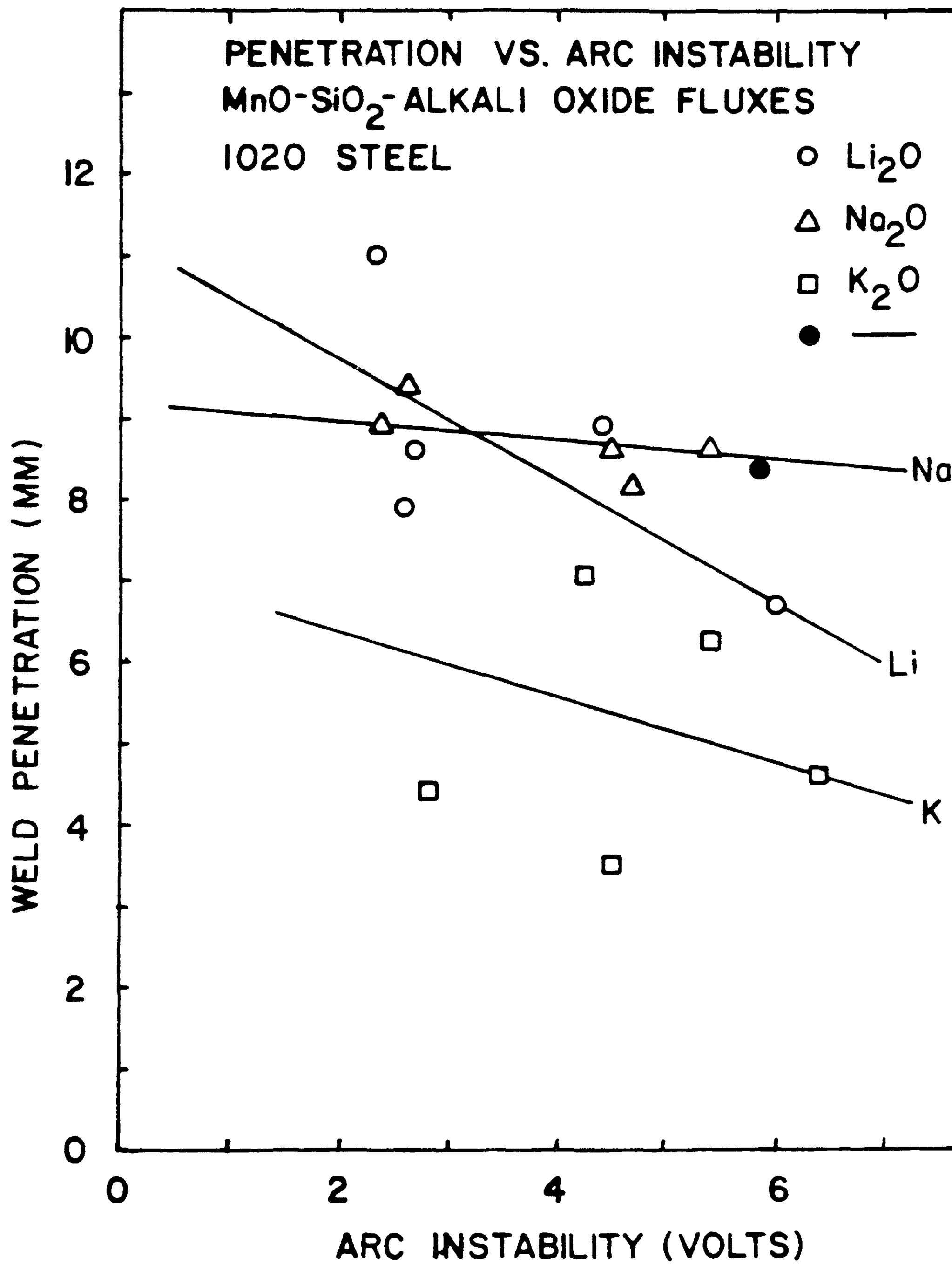

Fig. 49. Penetration vs. arc stability, 1020 steel.

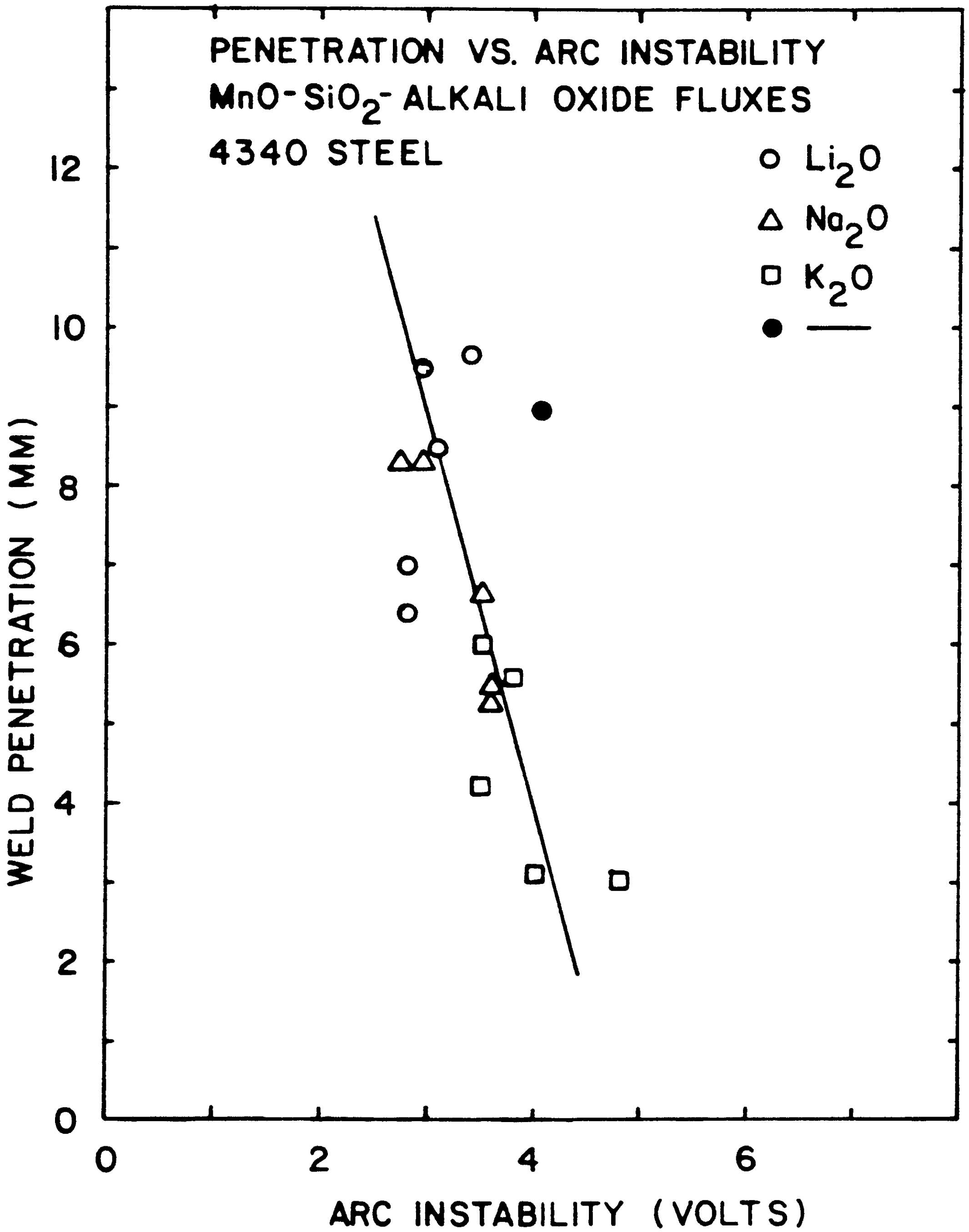

Fig. 50. Penetration vs. arc stability, 4340 steel.

C. The Relation of Flux Properties

It has been demonstrated that the effect of fluxes--viscosity, arc stability, and capillarity--all affect weld penetration. Because these three factors work simultaneously, it is often difficult to observe the effect of one single factor. The other two factors often mask the effect of variations in the third factor. For this reason, Hazlett[40] could not relate weld penetration to interfacial tensions.

Schwemmer noted in his investigations[18] that penetration was a linear function of the three factors mentioned above. From these observations he developed a single linear equation correlating the three factors to penetration:

$$\text{Penetration} = k\left[(\gamma_{FL} - \gamma_{FM}) \cdot \eta \cdot (V-\Delta V)\right] + C$$

where γ_{FL} and γ_{FM} are the flux-liquid metal and flux-solid metal interfacial tensions, η is the flux viscosity, and $(V-\Delta V)$ is the difference between the welding voltage and the measured arc stability. The slope k is a constant related to machine parameters and the intercept C corresponds to penetration when $(\gamma_{FL} - \gamma_{FM})$ is zero.[18] He found that this equation successfully described data from welds made on 1020 and 4340 steels with both MnO-SiO_2-FeO and MnO-SiO_2-CaO/CaF_2 fluxes. Figure 51 is a plot of penetration as a function of $[(\gamma_{FL} - \gamma_{FM}) \cdot \eta \cdot (30-\Delta V)$ for welds made on 1020 steel using the above two flux systems. Carmona also applied this equation to his data with some success.[19]

Figures 52 and 53 show penetration as a function of $[(\gamma_{FL} - \gamma_{FM}) \cdot \eta \cdot (30-\Delta V)]$ for 1020 and 4340 steels. The Schwemmer equation gives a reasonably linear relationship for data from 1020 steel; the slope of the best-fit line is about +0.074 and its intercept is about +9.5. Figure 53 shows that the equation does not work for data from 4340 steel welds.

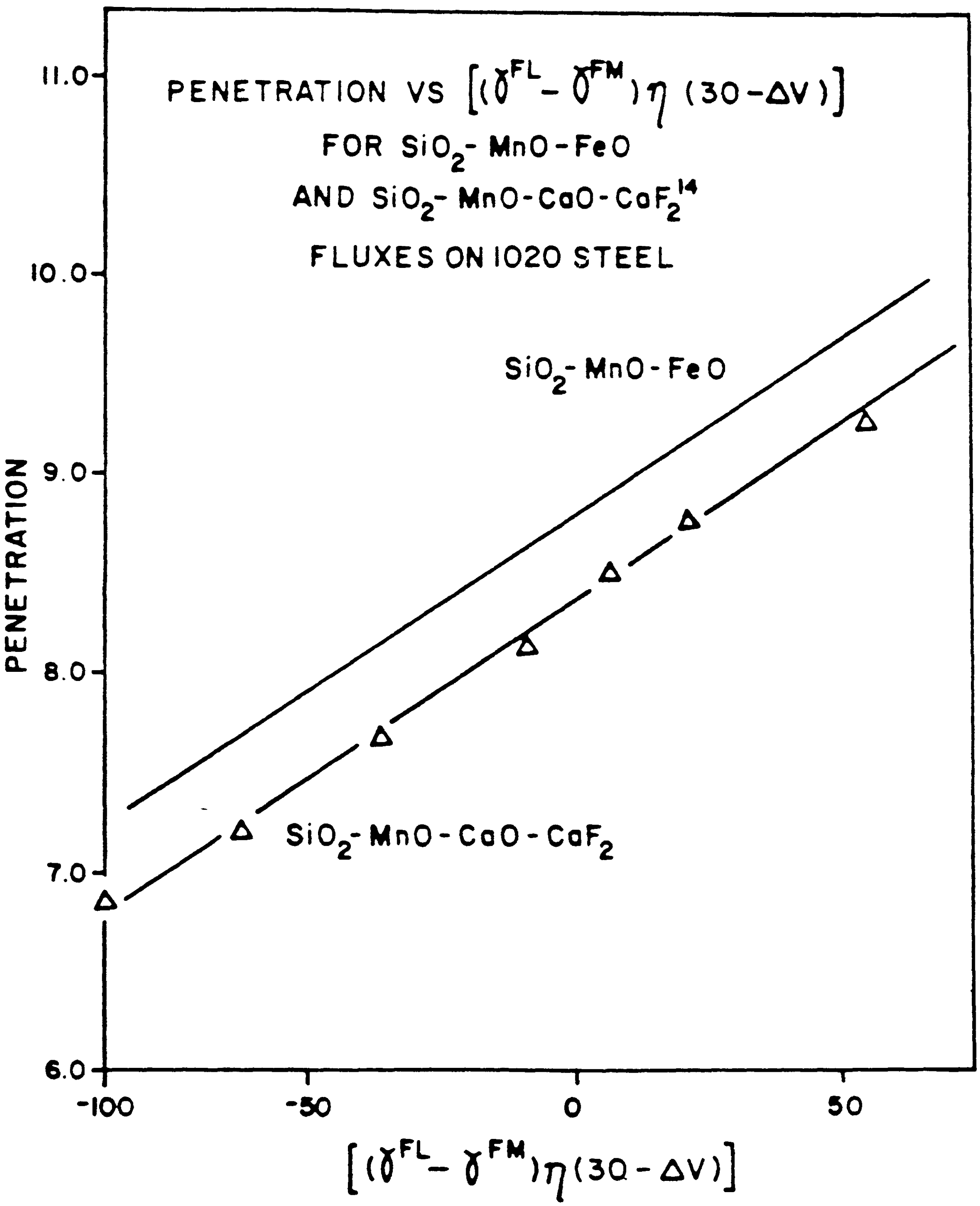

Fig. 51. Penetration vs. $[(\gamma_{FL} - \gamma_{FM}) \cdot \eta \cdot (30-\Delta V)]$, 1020 steel, SiO_2-MnO-FeO and SiO_2-MnO-CaO/CaF_2 fluxes.

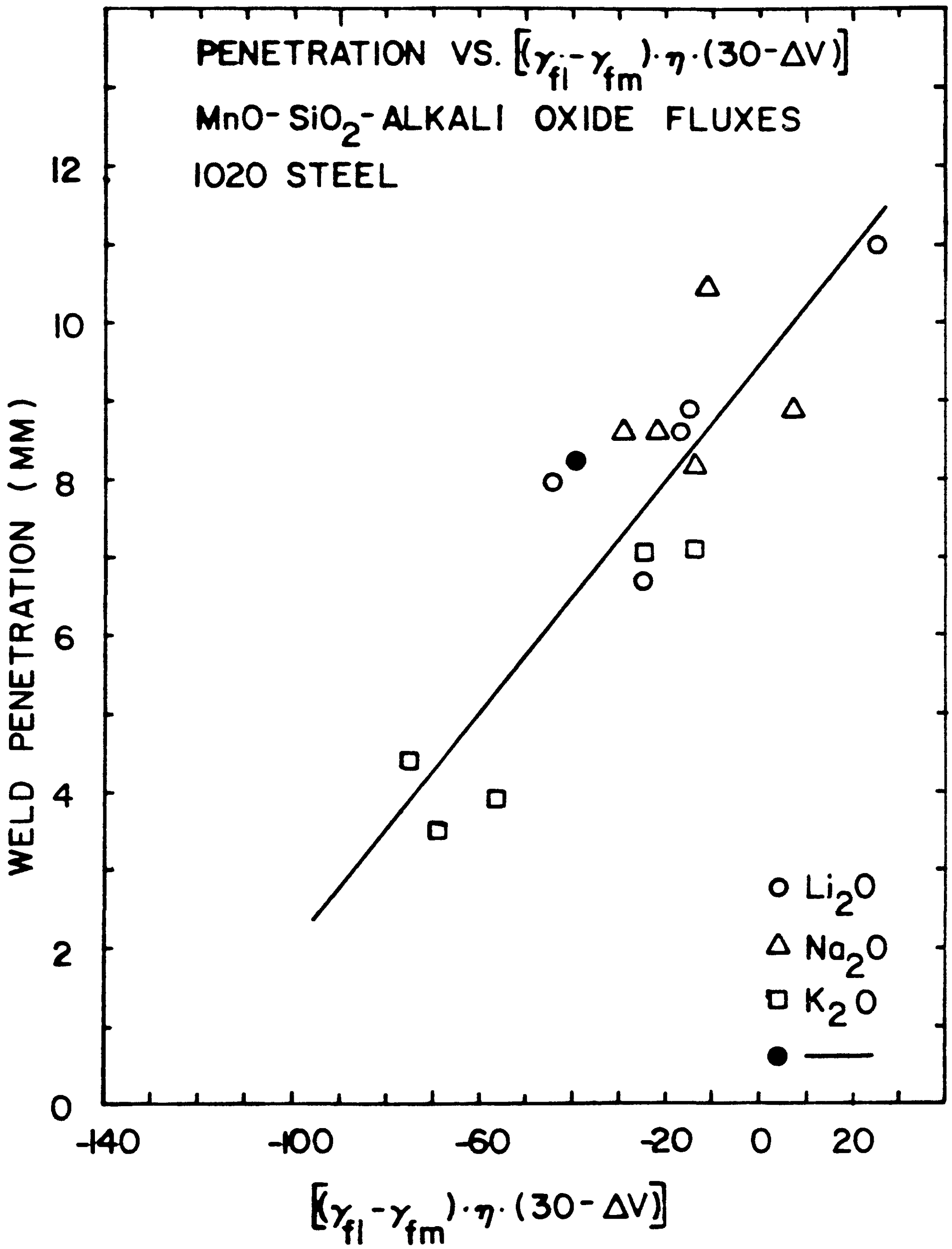

Fig. 52. Penetration vs. $[(\gamma_{FL} - \gamma_{FM}) \cdot \eta \cdot (30\text{-}\Delta V)]$, 1020 steel, alkali additions to $MnO\text{-}SiO_2$ fluxes.

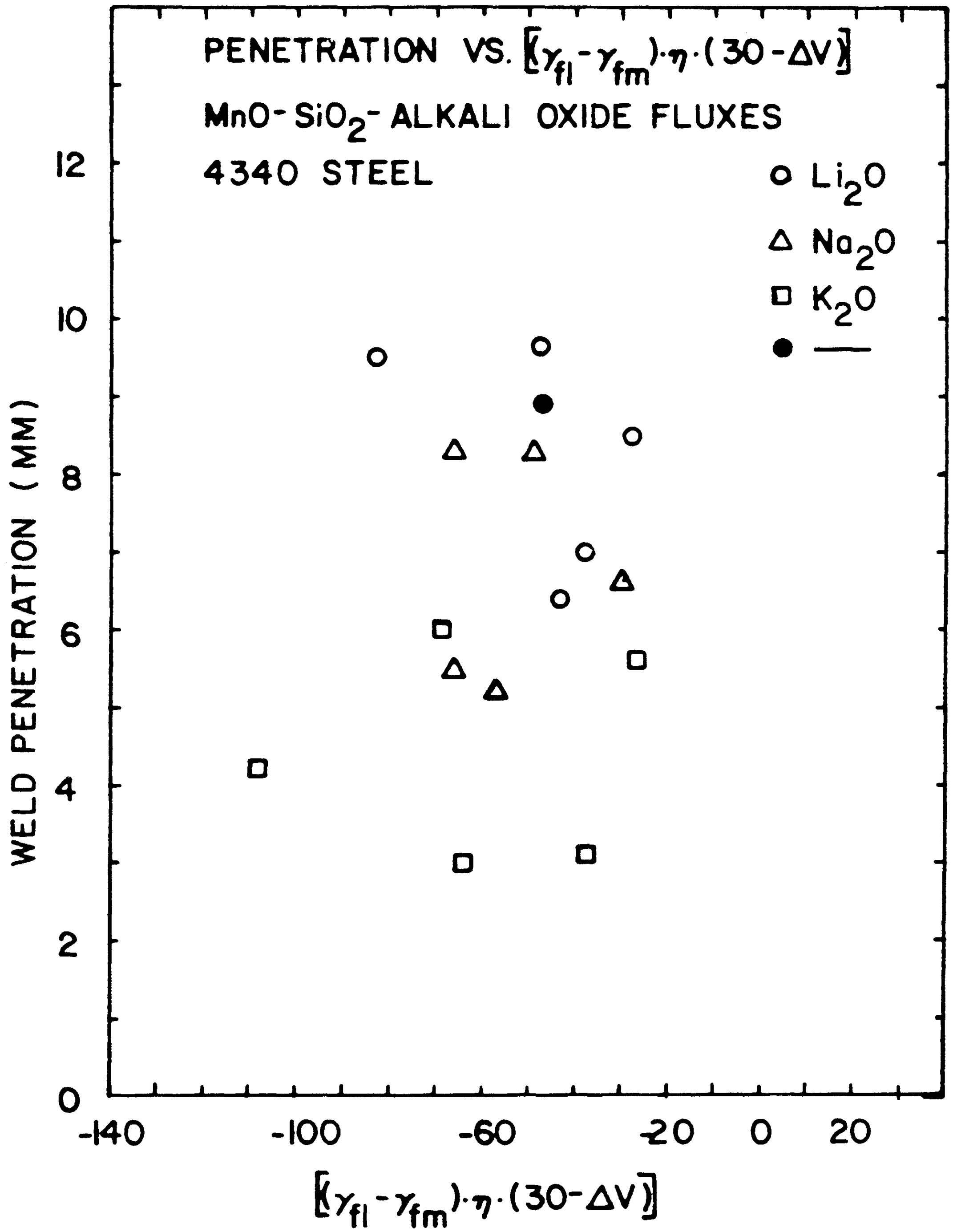

Fig. 53. Penetration vs. $[(\gamma_{FL} - \gamma_{FM}) \cdot \eta \cdot (30\text{-}\Delta V)$, 4340 steel, alkali additions to $MnO\text{-}SiO_2$ fluxes.

VII. DISCUSSION OF RESULTS

A. Flux Viscosity

The reason behind the initial decrease in flux viscosity at low alkali contents is fairly certain. Since the addition of alkalis in the place of manganese ions causes a viscosity decrease, it must be that the alkalis are more effective silicate network modifiers than manganese. In fact, Figures 15 and 16 show that the alkalis are generally more effective network modifiers than metal ions with greater valences. But the mechanism by which alkali additions beyond 3 ionic % cause flux viscosity increases is not clear at present. It is possible that above the 3% level the alkalis cause interactions between ions in the melt which strengthen the attractive forces between silicate anions. Unfortunately, little is known about the structures of silicates containing large quantities of metal oxides, so that the nature of such ionic interactions cannot be reported.[23]

Penetration in 1020 steel welds increased with increasing flux viscosity, but the opposite was observed for welds made on 4340 steel with fluxes containing potassium (refer back to Figure 48). It is possible that other factors--especially variation in surface tensions--interfere to the point that the effect of viscosity alone cannot be observed.

B. Arc Stability

Arcs on 4340 steel became slightly more stable when alkalis were added to fluxes. The fact that the increase in stability was small indicates that the alloying agents in the steel play a dominant role in determing arc stability. Whether they do so by virtue of their effect on the work function of the metal or by other means is not known.

Arc stability data for 1020 steel welds made with potassium-bearing fluxes was too scattered to observe a trend (refer back to Figure 27).

The plots of arc stability as a function of ionization potential from both this investigation (Figures 29 and 30) and the work of Carmona[19] (Figure 22) show that ionization potential is definitely not the controlling factor. Some other property or combination of properties (in which ionization potential may be included) must be controlling arc stability.

C. Interfacial Tensions

The effects of interfacial tensions on penetration in 1020 steel welds agree with the results of Schwemmer[18] and Carmona.[19] As the magnitude of γ_{FL} increases, the weld bead is more strongly confined and penetration increases. As γ_{FM} increases, the tendency for the bead to wet the plate grows stronger and penetration decreases.

The effects of interfacial tensions on 4340 steel weld penetration do not follow the same trend, with the exception of welds made with sodium-bearing fluxes. It is quite possible that changes in flux composition affect the fusion line interfacial tension γ_{LM}. This would invalidate the assumption of constant γ_{LM} used in the derivation of the expressions for the relative values of γ_{FL} and γ_{FM}. If none of the surface tensions remains relatively constant then it is impossible to calculate relative values for the other two tensions.

The behavior of these interfacial tensions is the primary reason that the equation developed by Schwemmer did not fit the data for 4340 steel welds.

VIII. CONCLUSIONS

From the results of this investigation and from reviews of the results of other CSM welding flux investigators, the following conclusions were made:

1. At low metal ion addition levels (under 3 ionic %), the alkali elements are more effective network modifiers than the alkaline earth and transition elements. But beyond the 3 ionic % level this situation changes because the alkali elements then cause flux viscosity to increase. The mechanism behind this viscosity increase is not clear.

2. Alkali elements act as arc stabilizers when added to manganese silicate welding fluxes. The stabilizing effect is more pronounced in arcs on 1020 steel, which indicates that the 4340 steel alloying agents play a dominant role in stabilizing the arc. It was also confirmed that the ionization potential of flux components is not the key factor in determining arc stability.

3. $MnO-SiO_2$ flux alkali content had little effect on the flux-weld pool interfacial tension, but the flux-solid metal tension value decreased with increasing sodium content for both 1020 and 4340 steel.

4. Flux viscosity, arc stability, and interfacial tensions all work together to determine weld penetration, and because of this, it is often difficult to observe the effects of any single factor. But the equation developed

by Schwemmer[18] relating these factors to penetration describes the data for 1020 steel reasonably well. The failure of the equation to do the same for 4340 steel is attributed to the effect of alloying agents and alkalis on the fusion line interfacial tension component.

REFERENCES

1. American Welding Society. "Terms and Definitions," AWS-A3.0.69.

2. Olson, D. L., Private communication, June 12, 1979.

3. AWS Welding Handbook Section Two: Welding Processes, 24.20 (1969).

4. Ibid., 22.11.

5. Davis, M. L. E. and Coe, F. R., "The Chemistry of Submerged Arc Fluxes." The Welding Institute, (1977).

6. Eagar, T. W., "Sources of Weld Metal Oxygen Contamination During Submerged Arc Welding," Welding Journal, 76s, March 1978.

7. Zaks, I. A. and Zhorova, R. S., "Effect of Various Fluxes on the Solidification Cracking Resistance and Properties of Austenitic Weld Metals," Svar Proiz, 7, 32 (1974).

8. Ito, Y. et al., "Effect of CaF_2 in Flux on Toughness of Weld Metal--Relation Between CaF_2 Content in Welding Flux and Impure Gas Content in Weld Metal," The Sumitomo Search, #16, November 1976.

9. Garland, J. G. and Kirkwood, P. R., "Towards Improved Submerged Arc Weld Metal Toughness," Metal Construction and British Welding Journal, May and June 1975.

10. Tuliani, S. et al., "Notch Toughness of Commercial Submerged Arc Weld Metal," Welding and Metal Fabrication. August 1969.

11. Belton, G. R., Moore, T. J., and Tankins, E. S., "Slag-Metal Reactions in Submerged Arc Welding," Welding Journal, 43, 289s (1963).

12. Bennett, A. P. and Stanley, P. J., "Fluxes for the Submerged Arc Welding of QT35 Steel," British Welding Journal, 13, 59 (1966).

13. Lewis, W. J., Faulkner, G. E., and Rieppel, P. J., "Fluxes and Filler Wire Developments for Submerged Arc Welding HY-80 Steel," Welding Journal, 41, 337s (1961).

14. Singleton, E. L., Carpenter, L., and Lundquist, R. V., "Studies of the MnO-SiO_2 Binary System," U.S. Bureau of Mines Report 5938 (1962).

15. Ferrera, K. P. and Olson, D. L., "Performance of $MnO-SiO_2$-CaO as a Welding Flux," Welding Journal, Vol. 58, p. 211s, July 1975.

16. Alizo, Quintini C., "Effects of SiO_2-MnO-CaO Flux Composition of the Physical Properties of Submerged Arc Weld Metal," Thesis T-1794, Colorado School of Mines, (1975).

17. Janzen, H. E., "An Investigation of the SiO_2-MnO-CaO/CaF_2 Welding Flux System," Thesis T-1970, Colorado School of Mines, (1977).

18. Schwemmer, D. D., Jr., "An Investigation of the SiO_2-MnO-FeO Welding Flux System," Thesis T-1989, Colorado School of Mines, (1977).

19. Carmona, Enrique L., "Influence of Alkaline-Earth and Transition Ion Additions on the Behavior of the $MnO-SiO_2$ Welding Flux System," Thesis T-2123, Colorado School of Mine, (1978).

20. Jackson, C. E., "Fluxes and Slags in Welding," WRC Bulletin #190, (1973).

21. Vennard, J. K., Elementary Fluid Mechanics, John Wiley and Sons, New York, NY, Fourth Edition, (1961).

22. Geiger, G. H. and Poirier, D. R., Transport Phenomena in Metallurgy, Addison-Wesley, Reading, Mass., 26, (1973).

23. Richardson, F. D., Physical Chemistry of Melts in Metallurgy, Academic Press, London, New York 78, (1974).

24. Warren, B. E. and Biscoe, J., Journal of the American Ceramic Society, 21, 259 (1938).

25. Biscoe, J. et al., Journal of the American Ceramic Society, 24, 116, (1941).

26. Kingery, W. D., Introduction to Ceramics, John Wiley and Sons, New York, p. 153 (1960).

27. Bockris, J. O'M., Mackenzie, J. D. and Kitchener, J. A., Transactions of the Faraday Society, 51, 1734 (1955).

28. Reinhart, T. L., Laboratory notebook for this investigation.

29. Jackson, C. E., "The Science of Arc Welding," Research Supplement to Welding Journal, Apr. 1960, pp. 129s-145s.

30. Welding Handbook, Section 2: Welding Processes. American Welding Society. Sixth Edition (1969).

31. Lancaster, J. F., "Energy Distribution in Argon Shielded Welding Arcs," British Welding Journal, Vol. 1, #9, 412 (1954).

32. Roper, J. R., "Capillarity Effects in the Gas Tungsten Arc Weldability of 21-6-9 Stainless Steel," Thesis T-1881, Colorado School of Mines (1977).

33. Bennett, W. S. and Mills, G. S., "Gas Tungsten Arc Weldability Studies on High Manganese Stainless Steel," Welding Journal, V., 53, #12, (1974).

34. Ludwig, H. C., "Current Density and Anode Spot Size in the Gas Tungsten Arc," Welding Journal, 47, 234s, (1968).

35. Russanevitz, N. F., Avtog. Delog., 9, 27, (1938).

36. Davidenko, I. D., Avtog. Delog., 9, 6, (1938).

37. Welding Handbook, Section Two: Welding Processes. American Welding Society, 24.20 (1969).

38. Jackson, C. E. and Shrubsall, A. E., "Control of Penetration and Melting Ratio with Welding Technique," Welding Journal, 32, 172s (1953).

39. Wassink, R. J. K., "Wetting of Solid Metal Surfaces by Molten Metal," Journal of the Institute of Metals, 92, 38, (1967).

40. Hazlett, T. H., "Coating Ingredients Influence on Surface Tension, Arc Stability and Bead Shape," Welding Journal, 36, 18s (1957).

41. Kozakevitch, P., "Surface Phenomena of Metals," Society of Chemical Industry Monograph 28, p. 223 (1968).

42. Spraragen, W. and Claussen, W. G., "Coatings and Fluxes in the Welding of Steels," Welding Journal, 17, 153 (1938).